國立臺灣大學植物科學研究所

博士論文

Institute of Plant Biology, College of Life Science
National Taiwan University

Doctoral dissertation

揭示小型調節 RNA 於阿拉伯芥光形態發育之多重貢獻

Unraveling multifaceted contributions of small regulatory RNAs to photomorphogenic development in *Arabidopsis*

林孟淳

Meng-Chun Lin

指導教授：吳素幸 博士

Advisors: Shu-Hsing Wu, Ph.D.

中華民國 106 年 7 月

July 2017

doi:10.6342/NTU201702588

國立臺灣大學博士學位論文
口試委員會審定書

揭示小型調節 RNA 於阿拉伯芥光形態發育之多重貢獻

Unraveling multifaceted contributions of small regulatory RNAs to photomorphogenic development in Arabidopsis

本論文係林孟淳君（學號 F97b42012）在國立臺灣大學植物科學研究所完成之博士學位論文，於民國 106 年 7 月 28 日承下列考試委員審查通過及口試及格，特此證明

口試委員：

（指導教授）　（簽名）

台灣大學植物科學研究所教授 鄭石通博士

中央研究院農業生物研究中心 陳荷明助研究員

中央研究院植物暨微生物研究所 涂世隆副研究員

台灣大學植物科學研究所 謝旭亮教授(所長)

系主任、所長　（簽名）

i

doi:10.6342/NTU201702588

致謝

感謝每一位在我求學過程中提供協助的人，沒有你們，我不可能通過這些試煉。特別謝謝我的指導老師吳素幸博士，在這五年半來給予我的教誨。期間最重要的，是讓我了解到，很多事情不能只從一個角度切入，要考慮所有可能的變數；研究如是，生活也是如此。同時也感謝我的碩士班指導老師謝旭亮博士，開啟了我對植物科學研究的道路。也感謝我的口試委員們，給予我許多寶貴的建議，讓我能夠審視自己研究的不足之處。也謝謝 A326 實驗室的同伴們，以及我所指導過的學生們，你們都是我學習的對象，讓我每一天都能持續精進。也感謝我的父母與弟弟，在我研究的途中，不斷給予精神上的支持。在遇見大家之前，我只是一個喜歡種植物的學生，現在除了保有熱愛植物的那份單純外，對植物的認識也更多了。我一直覺得，人生是一場很不容易玩的遊戲，但也因為這樣才好玩。感謝主，讓我能夠在人生中遇見你們，現在這個遊戲，變得更加有趣了。

doi:10.6342/NTU201702588

中文摘要

光形態發生，又稱幼苗去白化現象（seedling de-etiolation），對甫出土幼苗之生存，可謂至關重大；而小型調節 RNA（small regulatory RNA，sRNA），及其引起之轉錄後調控，對眾多生物之生長發育，有不可或缺的重要性。於阿拉伯芥中，當參與 sRNA 合成途徑之基因產生突變，植物會對光過度敏感，且有嚴重之發育缺陷。本實驗室先前之研究指出，依據有穩定 sRNA 之功能之甲基轉移酶，HUA ENHANCER 1，除藉其甲基轉移酶之功能穩定 sRNA 外，本身亦為光形態發生之負調節因子。已知 miRNAs，miR157 和 miR319，可分別調節光形態發生之正向及負向調控轉錄因子。先前之證據，雖可略窺 sRNA 對於光形態發生之作用；但若能提供全基因組規模之探討，可使此研究領域有更長足之進步。然而，截至目前為止，並未有此等規模之探討。因此，藉由 sRNA 及降解組定序分析，吾等發現照光 24 小時的去白化幼苗，有 335 件 mRNA 剪切現象，乃肇因於 sRNA 之作用；造成這些剪切現象之主因，為 sRNA 之表現量，而與目標基因（target mRNA）之表現量無關。饒富意味的是，無論 miRNA 本身之表現是否受光調節，與其對應之目標基因表現，多在光照後降低。負責攜帶 miRNA 並剪切目標基因之 ARGONAUTE1，其本身之 mRNA 於光中之表現，受 miR168a/b 負向調節。此外，吾等亦發現 miR396a/b，由抑制負調控者 *GROWTH REGULATING FACTOR*s mRNA 之累積，得以正向調節光形態發生。總結而論，最佳化光形態發生需要 sRNA。sRNA 藉由調控光形態發生正調控者及負調控者之基因表現，使阿拉伯芥幼苗，可以有即時且穩定之適應機制，以因應光照環境之改變。

關鍵詞

光、小型調節 RNA、次世代定序、轉錄後調控、光形態發生。

doi:10.6342/NTU201702588

Abstract

Photomorphogenesis, or seedling de-etiolation, is a vital step for seedling survival once they have emerged from soil. It was reported that many small RNA (sRNA) mediated post-transcriptional regulation is required for growth and development of diverse organisms. In *Arabidopsis*, many mutants of sRNA biogenesis show light hypersensitivity and severe morphological defects. In our previous study, we have also shown that HUA ENHANCER 1, a methyltransferase that stabilizes sRNA duplexes, is a negative regulator of photomorphogenesis. miR157 and miR319 were known to regulate positive and negative regulators of photomorphogenesis, respectively. Although previous evidence gave a glimpse of sRNA-mediated regulation of de-etiolation, a genome-wide profiling of sRNAs and their regulation of target genes during photomorphogenesis has been missing. I aimed to provide a comprehensive view of sRNA-controlled gene expression during photomorphogenesis. By profiling sRNAs and the 5' ends of degraded mRNAs during the first 24 h of light irradiation, I identified 335 sRNA-mediated mRNA cleavage events in de-etiolating seedlings. These cleavage events are mainly resulted from actions of highly expressed sRNAs and irrelevant to the abundance of target mRNAs. Interestingly, the target mRNAs with cleavage signature identified tend to show down-regulation by light, regardless of the miRNA expression pattern. The expression of the slicer protein gene *ARGONAUTE1* in the miRNA functioning pathway could be tuned down by miRNA168a/b. I also found that miR396a/b positively regulates photomorphogenesis by suppressing *GROWTH REGULATING FACTOR*s. Our results suggest that the sRNAs are required to optimize the target mRNAs and regulate photomorphogenesis. With sRNAs controlling

doi:10.6342/NTU201702588

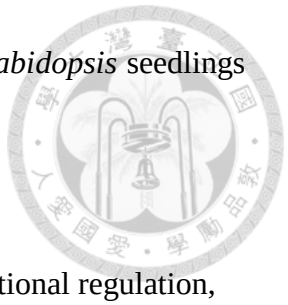

both positive and negative regulators of photomorphogenesis, young *Arabidopsis* seedlings can have a timely but robust development to adapt to light.

Keywords

Light, small regulatory RNA, next-generation sequencing, post-transcriptional regulation, photomorphogenesis

List of abbreviations

sRNA, small regulatory RNA; miRNA or miR, microRNA; siRNA, small interfering RNA; phasiRNAs, phased siRNA; piRNA, Piwi-interacting RNA; *PHAS*, phasiRNA-generating loci; *TAS*, trans-acting siRNA-generating loci; R, red; FR, far-red; B, blue; phy, phytochrome; cry, cryptochrome; HY5, ELONGATED-HYPOCOTYL 5; HYL1, HYPONASTIC LEAVES 1; HEN1, HUA ENHANCER1; HST, HASTY; AGO1, ARGONAUTE1; COP1, CONSTITUTIVE PHOTOMORPHOGENESIS 1; TCP, TEOSINTE BRANCHED 1, CYCLOIDEA AND PCF TRANSCRIPTION FACTOR; GRF, GROWTH REGULATING FACTOR; K-S test, Kolmogorov-Smirnov test; RPM, read per million reads; TE, transposable element; RdDM, RNA-dependent DNA methylation; Aub, Aubergine.

doi:10.6342/NTU201702588

目　錄

doi:10.6342/NTU201702588

List of Figures

doi:10.6342/NTU201702588

List of Tables

doi:10.6342/NTU201702588

Introduction

Plants have evolved a plethora of morphological alterations to adapt to their surroundings. Photomorphogenesis, or de-etiolation, is one such process when seedlings first experience light irradiation. The rate of hypocotyl elongation decreases in seedlings under light exposure, which allows for the formation of firm structural support for seedlings emerging from the soil surface. Also, the cotyledons open and expand to maximize the area of light perception and to expose the shoot apical meristem for the development of true leaves. Light also triggers the development of chloroplasts for photosynthesis so that plants can utilize light energy for autotrophic growth and development [1-3].

In *Arabidopsis*, photomorphogenesis is under the control of at least three types of photoreceptors, including the red (R)–far-red (FR) light photoreceptor phytochromes (phys), blue light (B) photoreceptor cryptochromes (crys) and the UV-B photoreceptor, UVR8 [3-8]. The perceived light signals trigger signaling cascades that reprogram gene expression for photomorphogenic development. Transcriptional profiling for *Arabidopsis* seedlings exposed to B, FR, R light and the light–dark transition have revealed differential expression of approximately one-third of the genome [9]. The light-regulated genome-wide transcriptomic adjustment requires the actions of transcription factors. One of the most well-characterized transcription factors conveying light signals to changes of gene expression is ELONGATED-HYPOCOTYL 5 (HY5). HY5 is a light-regulated bZIP transcription factor that upregulates the expression of many light-responsive genes during de-etiolation [10]. In addition to activating transcription, light also enhances the translational efficiency of thousands of genes, especially those committed to the translation

doi:10.6342/NTU201702588

apparatus and chloroplast functions [11, 12].

Plant small regulatory RNAs (sRNAs) are 20 to 24 nt long and can be classified into microRNAs (miRNAs) and small interfering RNAs (siRNAs) primarily according to different modes of biogenesis. MiRNAs originate from stem-loop structures of primary transcripts, and siRNAs are mostly derived from double-stranded RNAs [13]. Phased siRNAs (phasiRNAs) are a special group of siRNAs generated from mRNAs cleaved by 22-nt miRNAs or siRNAs [14-16]. Plant miRNAs can mediate the cleavage or translation inhibition of target mRNAs, whereas siRNAs function via RNA-dependent DNA methylation (RdDM) for transcriptional gene silencing or post-transcriptional target mRNA cleavage [17-22].

Previous studies have implied that sRNAs are involved in gene expression regulation during de-etiolation. Mutants defective in genes for miRNA biogenesis and functions have altered light responses. For example, in *Arabidopsis*, light hypersensitive phenotypes have been observed to carry mutations in the miRNA processor HYPONASTIC LEAVES 1 (HYL1), the sRNA methyltransferase HUA ENHANCER1 (HEN1), the sRNA transporter HASTY (HST), and the slicer protein ARGONAUTE1 (AGO1) [23-25]. A negative regulator of photomorphogenesis, CONSTITUTIVE PHOTOMORPHOGENESIS 1 (COP1), can protect HYL1 against degradation, thereby leading to a stabilized miRNA pool [26]. Transcripts of the positive regulator HY5 and negative regulator TEOSINTE BRANCHED 1, CYCLOIDEA AND PCF TRANSCRIPTION FACTORs (TCPs) of photomorphogenesis were shown to be under regulation by miR157d and miR319,

doi:10.6342/NTU201702588

respectively [25]. In addition, HY5 was found to bind to promoter regions of at least 8 miRNAs (*MIR*) loci and required for the accumulation of miR156d, miR402, miR408, miR775 and miR858 [27]. These studies provide a glimpse into photomorphogenic development shaped by the actions of a few sRNAs. A global investigation of sRNAs and their targets would greatly help in assessing the impact of post-transcriptional regulation in photomorphogenic development. However, such information is currently missing in de-etiolating seedlings.

In this study, I profiled sRNAs at 6 time points during the first 24 h of *Arabidopsis* photomorphogenic development. I also sequenced 5' ends of degraded mRNAs (degradome) in both dark- and light-grown seedlings to reveal sRNA-mediated cleavage of mRNAs during de-etiolation. Pairwise studies of sRNAs and their target mRNAs indicated that a high sRNA-to-target ratio is a key determinant for successful mRNA target repression by sRNAs. The high ratio is mainly contributed by the abundance of sRNAs. A total of 335 sRNA-target mRNA regulatory pairs were identified in de-etiolating seedlings, with several sRNAs demonstrated to regulate photomorphogenesis. The action of miR168 leads to reduced expression of *AGO1* under light, thereby offering a feedback regulation of miRNA functioning during de-etiolation. miR396 are identified to act as positive regulators of photomorphogenesis. In addition, I revealed that some 24-nt siRNAs had potential to cause target cleavage in de-etiolating seedlings. Our data indicate that sRNAs function in multiple regulatory circuits for optimized seedling growth under light illumination.

doi:10.6342/NTU201702588

Materials and Methods

Plant materials and growth conditions

Seeds of wild-type *Arabidopsis*, Col-0, L*er*, Ws, T-DNA insertion lines SALK_064047 (*mir396a*) and SAIL_1256_F08 (*grf7*) were acquired from stock centers, ABRC or NASC. Homozygous lines of T-DNA insertion lines were screened and confirmed for phenotype observation. The *grf1 grf2 grf3* triple mutant and *35S:MIR396aox* lines were kindly provided by Drs. Jeong Hoe Kim and DiQiu Yu, respectively. For phenotype observation, *Arabidopsis* seeds were surface-sterilized with diluted bleach (Distilled water: bleach = 7:3) and sown on half-strength Murashige and Skoog medium (Duchefa) without supplementing vitamin or sucrose, with 0.8% phyto agar at tissue culture grade (Duchefa, CAS number 9002-18-0). Seeds were stratified (4˚C for 4 days in the dark) to synchronize germination, then exposed to white light for 1 h to stimulate germination, and transferred to different light (W) conditions at 22℃ (Dark, W 12.5 and 50 μE for 4 days). The white light source was a PHILIPS LIFEMAX T-LD 18W/840 T25 cool white tube. Hypocotyl lengths of seedlings were measured by using ImageJ v1.47 [28]. The means and SEM were calculated from the measurements of at least 30 seedlings. At least 3 biological replicates for each line were used for each experiment.

Construction of *MIM396* lines

Primer sequences used in this study are listed in Appendix1. *35S:MIM396* target mimicry lines were generated as described [29]. Briefly, the genomic fragment of *IPS1* was amplified by using the iProof High-fidelity PCR kit (Bio-Rad) and cloned into the pGEMT-easy vector (Promega). The miR399 target site on original *IPS1* sequence was

doi:10.6342/NTU201702588

modified to sequester miR396a/b, as shown in Fig. 8a, by overlapping PCR during construction [29]. All constructs were then subcloned into the pCambia-1390 binary vector (CSIRO) digested with *Sal*I and *Sac*I. The constructs were transformed into *Agrobacterium tumefaciens* GV3101 strain, and introduced into *Arabidopsis* Col-0 by floral dipping. Two independent homozygous transgenic lines per construct were used for further analyses.

RNA sequencing and data analyses

For sRNA sequencing and data analyses, 4-d-old dark-grown *Arabidopsis* Col-0 seedlings were exposed to white light (100 μE) for 1, 3, 6, 12 and 24 h. The aerial tissues of approximately 5000 seedlings were collected for RNA isolation, with one biological replicate collected by Dr. Huang-Lung Tsai and 2 biological replicates collected by myself. Ten to 15 μg total RNA was size fractionated on 15% Tris-Borate-EDTA-Urea gel. sRNAs ranging from 17–30 nucleotides were gel-purified and used for cDNA library construction (Illumina Truseq for replicates 1 and 2, Small RNA v1.5 for replicates 3) and sequencing with the use of an Illumina HiSeq 2500. Twelve barcoded samples were sequenced in one single flowcell (a total of 240 M reads output per flowcell) at a read length of 50 nt. The adaptor-trimmed reads with size ≥ 18 nt were mapped to the *Arabidopsis* TAIR10 genome by using Bowtie [30] with the parameters -f –n 0 –e 80 –l 18 –a –m 5 –best –strata. For miRNA profiling, reads that perfectly matched to mature miRNA sequences were counted, normalized to total mapped reads of 20–24 nt and were shown as reads per million reads (RPM). Reads that mapped to miRNA families (e.g., miR156) were weighted by dividing the read count and equally assigning to each miRNA family member. For siRNA quantification, the Bowtie parameters were -f –n 0 –e 80 –l 18 –a –v 2 –best –strata with

doi:10.6342/NTU201702588

the aid of Dr. Sim-Lin Lim for filtering out known miRNAs. For phasiRNAs, the prediction of *PHAS* loci involved use of the UEA sRNA Workbench [31]. In brief, adaptor-trimmed reads longer than 16 nt were mapped to the TAIR10 genome, and the 21-nt phasing register was set to detect phasing within a 251-nt window, based on hypergeometric distributions described previously [14]. Among the uniquely mapped miRNA/siRNAs, only those with read counts ≥ 5 in ≥ 1 time point for all 3 biological replicates were considered expressed. Light-regulated sRNAs were defined as sRNAs with $p < 0.05$ on Student's t-test compared to dark treatment (W0h) for all 3 biological replicates. For mRNA transcriptome analysis, the RPKM for sRNA target genes were analyzed by using datasets published previously [12]. Potential targets included those predicted by use of psRNATarget [32] (with UPE = 25, expectation = 3), miRNA targets identified in previous studies [25, 33] and miRNA targets detected in our degradome analysis (see Table 6 for the number of targets). Expressed genes had RPKM > 0.01 in at least one time point in both biological replicates. The transcript levels of target genes with degradome signatures are in Tables 6 and 7.

For degradome sequencing, 100 μg total RNA was isolated from 4-d-old dark-grown seedlings and mixtures of 4-d-old dark-grown seedlings exposed to 1, 3, 6, 12 and 24 h of light. Degradome sequencing was performed as described [34-36]. Putative cleavage sites were identified by using Cleaveland v4.4.3 [37, 38]. Those with CleaveLand category ≤ 2, $p \leq 0.05$ and at least 5 reads at the predicted cleavage site were reported as valid targeting events.

doi:10.6342/NTU201702588

Northern blot analysis and qRT-PCR

In total, 20 to 50 μg total RNA was separated on 15% TBE-Urea gel (Invitrogen). SYBR-Gold (Life Technologies) was used for visualizing RNAs on gels. RNAs were then transferred to Hybond-N+ Nylon membrane (GE Healthcare), by using Transblot SD Semi-Dry Transfer Cell (Bio-Rad) and hybridized with γ-^{32}P-labeled miRNA probes as indicated at 37°C overnight in UltraHyb Oligo buffer (Ambion). Hybridized blots were washed and exposed to Phosphoimager (GE Healthcare), then analyzed by using Typhoon FLA 7000 (GE Healthcare Life Sciences), as described [14]. Images were quantified by using ImageJ v1.47 [28]. For qRT-PCR, cDNA was synthesized from 2 μg total RNA from 4-d-old de-etiolating *Arabidopsis* seedlings. The SuperScript II RT kit (Invitrogen) was used for reverse transcription of mRNA. For qRT-PCR, cDNA with 0.25 ng equivalence of mRNA was used as a template for each sample. PCR amplification and detection was as described [39]. Primers are in Appendix 1.

doi:10.6342/NTU201702588

Results

The expression and actions of small RNAs in de-etiolating *Arabidopsis* seedlings

I first used deep sequencing to survey the sRNAs in de-etiolating *Arabidopsis* seedlings. The sRNAs were isolated from 4-d-old dark-grown (W0h) seedlings and seedlings that were further treated with continuous white light irradiation for 1 to 24 h (W1h to W24h) and subjected to deep sequencing (Fig. 1). Approximately 18-22 million reads were obtained for each sample in 3 biological replicates. For each dataset, 94–98% of the filtered reads (see methods) could be mapped to the TAIR10 genome (Table 1). I first analyzed miRNAs and phasiRNAs, as they are frequently studied groups of plant sRNAs. Among the 427 *Arabidopsis* miRNAs annotated in miRBase 21 [40], 207 (48.5%) are considered expressed (see methods for criteria) (Table 2). Overall 58 phasiRNAs derived from 12 phasiRNA-generating loci (*PHAS*, or trans-acting siRNA-generating loci, *TAS*) [14] were expressed in de-etiolating seedlings (Table 3 and 4). In addition to miRNAs and phasiRNAs, 4,255 20–24 nt siRNAs were defined expressed in this developmental stage (Table 5).

Since both miRNAs and siRNAs can target mRNAs for cleavage [19, 41-43], I aimed to identify sRNA–target pairs that may be involved in photomorphogenic development. I performed degradome sequencing followed by CleaveLand analyses [38] to identify target mRNAs cleaved by expressed sRNAs in de-etiolating seedlings. The degraded mRNA samples were obtained from seedlings grown under dark (W0h) or light (equally mixed from samples treated with W for 1, 3, 6, 12 and 24 h). Approximately 50 million reads for each of the libraries were obtained; 81–85% could be mapped to TAIR10 cDNAs (Table 1). Our analyses suggested that 262 non-redundant sRNAs could mediate the cleavage of 306 *Arabidopsis* mRNAs (a total of 335 target cleavage sites). Among them, 142 cleavage

doi:10.6342/NTU201702588

events were mediated by miRNAs, 13 by phasiRNAs and 180 by other siRNAs (Fig. 1; Table 6 and 7). These newly identified sRNA-target pairs are potential players in post-transcriptional gene regulation in *Arabidopsis* photomorphogenesis.

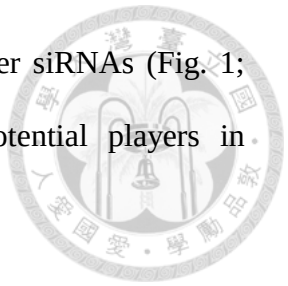

sRNA abundance determines the likelihood of target mRNA cleavage

When analyzing the mRNA degradomes, I noticed that although 90 miRNA families were expressed in de-etiolating seedlings (Table 2), target cleavage was detected for only members of 49 miRNA families (Table 6). The results prompted us to investigate factors affecting target cleavage or the identification of degradome signatures. Previous reports have shown that high target abundance compromised the repression activity of miRNAs and siRNAs when introduced via transfection in animal cell lines [44]. A computational model based on fixed concentration of miRNAs and mRNAs implicated that the concentration of miRNAs has a greater effect on miRNA-mRNA interaction in *Drosophila melanogaster* and in human [45]. In contrast to the seed pairing seen in most animal miRNA-mRNA interactions, most plant miRNAs interact with their target mRNAs at high complementarity that leads to cleavage of target mRNAs [19]. The availability of transcriptome data for mRNAs [12], sRNAs and degradome signatures in this study allowed us to investigate whether miRNAs/siRNAs or target abundance is important for effective miRNA/siRNA-mediated target cleavage in de-etiolating *Arabidopsis* seedlings.

Our analysis indicated that miRNAs causing target cleavage tended to have higher abundance, as compared with miRNAs that failed to generate detectable target degradome signatures (Fig. 2a). The results were similar for miRNAs expressed in both the dark ($p=5.2\times10^{-8}$, D = 0.4327 in Kolmogorov-Smirnov test, K-S test) and light ($p=3.0\times10^{-8}$, D =

doi:10.6342/NTU201702588

0.4394, K-S test) (Fig. 2a). In contrast, for mRNAs with miRNA target sites, the transcript abundance was comparable for mRNAs with or without degradome signatures identified (Fig. 2b). Pair-wise examination of miRNA-to-target ratios revealed relatively higher ratios for miRNA-mRNA pairs with observed cleavage under both dark ($p=1.3\times10^{-12}$, D = 0.4108, K-S test) and light ($p=2.5\times10^{-12}$, D = 0.4067, K-S test) (Fig. 2c). Therefore, miRNAs with high abundance may give rise to high miRNA-to-target ratios, thereby leading to successful target mRNA cleavage.

The above notion remains true when applied to siRNA-mediated mRNA cleavage (Fig. 3), although not as significant as for miRNAs (Fig. 2a). Among the 4,255 expressed siRNAs, only 180 have degradome signatures identified for their target mRNAs (Table 7), as compared with 155 targets resulting from 265 miRNA/phasiRNA-mediated cleavages (Table 6), possibly because of the significantly lower expression of most siRNAs than miRNAs (Fig. 2d).

Although the expression of most of the miRNAs remained unchanged before and after light treatment, light appears to down-regulate the expression of target mRNAs with degradome signatures but not that of mRNAs without evidence of cleavage (Fig. 2e). Therefore, instead of regulating miRNA expression, light signals may potentiate the target-cleavage activities of miRNAs to tune down the expression of their target genes during de-etiolation. Whether this reduction is achieved by regulating the expression or enzymatic activities of slicer complexes remains to be investigated.

doi:10.6342/NTU201702588

Light optimizes miRNA functioning via the action of miR168

Previously, we reported a feedback regulation between *HY5* and *HEN1*, which indicates that an sRNA equilibrium is required during photomorphogenic development [25]. Here, I sought to identify whether light regulates steps in sRNA biogenesis and functioning in addition to *HEN1*. In *Arabidopsis*, miR168 targets the sRNA slicer gene *AGO1* [46]. Deep sequencing and Northern blot results indicated that the expression pattern of miR168 only slightly fluctuated under light (Fig. 4a, b). However, the mean abundance of miR168a/b ranged from 880 to 1270 read per million reads (RPM) (Table 2), which is more than 10 times greater than the median level of miRNAs overall (Fig. 2a). Thus, miR168a/b has high potential in mediating the cleavage of *AGO1* transcript. Indeed, under light, *AGO1* cleavage signatures could be detected (Table 6), which led to the down-regulation of *AGO1* (Fig. 4c). The detection of *AGO1* cleavage signature only under light is also consistent with preferential light-mediated downregulation of miRNA target mRNAs (Fig. 2e). Thus, miR168a/b have potential to desensitize the sRNA actions by targeting *AGO1* for degradation during photomorphogenesis.

Light regulates the expression of some miRNAs and phasiRNAs

Although most miRNA levels were unchanged before and after light treatment in young *Arabidopsis* seedlings (Fig. 2d; Table 2), I still observed that 32% (67 of 207) of expressed miRNAs were regulated by light (Fig. 4; Table 8). Only 8 of 58 expressed phasiRNAs were differentially regulated by light (Table 4). Because sRNA abundance is a major determinant for target cleavage in seedlings (Fig. 2), any changes in sRNA levels under light may alter their target suppression capacity. Thus, the light regulation of miRNAs and phasiRNAs

doi:10.6342/NTU201702588

may provide a timely control of target mRNAs to shape photomorphogenic development. The light responsiveness of the 67 light-regulated miRNAs could be classified into 3 major clusters by k-mean clustering (Fig. 5; Table 2). miR163 belongs to cluster I, whose expression is barely detectable in the dark but is rapidly induced by light. miR163 has been shown to promote seed germination and primary root growth during early seedling development, but not involved in light-induced inhibition of hypocotyl elongation [47]. Cluster II miRNAs are also upregulated by light, and the up regulation is more prominent after prolonged light exposure. The miRNAs in cluster II include miR157d, reported to target *HY5* during photomorphogenic development [25]. The miRNAs in cluster III were down regulated by light, especially after 6-h light exposure.

miR396 promote photomorphogenesis by tuning *GRF* levels

In de-etiolating seedlings, the degradome signatures were most frequently found for mRNAs targeted by members in the miR156/157 and miR396 families (Fig. 6a). miR157d directly targets *HY5* to desensitize the light signals during photomorphogenesis [25], but the functions of miR396 in photomorphogenic development remain obscure.

The expression of miR396 was slightly decreased upon light treatment (Fig. 6b and 6c). miR396 can target 7 *GROWTH REGULATING FACTOR*s (*GRF*s) [33, 48], and the cleaved signatures of all 7 *GRF*s were detected in our degradome analysis (Table 6). *GRF1*, *GRF2*, *GRF3* and *GRF7* showed relatively higher degradome signature reads amongst the *GRF*s (Fig. 6d), and all showed clear down regulation under light (Fig. 6e). *GRF1*, *GRF2* and *GRF3* cooperatively regulate leaf and cotyledon development [49], whereas *GRF7* is a transcriptional repressor of abscisic acid and osmotic stress-responsive genes [50].

doi:10.6342/NTU201702588

However, their functions in photomorphogenesis remain unknown.

To assay the regulatory roles of miR396–*GRF* pairs in photomorphogenesis, I first isolated and analyzed the *mir396a* single mutant (SALK_064047; Fig. 7a). Although overall miR396 levels were reduced, the phenotypes of the *mir396a* mutant were indistinguishable from that of the wild type under dark or light (Fig. 7a and b). Possibly, the residual amount of miR396b in *mir396a* is sufficient for normal seedling development (Fig. 7a).

Because both miR396a and miR396b can suppress *GRFs* [48], I generated target mimicry lines (*MIM396*) to sequester these two miRNAs (Fig. 8a). The levels of *GRF1*, *GRF2*, *GRF3* and *GRF7* were indeed increased in two independent *MIM396* lines (Fig. 8a). The *MIM396* lines showed elongated hypocotyl length under 50 μE white light (Fig. 8b), which suggests that functional miR396 can positively regulate photomorphogenesis. I also examined the hypocotyl lengths of the *MIR396A* overexpression line (*MIR396Aox*) [48] and found that light sensitivity was not further exaggerated (Fig 7c and d), so the endogenous miR396 pool may be at a saturated level for its functions in light responses.

To further understand the mechanistic roles of miR396 in photomorphogenesis, I examined the hypocotyl lengths of *grf1 grf2 grf3* and *grf7* mutants. Compared to wild-type Ws, the *grf1 grf2 grf3* triple mutant showed short hypocotyl under 50 μE white light, which indicates that the three *GRF*s act as negative regulators of photomorphogenesis. In contrast, *grf7* showed a short hypocotyl only under dark (Fig. 8c). Together with the quick repression of *GRF7* expression by light (Fig. 6e), the major function of *GRF7* is likely to promote hypocotyl elongation under dark. In sum, miR396 can act as a positive regulator of hypocotyl elongation by suppressing the negative regulator *GRF*s.

Varied length and target properties of siRNAs in *Arabidopsis* seedlings

doi:10.6342/NTU201702588

Among the expressed siRNAs in de-etiolating seedlings, 164 are capable of mediating target cleavage (Table 7). Among them, 70 (> 40%) are 24 nt long (Fig. 9a), which is quite different from the typical 21- or 22-nt miRNAs/phasiRNAs that mediate target mRNA cleavage [14, 19, 51]. Most target genes with degradome signatures for both miRNAs/phaiRNAs and siRNAs are protein coding genes (Fig. 9b). Intriguingly, 30 cleavage events from the actions of siRNAs were identified from 18 transposable elements (TEs), which is significantly higher than the number targeted by miRNAs/phasiRNAs ($p = 3.2 \times 10^{-3}$ by Fisher's exact test). Most siRNA-targeted transposons are in the gypsy-like retrotransposon and CACTA-like transposase family. Eleven sRNAs that mediate TE mRNA cleavage are also derived from annotated TEs, with 4 sRNAs derived from their target loci (Table 7), so these TEs may be capable of self-suppressing through TE-derived siRNAs and self-targeted cleavage. Among the 30 cleavage events derived from TE mRNAs, 23 potentially resulted from cleavage mediated by 24-nt siRNAs. The 24-nt siRNAs derived from transposable elements can mediate silencing of their original transposable elements via RNA-dependent DNA methylation (RdDM) [17, 18]. Our results suggest that in addition to RdDM, siRNA-mediated cleavage may function as an additional mechanism to prevent TE mRNA accumulation, which may escape from incomplete RdDM.

doi:10.6342/NTU201702588

Discussion and future perspectives

Light regulates miRNA-target pairs in photomorphogenic development

In addition to the previously discovered miR157d–HY5 and miR319–TCP pairs [25], I found additional miRNA–target pairs that positively regulate photomorphogenesis. In this study, miR168 could tune down *AGO1* level under light (Fig. 4), which can counteract the actions of sRNAs stabilized by the light-induced *HEN1* expression. miR396 can act as positive regulators of photomorphogenesis by suppressing *GRF1*, *GRF2*, *GRF3* and *GRF7*. The *grf7* mutant shows shorter hypocotyl length under dark, so it may positively regulate hypocotyl elongation under dark. Under light conditions, the *grf7* mutant phenotype is comparable to that of the wild type possibly because light also markedly represses *GRF7* expression (Fig. 6e, Table 9).

I cannot rule out that light down-regulates the expression of *GRFs* at the transcriptional level. However, the detection of the miR396-mediated cleavage events on *GRFs* (Fig. 6, Table 6) suggested that miR396 indeed functions to optimize the *GRF* mRNA levels during de-etiolation. GRFs are known as transcription activators [52]; hence, future investigation of GRF downstream genes will help demystify genes regulated by the miR396-*GRF* lineage and provide a future research direction for their contribution in photomorphogenic development.

sRNAs regulate photomorphogenesis from multiple angles

Our results in Fig. 2 and 3 showed that abundant sRNAs have a better likelihood of mediating target mRNA cleavage during photomorphogenic development. Also, despite no negative correlation between the expression of miR168/miR396 and their target mRNAs

doi:10.6342/NTU201702588

(Fig. 4 and 6), degradome signatures from their target mRNAs were observed (Table 6, Fig. 6). This finding indicated that although light only slightly affect the accumulation of miR168 and miR396, these miRNAs can contribute to the expression repression of their target mRNAs in de-etiolating seedlings. The steady-state mRNA transcriptome during photomorphogenic growth likely is a finely orchestrated balance between the well-studied transcriptional regulation by light signals and target mRNA cleavage mediated by small regulatory RNAs as examples shown in this study.

Combined with our previous [25] and current discovery, sRNAs could fine-tune the expression of both positive (*HY5*) and negative (*TCPs*, *AGO1*, *GRF*s) regulators of photomorphogenesis (Fig. 10). Clearly, as key regulators of these complex and interlocked regulatory circuits, the whole plethora of sRNAs is crucial for an optimal transcriptome during photomorphogenesis. This observation also explains why mutations of single *MIR* or target gene usually show less prominent phenotypic changes (Fig. 8), as compared with mutants with a defective miRNA pathway [23-25, 42, 53-56]. I have observed a considerable amount of degradome signatures that were predicted to be results of siRNA-mediated mRNA cleavage. This suggests that, in addition to miRNAs, siRNAs also contribute considerably to down regulate their target mRNAs in de-etiolating seedlings. Further investigation of the miRNA- and siRNA-target pairs will continue to shed light on post-transcriptional regulation of photomorphogenic growth.

Finally, our observation suggests that siRNA-mediated TE mRNA cleavage may serve as an additional mode of TE silencing (Fig. 9). In *Arabidopsis*, TE mRNAs could also be cleaved by miR859 [57] and a tRNA-derived small RNA via the association with AGO1 in pollens [58]. In *Drosophila* germ cells, Piwi-interacting RNAs (piRNAs) can interact

doi:10.6342/NTU201702588

with Aubergine (Aub) or AGO3 for the cleavage of TE mRNAs [59, 60]. It remains to be clarified with which AGO protein(s) siRNAs interact for silencing plant TE mRNAs.

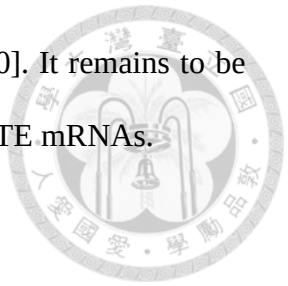

Conclusions

Photomorphogenesis is a coordinated result of gene expression regulation at multiple levels. Our analyses revealed multiple sRNA–mRNA pairs contributing to this important development process. I also confirmed a comprehensive impact of sRNAs on regulating post-transcriptional gene expression during de-etiolation in *Arabidopsis*. sRNAs target multiple positive and negative regulators of photomorphogenesis, offering sophisticated fine-tuning power for regulating gene expression during de-etiolation. The potency of an sRNA in target cleavage is primarily determined by its abundance, adding an extra regulation dimension in addition to target recognition

.

doi:10.6342/NTU201702588

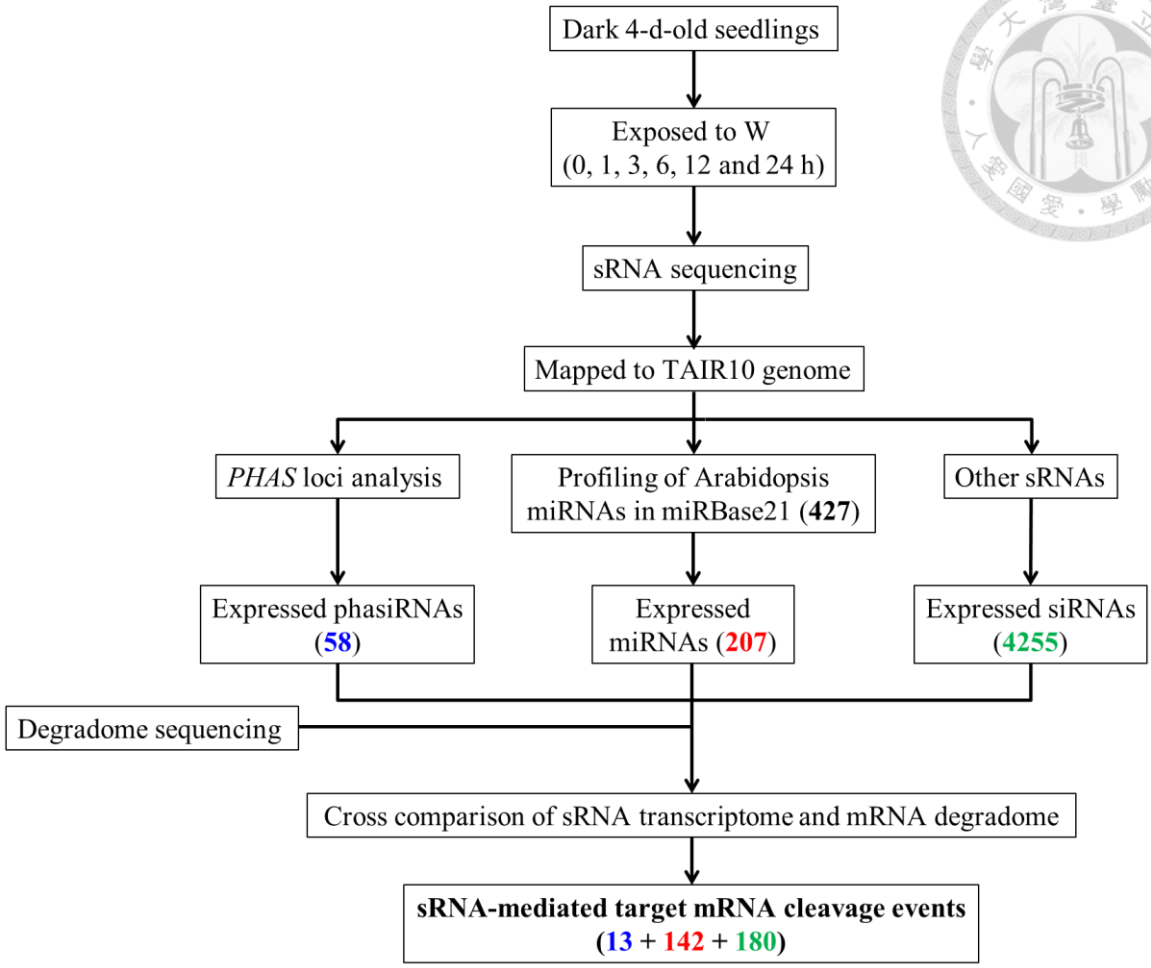

Fig. 1 Pipeline for investigating sRNA-mediated regulation in de-etiolating *Arabidopsis* seedlings.

Four-d-old dark-grown seedlings (W0h) were exposed to continuous white light (W; 100 μE) for 1, 3, 6, 12 and 24 h; 18 – 22 million (M) reads per library were acquired. Degradome sequencing for dark- (Dark) and light- (equally pooled from the five light-treated time points) grown seedlings were used for identifying sRNA-mediated cleavage of target mRNA. sRNAs with read ≥ 5 in ≥ 1 time point for all three biological replicates were defined as expressed siRNA. Colored numbers in parentheses indicate the number of sRNAs/targets passing the corresponding filtering criteria.

doi:10.6342/NTU201702588

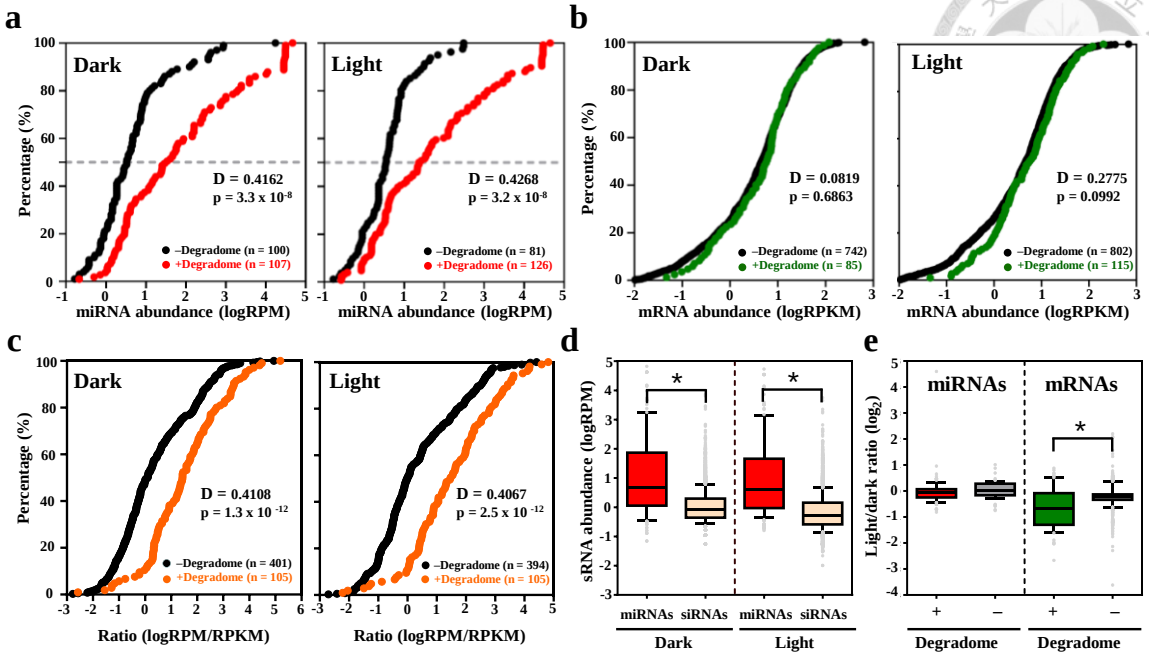

Fig. 2 The miRNA abundance, rather than target mRNA abundance, is the major determinant of target cleavage.

a miRNAs causing target cleavage tend to have higher abundance. Kolmogorov-Smirnov (KS) plot showing the abundance of expressed miRNAs in dark and light (W3h). + Degradome (red) indicates miRNAs with valid target cleavages identified; - degradome (black) indicates expressed miRNAs without target cleavage identified. Dashed lines indicate 50th percentile of sRNAs. **b** Target mRNA abundance was relatively unchanged regardless of being cleaved. KS plot showing the abundance of target mRNA with (green) or without (black) degradome signatures under dark or light (W4h). Only expressed target genes with RPKM > 0.01 were plotted. **c** Degradome signatures were preferentially detected in mRNAs with high miRNA-to-target ratios. KS plot showing distribution of pairwise miRNA-to-target ratios in dark and light (W3h/W4h). + Degradome (orange) indicates miRNA–target pairs with target cleavage validated; - degradome (black) indicates miRNA–target pairs without target cleavage validated. **d** The abundance is relatively lower

doi:10.6342/NTU201702588

for siRNAs than expressed miRNAs. **e** Target mRNAs, but not miRNAs, are downregulated by light. Light/dark ratios indicate the relative levels of miRNAs (W3h/W0h) and mRNAs (W4h/W0h). + and – degradome indicate miRNAs/targets with or without identified degradome signatures, respectively. Data are the mean of all biological replicates (three replicates for sRNAs and two for mRNAs). * $p < 0.01$ by Student's t-test. The bottom, middle, and top of the box represent the 25^{th}, 50^{th}, and 75^{th} percentiles, and whiskers are the 10^{th} and 90^{th} percentiles, respectively.

doi:10.6342/NTU201702588

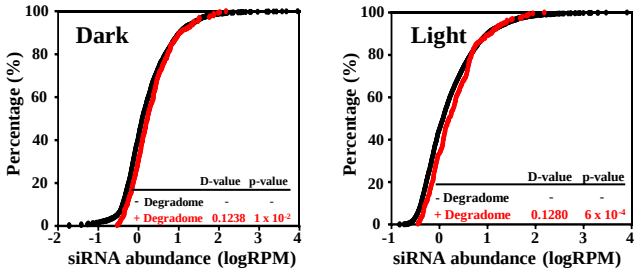

Fig. 3 miRNAs/siRNAs with target cleavage capability tend to be more abundant than miRNAs/siRNAs that did not show target cleavage signatures.

KS plot showing distribution of siRNAs. + Degradome (red) indicates sRNA with target mRNA signature identified; - degradome indicates expressed siRNAs without target signature identified in de-etiolating seedlings. Data are calculated from average of three biological replicates. p-values and D-values were calculated from KS test.

doi:10.6342/NTU201702588

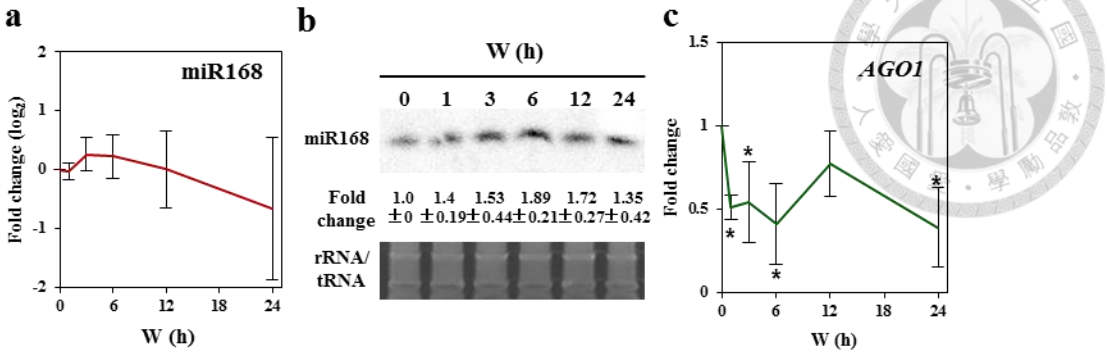

Fig. 4 The expression of miR168 and *AGO1* in de-etiolating *Arabidopsis*.

a Expression pattern of miR168. Data are mean ± SD from three biological replicates of sRNA sequencing. **b** Northern blot analysis of miR168 level during the times examined. The values of mean ± SD are calculated from three biological replicates. SYBR-gold stained rRNA/tRNA was a loading control. **c** Light down regulates *AGO1*. qRT-PCR results were shown as mean ± SD calculated from three biological replicates. Asterisks indicate $p < 0.01$ in Student's t-test.

doi:10.6342/NTU201702588

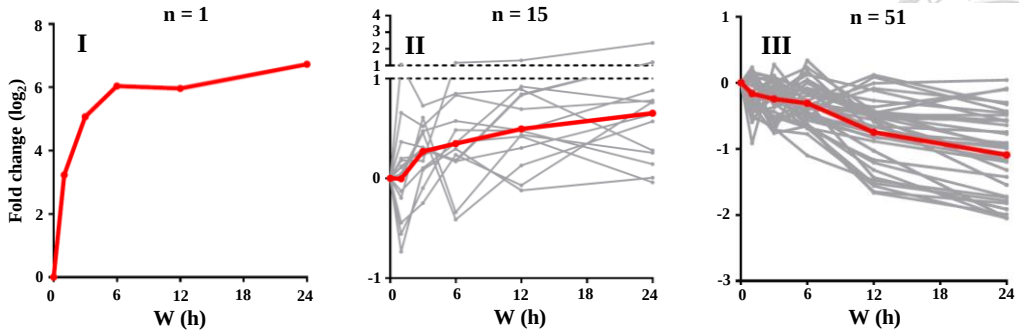

Fig. 5 Clustering analysis of light-regulated miRNAs.

Student's t-test was performed to identify miRNAs with significant fold changes against dark (W0h) in all three replicates. The expression patterns of miRNAs in response to light treatments were classified into three clusters by use of k-mean clustering (by Euclidean distance). Gray lines indicate the average fold change of each miRNA from three biological replicates; red lines indicate average fold changes within the cluster.

doi:10.6342/NTU201702588

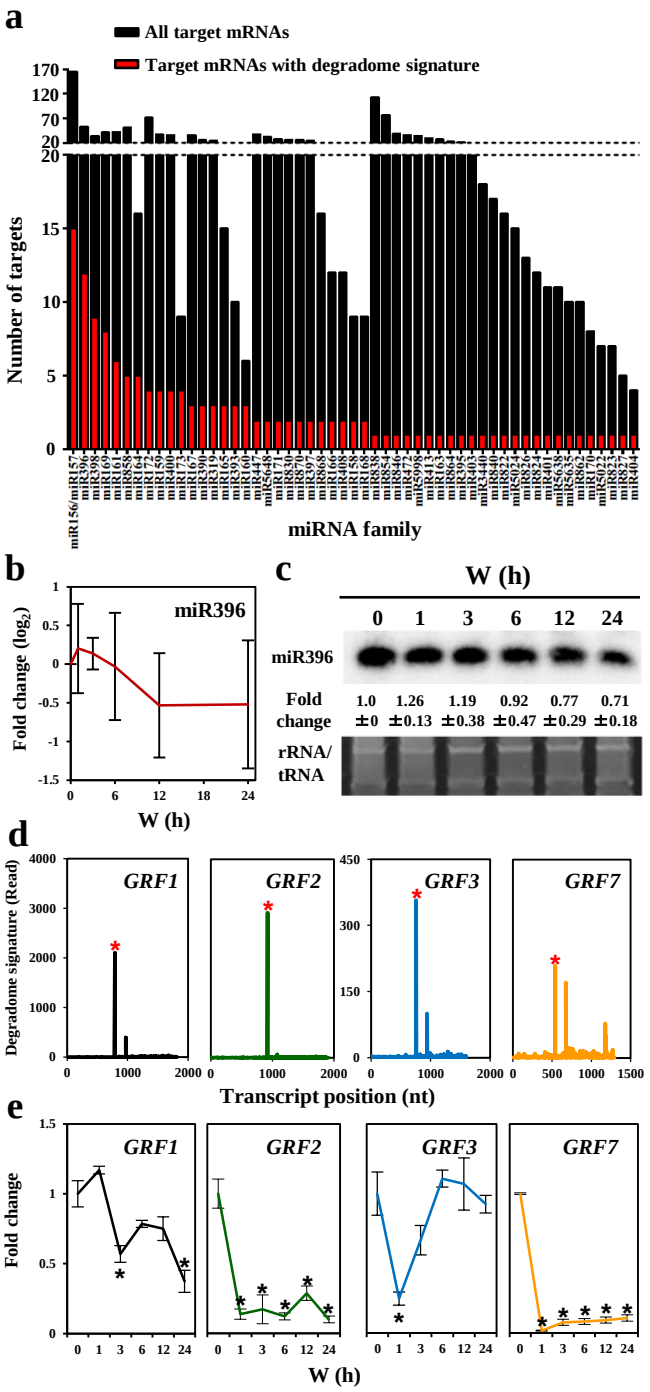

Fig. 6 miRNA families with valid targets and the expression patterns of miR396–*GRF* regulatory pairs in de-etiolating seedlings. a Expressed miRNA families with predicted (black) or valid (red) target cleavages in de-etiolating *Arabidopsis*. **b** Expression of miR396

doi:10.6342/NTU201702588

is transiently upregulated and gradually decreased on W exposure. Data are mean ± SD from three biological replicates of sRNA sequencing. **c** Northern blot analyses confirmed the expression of miR396 in de-etiolating *Arabidopsis*. One representative gel image is shown. Data are mean ± SD for the relative expression from three biological replicates. SYBR-Gold-stained rRNA/tRNA was a loading control. **d** Degradome T-plot marked the miR396-mediated *GRF1/GRF2/GRF3/GRF7* mRNA cleavage in de-etiolating seedlings. Red asterisks indicate the degradome signatures detected at expected miR396-guided cleavage sites for *GRF1*, *GRF2*, *GRF3* and *GRF7*. **e** Light regulation of *GRF1*, *GRF2*, *GRF3* and *GRF7*. Data are mean ± SD from three technical replicates of one representative qRT-PCR experiment. * $p < 0.01$ in Student's t-test. Three biological replicates were performed with similar results.

doi:10.6342/NTU201702588

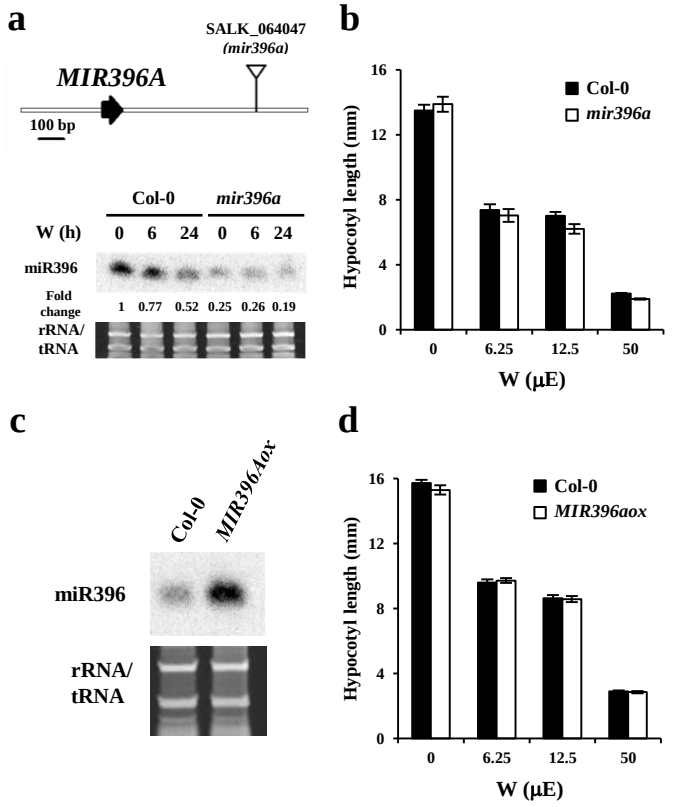

Fig. 7 Molecular and phenotypic analyses of *mir396a* mutant and *MIR396aox* lines. a Illustration of T-DNA insertion site and the confirmation of reduced miR396 levels in *mir396a* (SALK_064047). **b** Comparable hypocotyl lengths between *mir396a* mutant and wild-type *Arabidopsis* under both dark and W conditions. One representative result is shown, n ≥ 30. Three biological replicates were performed with similar results. **c** Northern blot analysis of confirmed overexpression of miR396 in *MIR396aox* line. Four-d-old dark-grown seedlings were used for RNA isolation. SYBR-Gold stained rRNA/tRNA was a loading control. **d** Comparable hypocotyl lengths between *MIR396aox* line and wild-type *Arabidopsis* under dark and W conditions. One representative result is shown, n ≥ 30. Three biological replicates were performed with similar results.

doi:10.6342/NTU201702588

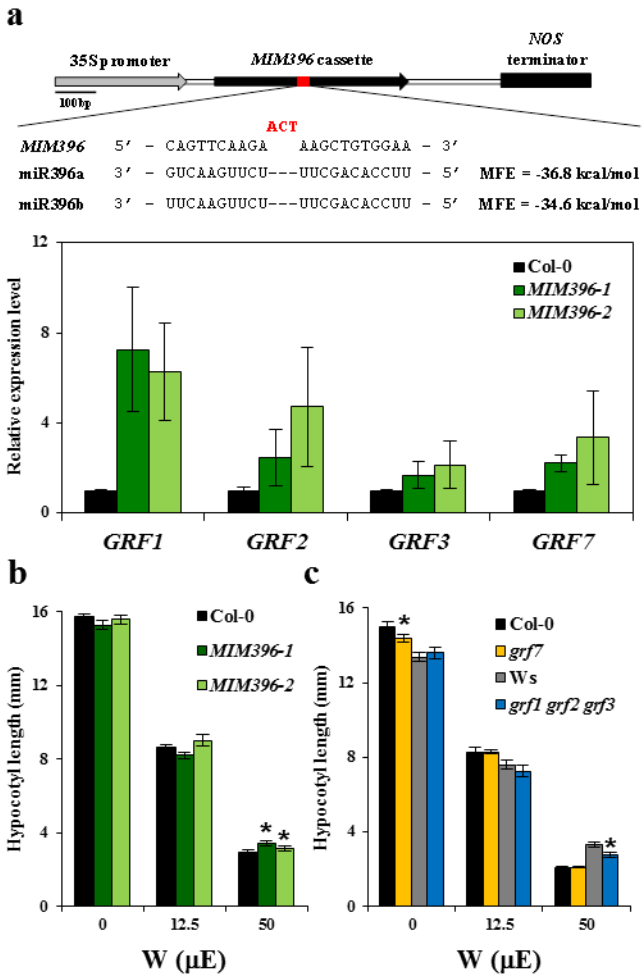

Fig. 8 miR396 positively regulate photomorphogenesis by suppressing *GRF* levels.

a Illustration of the *35S:MIM396* (*MIM396*) target mimicry construct. The nucleotides generating a bulge at the miR396 target site is highlighted in red. Minimum free energy (MFE) for *MIM396* binding to miR396a and miR396b was calculated by RNAHybrid. The expression of *GRF1*, *GRF2*, *GRF3* and *GRF7* is increased in the two independent *MIM396* T_4 lines. Data are mean ± SD calculated from three biological replicates. **b** The *MIM396* T_4 homozygous lines show long hypocotyl length under W at 50 µE. Data are mean ± SE of hypocotyl length for one representative result. * $p < 0.01$ by Student's t-test, $n \geq 30$. Three biological replicates were performed with similar results. **c** The *grf1 grf2 grf3* triple

doi:10.6342/NTU201702588

mutant and the *grf7* single mutant shows shorter hypocotyl than their corresponding wild types, Ws and Col-0, under W and dark conditions, respectively. * $p < 0.01$ by Student's t-test, $n \geq 30$. Data are one representative result from three biological replicates performed with similar results.

doi:10.6342/NTU201702588

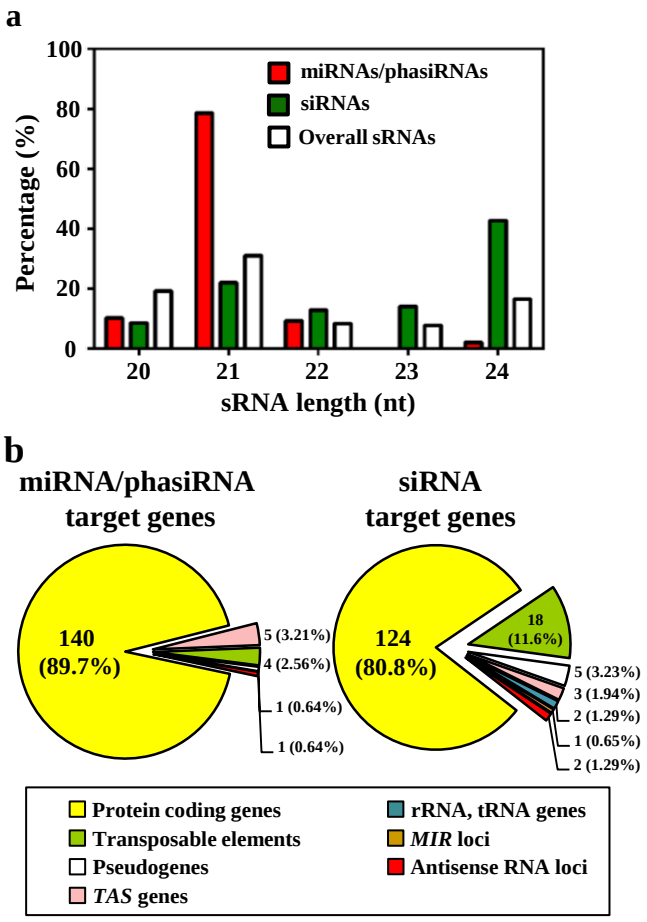

Fig. 9 siRNA sizes and target gene features in de-etiolating seedlings.

a Length distribution of sRNAs with targeted cleavage signatures identified (red and green).

b Categorization of mRNAs with distinct degradome signatures from targeted cleavage by miRNAs/phasiRNAs or siRNAs.

doi:10.6342/NTU201702588

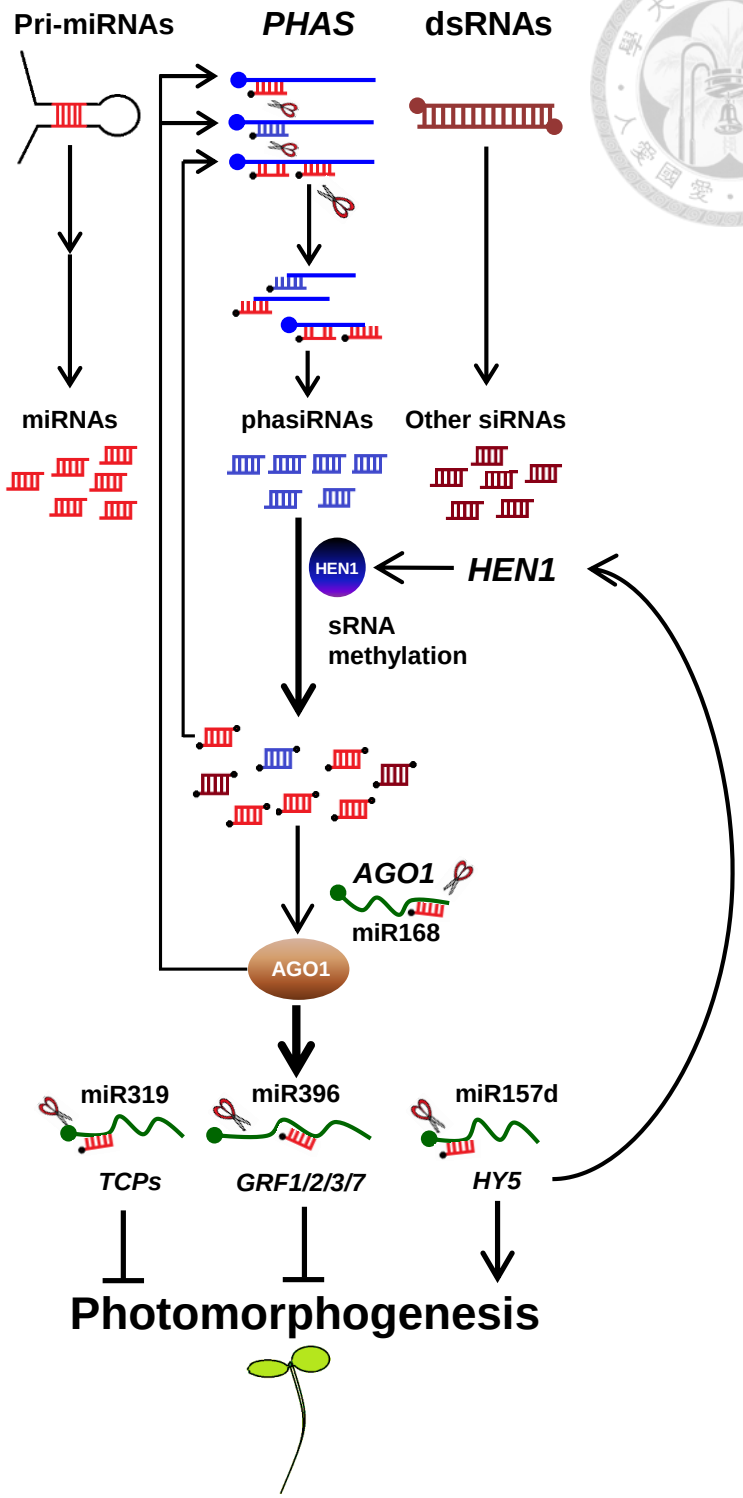

Fig. 10 A proposed model for sRNA-mediated gene expression regulation during photomorphogenesis.

doi:10.6342/NTU201702588

Table 1. Sequencing and mapping statistics.

		Total filtered reads	Mapped to TAIR10 (%)
sRNA sequencing	**W 0h_r1**	18439145	18146072 (98.41)
	W 0h_r2	18682024	18407313 (98.53)
	W 0h_r3	18560002	17639306 (95.04)
	W 1h_r1	19412255	19087424 (98.32)
	W 1h_r2	18390959	18093486 (98.38)
	W 1h_r3	19753930	18932617 (95.84)
	W 3h_r1	18188712	17660361 (97.10)
	W 3h_r2	19877564	19435501 (97.76)
	W 3h_r3	21973959	20906003 (95.14)
	W 6h_r1	20113158	19665226 (97.77)
	W 6h_r2	18960873	18661473 (98.42)
	W 6h_r3	20580490	19454549 (94.53)
	W 12h_r1	18936937	18202597 (96.12)
	W12h_r2	19319775	18822788 (97.43)
	W 12h_r3	18720032	17579785 (93.91)
	W 24h_r1	18322471	17887523 (97.63)
	W 24h_r2	21824208	21516866 (98.59)
	W 24h_r3	19769062	18906022 (95.63)
Degradome sequencing	**Dark (W0h)**	59810548	48766970 (81.54)
	Light*	54268999	46178774 (85.09)

*: RNA sample mixed from W1h, W3h, W6h, W12h and W24h.

The total filtered reads indicate the reads ≥ 15 nt after adaptor removal.

r1, r2 and r3 indicate 3 biological replicates.

doi:10.6342/NTU201702588

Table 2. Expressed miRNAs in de-etiolating Arabidopsis seedlings. Average read per million reads (RPM) from three biological replicates were listed.

			Averaged RPM						Averaged fold change					
miRNA family	miRNA	Sequence	W0h	W1h	W3h	W6h	W12h	W24h	W0h	W1h	W3h	W6h	W12h	W24h
miR156	ath-miR156a-3p	GCUCACUGCUCUUUCUGUCAGA	2.05	2.47	3.98	2.21	4.30	4.77	1.00	1.29	2.11	1.18	2.55	2.33
	ath-miR156a-5p	UGACAGAAGAGAGUGAGCAC	28417.76	27105.62	27623.22	25733.96	23309.12	23513.08	1.00	0.88	0.94	0.87	0.67	0.58
	ath-miR156b-5p	UGACAGAAGAGAGUGAGCAC	29604.64	28227.97	28786.09	26963.36	24248.38	24407.60	1.00	0.89	0.93	0.88	0.67	0.58
	ath-miR156b-3p	UGCUCACCUCUCUUUCUGUCAGU	2.33	2.68	3.18	1.54	2.63	3.17	1.00	1.13	1.35	0.67	1.16	1.36
	ath-miR156c-5p	UGACAGAAGAGAGUGAGCAC	28417.76	27105.62	27623.22	25733.96	23309.12	23513.08	1.00	0.88	0.94	0.87	0.67	0.58
	ath-miR156c-3p	GCUCACUGCUCUAUCUGUCAGA	14.92	17.63	20.70	14.01	20.09	20.81	1.00	1.08	1.38	0.83	1.18	1.54
	ath-miR156d-5p	UGACAGAAGAGAGUGAGCAC	28805.75	27459.09	27944.93	26091.81	23673.68	23989.82	1.00	0.88	0.93	0.87	0.67	0.58
	ath-miR156e	UGACAGAAGAGAGUGAGCAC	28416.25	27105.80	27622.63	25731.84	23307.20	23511.10	1.00	0.88	0.94	0.87	0.67	0.58
	ath-miR156f-5p	UGACAGAAGAGAGUGAGCAC	28416.25	27105.80	27622.63	25731.84	23307.20	23511.10	1.00	0.88	0.94	0.87	0.67	0.58
	ath-miR156f-3p	GCUCACUCUCUAUCCGUCACC	282.71	312.89	391.29	273.74	398.81	296.40	1.00	1.07	1.36	0.88	1.16	1.09
	ath-miR156g	CGACAGAAGAGAGUGAGCAC	295.62	261.96	274.86	284.18	227.63	173.09	1.00	0.89	0.93	0.96	0.78	0.59
	ath-miR156h	UGACAGAAGAAAGAGAGCAC	17.58	17.33	16.38	17.35	14.45	17.48	1.00	0.75	0.78	0.89	0.78	0.95
	ath-miR156i	UGACAGAAGAGAGAGAGCAG	1.43	1.39	1.53	1.44	1.28	1.08	1.00	0.97	1.06	0.97	0.79	0.61
	ath-miR156j	UGACAGAAGAGAGAGAGCAC	53.13	48.37	49.44	55.48	52.97	52.59	1.00	0.83	0.95	0.87	0.70	0.55
miR157	ath-miR157a-3p	GCUCUCUAGCCUUCUGUCAUC	160.04	171.27	126.23	151.26	121.63	288.83	1.00	1.10	1.30	1.16	2.14	2.38
	ath-miR157a-5p	UUGACAGAAGAUAGAGAGCAC	3919.67	3961.65	3874.22	3996.10	4349.27	6571.46	1.00	1.01	1.11	1.32	1.32	2.48
	ath-miR157b-5p	UUGACAGAAGAUAGAGAGCAC	3919.67	3961.65	3874.22	3996.10	4349.27	6571.46	1.00	1.01	1.11	1.32	1.32	2.48
	ath-miR157b-3p	GCUCUCUAGCCUUCUGUCAUC	160.09	171.29	126.25	151.26	121.65	288.83	1.00	1.10	1.29	1.15	2.12	2.36
	ath-miR157c-3p	GCUCUCUAUACUUCUGUCACC	1.12	1.26	1.77	2.64	2.85	5.19	1.00	1.16	1.32	2.26	2.48	5.39
	ath-miR157c-5p	UUGACAGAAGAUAGAGAGCAC	3955.62	3997.16	3914.75	4062.01	4426.78	6749.29	1.00	1.02	1.13	1.41	1.40	2.41
	ath-miR157d	UGACAGAAGAUAGAGAGCAC	40.35	41.97	41.81	42.00	46.98	68.19	1.00	1.31	1.26	1.21	1.27	1.57
miR158	ath-miR158a-3p	UCCCAAAUGUAGACAAAGCA	17470.90	22833.10	14562.02	20515.69	13487.01	10482.70	1.00	1.16	0.87	1.10	0.72	0.59
	ath-miR158a-5p	CUUUGUCUACAAUUUUGGAAA	1.45	0.92	1.13	1.68	1.15	1.18	1.00	0.71	0.82	1.21	1.00	0.98
	ath-miR158b	CCCCAAAUGUAGACAAAGCA	161.50	155.59	142.09	154.78	102.37	89.72	1.00	1.14	0.85	1.09	0.74	0.59
miR159	ath-miR159a	UUUGGAUUGAAGGGAGCUCUA	5475.71	5074.37	4961.39	4396.70	2959.00	6011.02	1.00	1.28	1.21	1.69	0.80	1.37
	ath-miR159b-3p	UUUGGAUUGAAGGGAGCUCUU	1849.12	1629.53	1676.71	1514.24	1172.39	1622.50	1.00	1.14	1.19	1.69	0.94	1.16
	ath-miR159c	UUUGGAUUGAAGGGAGCUCCU	45.80	40.48	44.73	51.81	98.64	196.76	1.00	0.88	1.12	1.27	1.99	3.38
miR160	ath-miR160a-5p	UGCCUGGCUCCCUGUAUGCCA	25.53	19.57	21.63	22.94	21.32	20.17	1.00	0.80	0.86	0.92	0.84	0.82
	ath-miR160b	UGCCUGGCUCCCUGUAUGCCA	12.91	9.42	11.44	10.90	9.35	6.75	1.00	0.88	0.95	0.91	0.79	0.70
	ath-miR160c-3p	CGUACAAGGAGUCAAGCAUGA	60.94	62.95	48.54	47.22	65.57	70.17	1.00	0.90	0.82	0.79	1.01	1.04
	ath-miR160c-5p	UGCCUGGCUCCCUGUAUGCCA	25.48	19.50	21.45	22.92	21.27	19.97	1.00	0.80	0.86	0.92	0.84	0.81
miR161	ath-miR161.2	UCAAUGCAUUGAAAGUGACUA	145.81	181.09	146.14	159.91	144.59	167.56	1.00	1.12	0.95	1.12	0.99	1.15
	ath-miR161.1	UGAAAGUGACUACAUCGGGGU	2073.93	1893.10	2156.48	1824.79	1705.49	1807.71	1.00	0.91	1.03	0.86	0.80	0.86
miR162	ath-miR162a-3p	UCGAUAAACCUCUGCAUCCAG	364.01	346.25	306.31	293.60	218.48	133.08	1.00	1.29	0.79	1.13	0.72	0.41
	ath-miR162a-5p	UGGAGGCAGCGGUUCAUCGAUC	8.11	7.49	6.81	6.50	5.20	4.55	1.00	0.92	0.82	0.79	0.51	0.38
	ath-miR162b-3p	UCGAUAAACCUCUGCAUCCAG	363.97	345.95	306.03	293.41	218.29	133.05	1.00	1.29	0.79	1.13	0.72	0.41
	ath-miR162b-5p	UGGAGGCAGCGGUUCAUCGAUC	6.35	6.31	5.69	5.58	5.13	4.12	1.00	1.04	0.88	1.15	0.63	0.51
miR163	ath-miR163	UUGAAGAGGACUUGGAACUUCGAU	0.88	5.29	21.26	32.84	37.96	54.78	1.00	12.61	38.66	109.80	74.37	164.09
miR164	ath-miR164a	UGGAGAAGCAGGGCACGUGCA	56.94	37.13	39.76	37.66	40.32	47.33	1.00	0.79	0.87	1.37	2.00	1.85
	ath-miR164b-3p	CAUGUGCCCAUCUUCACCAUC	0.50	0.47	0.38	0.59	0.22	0.41	1.00	2.66	0.83	2.32	1.30	1.49
	ath-miR164b-5p	UGGAGAAGCAGGGCACGUGCA	57.41	37.43	40.07	38.26	40.98	47.90	1.00	0.79	0.93	1.35	2.18	1.86
miR165	ath-miR165a-5p	GGAAUGUUGUCUGGAUCGAGG	33.90	32.96	34.50	35.96	29.52	25.06	1.00	0.98	1.02	1.06	0.86	0.71
	ath-miR165a-3p	UCGGACCAGGCUUCAUCCCCC	11142.34	11856.21	11416.79	10623.66	8750.96	7863.14	1.00	1.17	1.15	1.05	0.87	0.95
	ath-miR165b	UCGGACCAGGCUUCAUCCCCC	10304.01	11029.09	10533.92	9851.53	8129.08	7260.41	1.00	1.17	1.15	1.06	0.87	0.94
miR166	ath-miR166a-3p	UCGGACCAGGCUUCAUUCCCC	47014.84	49194.87	45177.38	42029.35	31576.68	25868.42	1.00	1.11	1.07	0.93	0.71	0.72

doi:10.6342/NTU201702588

miR166	ath-miR166a-5p	GGACUGUUGUCUGGCUCGAGG	160.97	140.77	125.81	92.20	65.55	52.87	1.00	0.91	0.81	0.63	0.45	0.39
	ath-miR166b-3p	UCGGACCAGGCUUCAUUCCCC	31162.49	33054.24	29767.43	28100.33	20643.76	17143.66	1.00	1.12	1.07	0.93	0.70	0.72
	ath-miR166b-5p	GGACUGUUGUCUGGCUCGAGG	160.97	140.77	125.81	92.20	65.55	52.87	1.00	0.91	0.81	0.63	0.45	0.39
	ath-miR166c	UCGGACCAGGCUUCAUUCCCC	31306.44	33194.14	29890.98	28220.36	20732.55	17215.87	1.00	1.12	1.07	0.93	0.70	0.72
	ath-miR166d	UCGGACCAGGCUUCAUUCCCC	31305.14	33193.37	29889.81	28219.23	20731.77	17215.31	1.00	1.12	1.07	0.93	0.70	0.72
	ath-miR166e-3p	UCGGACCAGGCUUCAUUCCCC	31115.43	33004.15	29723.00	28059.83	20615.00	17120.48	1.00	1.12	1.07	0.93	0.70	0.72
	ath-miR166e-5p	GGAAUGUUGUCUGGCACGAGG	11.39	7.89	6.92	5.50	3.96	4.08	1.00	0.72	0.62	0.47	0.37	0.31
	ath-miR166f	UCGGACCAGGCUUCAUUCCCC	31114.64	33003.19	29722.40	28059.38	20614.80	17120.30	1.00	1.12	1.07	0.93	0.70	0.72
	ath-miR166g	UCGGACCAGGCUUCAUUCCCC	31258.05	33143.50	29845.46	28178.74	20702.99	17192.14	1.00	1.12	1.07	0.93	0.70	0.72
miR167	ath-miR167a-3p	GAUCAUGUUCGCAGUUUCACC	2.11	2.18	2.93	3.12	2.94	4.27	1.00	1.04	1.42	1.50	1.40	2.06
	ath-miR167a-5p	UGAAGCUGCCAGCAUGAUCUA	2435.37	2025.82	3002.33	1605.80	2035.98	2503.60	1.00	0.77	1.00	0.78	1.04	0.86
	ath-miR167b	UGAAGCUGCCAGCAUGAUCUA	2438.74	2026.00	2999.89	1605.93	2039.81	2506.92	1.00	0.77	1.00	0.78	1.03	0.87
	ath-miR167c-3p	UAGGUCAUGCUGGUAGUUUCACC	1.30	1.66	1.00	0.99	1.17	1.87	1.00	1.29	0.74	0.75	0.85	1.44
	ath-miR167c-5p	UAAGCUGCCAGCAUGAUCUUG	29.83	24.66	34.80	18.71	23.85	30.06	1.00	0.88	1.01	0.76	0.95	0.79
	ath-miR167d	UGAAGCUGCCAGCAUGAUCUGG	234.65	191.81	221.01	184.22	170.07	152.51	1.00	0.82	0.98	0.76	0.74	0.69
miR168	ath-miR168a-5p	UCGCUUGGUGCAGGUCGGGAA	880.41	921.45	1221.11	1252.86	1270.91	1223.21	1.00	0.99	1.23	1.21	1.11	0.88
	ath-miR168a-3p	CCCGCCUUGCAUCAACUGAAU	394.62	447.02	545.97	553.87	369.75	214.19	1.00	0.97	1.25	1.28	0.94	0.73
	ath-miR168b-5p	UCGCUUGGUGCAGGUCGGGAA	852.26	889.71	1180.84	1216.71	1238.30	1201.29	1.00	0.98	1.21	1.19	1.09	0.86
	ath-miR168b-3p	CCCGUCUUGUAUCAACUGAAU	5.63	5.20	4.46	3.86	3.27	2.97	1.00	1.36	0.81	1.15	0.91	0.81
miR169	ath-miR169a-5p	CAGCCAAGGAUGACUUGCCGA	84.13	84.74	96.93	78.78	87.14	79.83	1.00	1.04	1.19	1.11	1.41	1.14
	ath-miR169a-3p	GGCAAGUUGUCCUUGGCUAC	25.00	19.64	23.35	23.51	18.71	12.56	1.00	0.79	0.93	0.96	0.76	0.50
	ath-miR169b-3p	GGCAAGUUGUCCUUCGGCUACA	3.99	4.07	4.16	2.79	4.19	3.25	1.00	1.04	1.09	0.70	1.08	0.81
	ath-miR169b-5p	CAGCCAAGGAUGACUUGCCGG	5.69	6.00	6.64	6.09	4.89	5.67	1.00	0.98	1.05	1.04	0.82	1.06
	ath-miR169c	CAGCCAAGGAUGACUUGCCGG	5.11	4.59	4.65	4.76	3.99	4.61	1.00	0.87	0.89	0.92	0.77	0.91
	ath-miR169f-3p	GCAAGUUGACCUUGGCUCUGC	2.59	1.94	2.59	3.36	3.94	5.01	1.00	0.96	1.07	1.38	1.36	1.58
	ath-miR169h	UAGCCAAGGAUGACUUGCCUG	1.62	1.36	1.59	1.27	1.60	1.36	1.00	0.87	1.05	0.82	1.02	0.82
	ath-miR169i	UAGCCAAGGAUGACUUGCCUG	3.42	3.36	3.54	2.56	3.00	2.74	1.00	0.88	1.12	0.76	1.01	0.82
	ath-miR169j	UAGCCAAGGAUGACUUGCCUG	3.31	3.23	3.41	2.42	2.94	2.70	1.00	0.87	1.15	0.76	1.10	0.86
	ath-miR169k	UAGCCAAGGAUGACUUGCCUG	1.66	1.36	1.61	1.27	1.60	1.38	1.00	0.85	1.04	0.80	0.99	0.81
	ath-miR169l	UAGCCAAGGAUGACUUGCCUG	3.27	3.17	3.40	2.44	2.92	2.69	1.00	0.85	1.14	0.78	1.10	0.86
	ath-miR169m	UAGCCAAGGAUGACUUGCCUG	1.78	1.60	1.87	1.41	1.87	1.42	1.00	0.96	1.14	0.84	1.14	0.80
	ath-miR169n	UAGCCAAGGAUGACUUGCCUG	3.31	3.23	3.41	2.42	2.94	2.70	1.00	0.87	1.15	0.76	1.10	0.86
miR170	ath-miR170-3p	UGAUUGAGCCGUGUCAAUAUC	1.55	1.93	1.96	2.06	2.08	1.63	1.00	1.22	1.26	1.31	1.34	1.04
miR171	ath-miR171a-3p	UGAUUGAGCCGCGCCAAUAUC	24.35	26.98	26.89	29.42	32.51	39.00	1.00	1.03	1.16	1.19	1.48	1.79
	ath-miR171b-5p	AGAUAUUAGUGCGGUUCAAUC	16.38	13.02	10.06	9.84	10.19	9.22	1.00	0.75	0.59	0.57	0.59	0.52
	ath-miR171b-3p	UUGAGCCGUGCCAAUAUCACG	2.96	2.93	2.46	2.56	1.98	1.72	1.00	1.08	0.90	1.02	0.84	0.75
	ath-miR171c-5p	AGAUAUUGGUGCGGUUCAAUC	2.07	1.92	1.53	1.93	1.94	2.90	1.00	0.85	0.70	0.84	0.77	1.06
	ath-miR171c-3p	UUGAGCCGUGCCAAUAUCACG	2.96	2.93	2.46	2.56	1.98	1.72	1.00	1.08	0.90	1.02	0.84	0.75
miR173	ath-miR173-5p	UUCGCUUGCAGAGAGAAAUCAC	232.34	207.44	192.17	190.31	175.11	199.37	1.00	0.97	0.83	0.82	0.70	0.57
	ath-miR173-3p	UGAUUCUCUGUGUAAGCGAAA	4.03	3.95	3.35	3.01	2.99	2.83	1.00	0.78	0.70	0.63	0.74	0.59
miR1886	ath-miR1886.1	UGAGAGAAGUGAGAUGAAAUC	0.93	1.11	0.89	0.69	0.56	0.70	1.00	1.21	0.98	0.74	0.64	0.79
	ath-miR1886.2	UGAGAUGAAAUCUUUGAUUGG	8.26	6.76	7.38	6.61	4.47	4.83	1.00	0.83	0.89	0.80	0.50	0.54
miR1888a	ath-miR1888a	UAAGUUAAGAUUUGUGAAGAA	0.67	0.77	0.87	0.72	0.56	0.96	1.00	1.01	1.05	0.93	0.72	0.98
miR2111b	ath-miR2111b-3p	AUCCUCGGGAUACAGUUUACC	1.65	1.28	1.66	1.13	0.84	0.90	1.00	1.08	1.71	1.08	0.54	0.51
miR2933	ath-miR2933a	GAAAUCGGAGAGGAAAUUCGCC	0.73	0.63	0.90	0.91	0.73	0.86	1.00	0.66	1.08	1.23	0.93	1.13
	ath-miR2933b	GAAAUCGGAGAGGAAAUUCGCC	0.73	0.63	0.90	0.91	0.73	0.86	1.00	0.66	1.08	1.23	0.93	1.13
miR319	ath-miR319a	UUGGACUGAAGGGAGCUCCCU	745.98	677.16	710.37	612.74	432.53	395.01	1.00	1.10	1.05	1.20	0.70	0.63
	ath-miR319b	UUGGACUGAAGGGAGCUCCCU	396.72	360.19	390.15	353.91	271.49	254.38	1.00	1.13	1.01	1.27	0.75	0.64
	ath-miR319c	UUGGACUGAAGGGAGCUCCUU	145.12	130.36	152.63	223.22	247.34	244.75	1.00	1.16	1.08	1.80	1.41	1.57
miR390	ath-miR390a-3p	CGCUAUCCAUCCUGAGUUUCA	1.39	1.53	1.40	1.34	1.59	1.85	1.00	1.09	1.00	0.97	1.14	1.28
	ath-miR390a-5p	AAGCUCAGGAGGGAUAGCGCC	262.43	263.85	213.03	179.30	157.29	155.09	1.00	1.04	0.85	0.70	0.56	0.53

doi:10.6342/NTU201702588

miR390	ath-miR390b-5p	AAGCUCAGGAGGGAUAGCGCC	262.77	264.20	213.47	179.68	157.91	155.40	1.00	1.04	0.85	0.70	0.56	0.53
	ath-miR390b-3p	CGCUAUCCAUCCUGAGUUCC	9.29	7.34	5.29	5.38	2.74	2.08	1.00	0.80	0.59	0.66	0.35	0.28
nuR393	ath-miR393a-3p	AUCAUGCUAUCUCUUUGGAUU	0.36	0.33	0.27	0.24	0.32	0.32	1.00	1.02	2.55	1.39	1.07	1.07
	ath-miR393b-3p	AUCAUGCGAUCUCUUUGGAUU	7.40	5.79	5.84	6.28	5.27	5.29	1.00	0.89	0.86	0.91	0.72	0.71
miR394	ath-miR394a	UUGGCAUUCUGUCCACCUCC	9.16	8.53	8.41	7.73	6.87	6.24	1.00	0.96	1.00	0.89	0.85	0.79
	ath-miR394b-5p	UUGGCAUUCUGUCCACCUCC	9.24	8.57	8.35	7.63	6.73	6.26	1.00	0.96	0.98	0.86	0.83	0.79
miR395	ath-miR395a	CUGAAGUGUUUGGGGGAACUC	1.36	0.90	0.84	1.05	0.47	0.35	1.00	0.75	0.66	0.88	0.39	0.29
	ath-miR395b	CUGAAGUGUUUGGGGGGACUC	0.38	0.32	0.27	0.28	0.19	0.11	1.00	0.85	0.72	0.74	0.50	0.28
	ath-miR395c	CUGAAGUGUUUGGGGGGACUC	0.38	0.32	0.27	0.28	0.19	0.11	1.00	0.85	0.72	0.74	0.50	0.28
	ath-miR395d	CUGAAGUGUUUGGGGGAACUC	1.36	0.90	0.84	1.05	0.47	0.35	1.00	0.75	0.66	0.88	0.39	0.29
	ath-miR395e	CUGAAGUGUUUGGGGGAACUC	1.36	0.90	0.84	1.05	0.47	0.35	1.00	0.75	0.66	0.88	0.39	0.29
	ath-miR395f	CUGAAGUGUUUGGGGGGACUC	0.38	0.32	0.26	0.28	0.19	0.11	1.00	0.85	0.69	0.74	0.50	0.28
miR396	ath-miR396a-3p	GUUCAAUAAAGCUGUGGGAAG	87.86	77.11	53.37	50.51	28.87	20.61	1.00	0.97	0.62	0.63	0.36	0.26
	ath-miR396a-5p	UUCCACAGCUUUCUUGAACUG	1513.45	1648.28	1803.35	1398.72	976.76	1109.73	1.00	1.01	1.22	0.89	0.75	0.89
	ath-miR396b-5p	UUCCACAGCUUUCUUGAACUU	728.69	720.88	699.23	560.45	323.39	272.31	1.00	1.48	1.00	1.31	0.77	0.70
	ath-miR396b-3p	GCUCAAGAAAGCUGUGGGAAA	22.82	29.39	23.23	19.29	16.15	19.21	1.00	0.93	0.86	0.72	0.63	0.53
miR397	ath-miR397a	UCAUUGAGUGCAGCGUUGAUG	0.96	0.56	0.86	0.79	0.50	0.37	1.00	0.70	0.81	0.72	0.67	0.72
	ath-miR397b	UCAUUGAGUGCAUCGUUGAUG	7.99	7.47	8.09	7.95	5.82	5.24	1.00	2.43	2.97	3.53	4.33	2.07
miR398	ath-miR398a-5p	AAGGAGUGGCAUGUGAACACA	2.14	3.19	2.70	2.63	2.06	2.40	1.00	1.82	1.32	1.29	1.26	1.30
	ath-miR398b-3p	UGUGUUCUCAGGUCACCCCUG	1003.69	998.46	1009.51	899.96	530.67	285.90	1.00	1.22	0.74	1.45	0.70	0.35
	ath-miR398b-5p	AGGGUUGAUAUGAGAACACAC	3.47	2.85	4.00	3.96	3.16	4.45	1.00	1.12	1.05	1.69	0.99	2.58
	ath-miR398c-5p	AGGGUUGAUAUGAGAACACAC	3.32	2.73	3.94	3.69	2.88	4.24	1.00	1.12	1.07	1.67	0.96	2.57
	ath-miR398c-3p	UGUGUUCUCAGGUCACCCCUG	1003.69	998.46	1009.51	899.96	530.67	285.90	1.00	1.22	0.74	1.45	0.70	0.35
miR399	ath-miR399b	UGCCAAAGGAGAGUUGCCCUG	10.93	9.42	10.16	7.94	6.17	4.82	1.00	0.81	0.99	0.68	0.58	0.45
	ath-miR399c-3p	UGCCAAAGGAGAGUUGCCCUG	10.24	9.08	9.26	7.80	5.82	4.53	1.00	0.92	1.04	0.71	0.60	0.47
miR400	ath-miR400	UAUGAGAGUAUUAUAAGUCAC	2.91	3.29	3.87	3.01	3.38	3.44	1.00	1.10	1.22	1.05	1.03	0.93
miR402	ath-miR402	UUCGAGGCCUAUUAAACCUCUG	29.74	31.52	30.61	25.48	21.30	17.94	1.00	0.94	1.00	0.81	0.76	0.68
miR403	ath-miR403-3p	UUAGAUUCACGCACAAACUCG	834.09	736.80	685.12	641.13	367.18	349.09	1.00	1.08	0.88	0.91	0.60	0.58
	ath-miR403-5p	UGUUUUGUGCUUGAAUCUAAUU	1.07	0.91	0.91	0.95	0.69	1.08	1.00	0.99	0.77	1.05	0.60	1.17
miR408	ath-miR408-5p	ACAGGGAACAAGCAGAGCAUG	124.00	101.34	134.26	86.62	89.38	75.54	1.00	0.74	0.90	0.64	0.48	0.36
	ath-miR408-3p	AUGCACUGCCUCUUCCCUGGC	594.28	499.96	543.29	660.30	495.56	311.76	1.00	0.84	0.90	1.09	0.93	0.71
miR4228	ath-miR4228-3p	UCGGAUGCGAAACGGUGGUGU	2.37	2.63	2.86	2.66	3.08	3.52	1.00	1.21	1.06	1.05	1.45	1.75
miR447	ath-miR447a.2-3p	UAUGGAAGAAAUUGUAGUAUU	4.25	4.53	3.45	4.04	2.59	3.05	1.00	1.22	0.82	1.07	0.74	0.87
	ath-miR447a-3p	UUGGGGACGAGAUGUUUUGUUG	3.31	3.68	3.32	3.40	2.70	2.68	1.00	1.11	0.97	0.98	0.78	0.65
	ath-miR447b	UUGGGGACGAGAUGUUUUGUUG	3.31	3.68	3.32	3.40	2.70	2.68	1.00	1.11	0.97	0.98	0.78	0.65
miR472	ath-miR472-3p	UUUUUCCUACUCCGCCCAUACC	12.31	11.98	11.77	12.27	8.08	8.44	1.00	1.29	1.09	1.20	0.81	1.11
	ath-miR472-5p	AUGGUCGAAGUAGGCAAAAUC	38.47	37.65	32.60	34.64	34.36	35.75	1.00	0.70	0.73	0.80	1.11	0.92
miR5012	ath-miR5012	UUUUACUGCUACUUGUGUUCC	2.70	2.26	1.80	1.49	0.68	0.69	1.00	0.78	0.76	0.63	0.44	0.31
miR5024	ath-miR5024-3p	CCGUAUCUUGGCCUUGUCAUU	5.72	5.05	4.79	3.60	2.28	1.12	1.00	0.73	0.95	0.65	0.40	0.26
	ath-miR5024-5p	AUGACAAGGCCAAGAUAUAACA	1.19	1.29	1.48	1.17	0.73	0.87	1.00	1.22	1.30	1.05	0.56	0.72
miR5026	ath-miR5026	ACUCAUAAGAUCGUGACACGU	23.50	24.86	32.71	18.54	21.57	32.00	1.00	0.91	1.53	0.81	1.41	1.23
miR5027	ath-miR5027	ACCGGUUGGAACUUGCCUUAA	0.32	0.54	0.52	0.46	0.35	0.28	1.00	5.23	4.70	3.20	3.53	2.34
miR5634	ath-miR5634	AGGGACUUUGUGAAUUUAGGG	1.06	0.83	0.75	0.63	0.57	0.41	1.00	0.91	0.70	0.63	0.60	0.45
miR5635	ath-miR5635b	UGUUAAGGAGUGUUAACGGUG	1.47	1.32	1.53	1.34	1.37	1.18	1.00	1.39	1.91	1.14	1.44	1.55
	ath-miR5635c	UGUUAAGGAGUGUUAACGGUG	1.47	1.32	1.53	1.34	1.37	1.18	1.00	1.39	1.91	1.14	1.44	1.55
	ath-miR5635d	UGUUAAGGAGUGUUAACGGUG	1.46	1.36	1.53	1.54	1.69	1.62	1.00	2.22	2.39	1.73	3.18	4.08
miR5640	ath-miR5640	UGAGAGAAGGAAUUAGAUUCA	25.09	23.75	21.83	18.68	11.94	9.61	1.00	1.23	0.93	1.21	1.10	0.58
miR5642	ath-miR5642a	UCUCGCGCUUGUACGGCUUU	60.36	58.13	69.21	77.58	122.11	135.11	1.00	0.93	1.08	1.32	1.90	1.86
	ath-miR5642b	UCUCGCGCUUGUACGGCUUU	16.51	16.18	18.42	24.64	21.14	9.94	1.00	0.94	1.08	1.53	1.41	0.72
miR5643	ath-miR5643a	AGGCUUUUAAGAUCUGGUUGC	2.79	2.92	3.57	2.92	3.05	3.29	1.00	0.95	1.59	1.25	0.87	1.33

doi:10.6342/NTU201702588

miR5643	ath-miR5643b	AGGCUUUUAAGAUCUGGUUGC	2.79	2.92	3.57	2.92	3.05	3.29	1.00	0.95	1.59	1.25	0.87	1.33
miR5644	ath-miR5644	GUGGGUUGCGGAUAACGGUA	4.54	3.32	3.94	4.34	3.75	3.31	1.00	0.73	0.87	0.96	0.83	0.74
miR5646	ath-miR5646	GUUCGAGGCACGUUGGGAGG	0.54	0.36	0.46	0.34	0.19	0.18	1.00	0.76	0.89	0.66	0.34	0.30
miR5651	ath-miR5651	UUGUGCGGUUCAAAUAGUAAC	4.26	3.52	4.15	3.85	3.31	4.40	1.00	0.93	1.14	0.90	0.91	1.28
miR5652	ath-miR5652	UUGAAUGUGAAUGAAUCGGGC	2.98	2.92	2.56	2.18	2.20	1.63	1.00	0.96	0.84	0.67	0.67	0.50
miR5653	ath-miR5653	UGGGUUGAGUUGAGUUGAGUUGGC	7.95	6.72	6.55	7.73	6.46	6.32	1.00	0.80	0.77	0.92	0.77	0.70
miR5656	ath-miR5656	ACUGAAGUAGAGAUUGGGUUU	4.68	5.24	4.49	4.18	3.95	3.62	1.00	1.83	1.26	1.37	0.53	0.50
miR5659	ath-miR5659	CGAUGAAGGUCUUUGGAACGGUA	7.10	7.04	7.25	7.52	5.99	6.74	1.00	1.86	1.53	2.15	0.99	1.50
miR5663	ath-miR5663-5p	AGCUAAGGAUUUGCAUUCUCA	2.01	2.61	2.25	2.24	2.36	2.86	1.00	1.27	1.13	1.09	1.15	1.69
miR5665	ath-miR5665	UUGGUGGACAAGAUCUGGGAU	0.16	0.21	0.33	0.30	0.15	0.12	1.00	1.60	3.03	2.41	1.21	0.80
miR773	ath-miR773a	UUUGCUUCCAGCUUUUGUCUC	3.96	4.36	5.29	3.76	4.18	5.36	1.00	1.10	1.34	0.95	1.05	1.36
miR775	ath-miR775	UUCGAUGUCUAGCAGUGCCA	44.76	38.45	45.48	30.74	30.85	29.38	1.00	0.88	0.99	0.69	0.66	0.59
miR777	ath-miR777	UACGCAUUGAGUUUCGUUGCUU	1.11	1.16	1.48	0.93	1.29	1.17	1.00	1.09	1.26	0.84	1.14	0.97
miR779	ath-miR779.2	UGAUUGGAAAUUUCGUUGACU	4.57	3.94	4.26	3.87	2.38	1.51	1.00	1.40	1.60	0.98	1.15	0.56
miR8165	ath-miR8165	AAUGGAGGCAAGUGUGAAGGA	5.98	5.74	6.55	7.09	6.43	7.50	1.00	0.63	0.69	1.06	0.67	0.73
miR8166	ath-miR8166	AGAGAGUGUAGAAAGUUUCUCA	1.84	2.04	2.04	2.23	1.85	1.87	1.00	1.26	1.12	1.49	0.99	1.04
miR8167	ath-miR8167a	AGAUGUGGAGAUCGUGGGGAUG	1.87	1.60	2.31	2.19	2.11	2.53	1.00	0.85	1.08	1.20	1.11	1.05
	ath-miR8167b	AGAUGUGGAGAUCGUGGGGAUG	1.87	1.60	2.31	2.19	2.11	2.53	1.00	0.85	1.08	1.20	1.11	1.05
	ath-miR8167c	AGAUGUGGAGAUCGUGGGGAUG	1.87	1.60	2.31	2.19	2.11	2.53	1.00	0.85	1.08	1.20	1.11	1.05
	ath-miR8167d	AGAUGUGGAGAUCGUGGGGAUG	1.87	1.60	2.31	2.19	2.11	2.53	1.00	0.85	1.08	1.20	1.11	1.05
	ath-miR8167e	AGAUGUGGAGAUCGUGGGGAUG	1.87	1.60	2.31	2.19	2.11	2.53	1.00	0.85	1.08	1.20	1.11	1.05
	ath-miR8167f	AGAUGUGGAGAUCGUGGGGAUG	1.87	1.60	2.31	2.19	2.11	2.53	1.00	0.85	1.08	1.20	1.11	1.05
miR8172	ath-miR8172	AUGGAUCAUCUAGAUGGAGAU	1.10	0.67	1.15	0.83	0.55	0.73	1.00	0.59	1.05	0.76	0.52	0.70
miR8174	ath-miR8174	AUGUGUAUAGGGAAGCUAAUC	0.74	0.73	0.70	0.69	0.46	1.01	1.00	1.15	1.13	0.96	0.86	1.10
miR8175	ath-miR8175	GAUCCCCGGCAACGGCGCCA	426.54	323.70	289.76	704.79	1351.58	554.15	1.00	0.79	0.76	1.28	2.41	1.61
miR8180	ath-miR8180	UGCGGUGCGGGAGAAGUGC	27.45	26.11	25.77	28.28	24.93	23.51	1.00	0.97	1.29	1.24	1.32	0.68
miR822	ath-miR822-3p	UGUGCAAAUGCUUUCUACAGG	4.32	3.20	4.31	2.47	3.15	2.64	1.00	0.74	0.99	0.57	0.72	0.61
	ath-miR822-5p	UGCGGGAAGCAUUUGCACAUG	430.42	406.18	366.82	350.04	294.11	288.99	1.00	0.80	0.76	0.76	0.54	0.48
miR823	ath-miR823	UGGGUGGUGAUCAUAUAAGAU	5.47	4.57	5.88	3.91	3.44	3.42	1.00	0.84	1.08	0.74	0.63	0.59
miR824	ath-miR824-5p	UAGACCAUUUGUGAGAAGGGA	11.80	13.38	13.97	11.23	9.52	11.52	1.00	0.82	0.99	0.97	0.64	0.86
	ath-miR824-3p	CCUUCUCAUCGAUGGUCUAGA	64.91	59.13	62.22	61.12	55.68	46.55	1.00	1.13	1.25	1.06	0.94	1.00
miR825	ath-miR825	UUCUCAAGAAGGUGCAUGAAC	4.68	3.34	4.43	6.46	6.38	5.41	1.00	0.69	0.94	1.41	1.43	1.13
miR827	ath-miR827	UUAGAUGACCAUCAACAAACU	0.21	0.44	0.32	0.33	0.39	0.42	1.00	2.56	3.15	2.14	2.60	3.51
miR829	ath-miR829-3p.1	AGCUCUGAUACCAAAUGAUGGAAU	141.83	128.55	146.96	132.20	83.61	73.41	1.00	0.89	1.00	0.91	0.60	0.55
	ath-miR829-5p	ACUUUGAAGCUUUGAUUUGAA	3.63	3.67	3.15	2.86	2.19	2.03	1.00	1.02	0.84	0.80	0.64	0.62
miR833	ath-miR833a-5p	UGUUUGUUGUACUCGGUCUAGU	0.22	0.19	0.24	0.14	0.35	1.09	1.00	0.81	2.04	1.12	2.88	9.97
	ath-miR833b	UGUUUGUUGACAUCGGUCUAG	0.21	0.44	0.38	0.38	0.40	0.27	1.00	2.13	1.79	1.80	1.91	1.25
miR839	ath-miR839-5p	UACCAACCUUUCAUCGUUCCC	0.51	0.40	0.61	0.47	0.53	0.31	1.00	0.84	1.21	1.02	1.05	0.59
miR840	ath-miR840-3p	UUGUUUAGGUCCCUUAGUUUC	0.72	0.78	0.71	0.84	0.46	0.47	1.00	1.61	1.46	3.23	1.10	1.97
	ath-miR840-5p	ACACUGAAGGACCUAAACUAAC	4.17	4.09	4.30	2.87	2.21	0.99	1.00	1.45	1.04	1.08	0.69	0.62
miR841	ath-miR841a-5p	UACGAGCCACUUGAAACUGAA	14.17	11.86	13.99	9.86	6.08	4.12	1.00	0.91	1.27	0.79	0.61	0.53
	ath-miR841a-3p	AUUUCUAGUGGGUCGUAUUCA	7.34	7.46	7.06	6.06	4.89	4.91	1.00	0.98	1.26	0.93	0.88	1.08
	ath-miR841b-3p	CAAUUUCUAGUGGGUCGUAUU	7.46	7.56	7.20	6.18	4.96	5.20	1.00	0.99	1.19	0.90	0.77	1.16
	ath-miR841b-5p	UACGAGCCACUGGAAACUGAA	9.72	8.76	11.26	9.03	10.28	9.29	1.00	1.21	1.43	1.19	1.78	2.24
miR842	ath-miR842	UCAUGGUCAGAUCCGUCAUCC	1.65	1.40	1.75	1.80	1.49	1.56	1.00	0.81	1.12	1.09	0.96	1.02
miR844	ath-miR844-3p	UUAUAAGCCAUCUUACUAGUU	0.28	0.17	0.17	0.10	0.14	0.19	1.00	0.60	0.56	0.41	0.44	0.71
miR845	ath-miR845a	CGGCUCUGAUACCAAUUGAUG	2.60	2.47	2.16	2.37	1.88	1.80	1.00	1.35	1.00	1.09	0.90	1.22
miR846	ath-miR846-3p	UUGAAUUGAAGUGCUUGAAUU	48.31	48.03	41.87	39.57	23.26	25.78	1.00	1.00	0.94	0.82	0.56	0.62
	ath-miR846-5p	CAUUCAAGGACUUCUAUUCAG	7.46	7.74	8.25	7.08	4.05	4.45	1.00	1.13	1.20	1.03	0.62	0.72

doi:10.6342/NTU201702588

miR848	ath-miR848	UGACAUGGGACUGCCUAAGCUA	3.63	3.77	3.83	3.99	3.48	3.38	1.00	0.99	1.07	1.23	1.18	0.79
miR850	ath-miR850	UAAGAUCCGGACUACAACAAAG	5.98	5.92	6.68	5.67	5.27	3.59	1.00	1.03	0.97	0.88	1.01	0.68
miR852	ath-miR852	AAGAUAAGCGCCUUAGUUCUG	4.81	5.12	4.36	4.17	3.84	4.48	1.00	0.89	1.23	1.19	1.26	0.97
miR853	ath-miR853	UCCCCUCUUUAGCUUGGAGAAG	0.76	0.69	0.45	0.60	0.49	0.39	1.00	1.09	0.67	0.84	0.56	0.82
miR858	ath-miR858a	UUUCGUUGUCUGUUCGACCUU	14.24	15.14	16.86	16.96	23.71	23.07	1.00	2.17	1.56	2.49	1.64	1.73
	ath-miR858b	UUCGUUGUCUGUUCGACCUUG	2.93	2.36	3.32	2.85	3.98	3.76	1.00	1.21	1.33	1.60	1.28	1.28
miR860	ath-miR860	UCAAUAGAUUGGACUAUGUAU	0.90	1.69	1.24	1.40	1.35	1.86	1.00	1.22	3.41	3.04	3.60	2.03
miR861	ath-miR861-3p	GAUGGAUAUGUCUUCAAGGAC	7.72	4.97	5.30	4.68	3.27	3.40	1.00	0.58	0.77	0.53	0.55	0.59
miR862	ath-miR862-5p	UCCAAUAGGUCGAGCAUGUGC	1.08	1.11	0.97	0.50	0.84	0.66	1.00	1.30	1.33	0.70	1.12	1.12
miR863	ath-miR863-3p	UUGAGAGCAACAAGACAUAAU	0.69	0.90	0.81	0.51	0.54	0.71	1.00	1.03	0.93	0.52	0.57	0.78
miR866	ath-miR866-5p	UCAAGGAACGGAUUUUGUUAA	0.87	1.06	1.01	0.74	0.84	1.00	1.00	1.16	1.30	0.83	0.82	1.05
miR869	ath-miR869.2	UCUGGUGUUGAGAUAGUUGAC	3.37	2.49	2.88	4.16	4.76	9.81	1.00	0.73	0.87	1.18	1.03	1.95
Median			4.68	4.44	4.93	4.59	3.89	4.30						

doi:10.6342/NTU201702588

Table 3. Expressed *PHAS* loci in de-etiolating seedlings.

***PHAS* locus**	**Gene**	**Chromosome**	**phasiR trigger**	**Start**	**End**	**n**	**k**	**p-value**
At1g62910	*RFL9 (PPR)*	1	TAS2 3'-D6 (-)	23299624	23299875	77	14	2.0×10^{-7}
At1g63130	*RPF6*	1	ta-siR2140	23413391	23413642	13	7	7.3×10^{-7}
At1g50055	*TAS1B*	1	miR173	18549441	18549692	60	12	9.7×10^{-7}
At1g63070	*PPR*	1	ta-siR2140	23386420	23386671	50	11	1.3×10^{-6}
At1g63150	*	1	TAS2 3'-D6 (-)	23420003	23420254	80	12	2.7×10^{-5}
At1g62930	*RPF3 (PPR)*	1	miR161.1	23307125	23307466	99	13	4.5×10^{-5}
At1g63080	*PPR*	1	ta-siR2140	23389990	23390241	58	10	5.5×10^{-5}
At1g62590	*PPR-AC*	1	TAS2 3'-D6 (-)	23178438	23178689	27	7	7.1×10^{-5}
At2g39681	*TAS2*	2	miR173	16539919	16540170	12	9	1.9×10^{-9}
At2g39675	*TAS1C*	2	miR173	16537860	16538111	10	7	1.5×10^{-8}
At2g27400	*TAS1A*	2	miR173	11722009	11722260	21	8	6.2×10^{-7}
At3g17185	*TAS3*	3	miR390	5682143	5682394	80	14	3.4×10^{-7}

n: Number of distinct alignments.

k: Number of phased alignments, based on hypergeometric distribution.

***: Reported *PHAS* locus.**

Loci with $p < 10^{-4}$ are listed.

doi:10.6342/NTU201702588

Table 4. Expressed phasiRNAs in de-etiolating seedlings.
Light regulation was defined as phasiRNAs passed p < 0.05 in Student's t-test against W0h. Average RPM from 3 replicates were listed. Light regulated phasiRNAs were highlighted in red.

							Averaged RPM						Averaged fold change					
phasiRNA	**Locus**	**Chr**	**Start**	**End**	**Strand**	**Sequence**	**W0h**	**W1h**	**W3h**	**W6h**	**W12h**	**W24h**	**W0h**	**W1h**	**W3h**	**W6h**	**W12h**	**W24h**
phasiR_20	*AT1G63080*	1	23390072	23390092	C	AATGGATTATGTAAGAGAGGT	75.43	84.88	78.76	73.84	64.91	65.68	1.00	0.95	1.02	0.88	0.63	0.70
phasiR_21	*AT1G63080*	1	23390135	23390155	C	TTAGTTGAACGGATGGTTGTG	9.17	8.82	10.26	8.82	6.42	6.81	1.00	0.64	0.97	0.75	0.31	0.25
phasiR_31	*AT1G63080*	1	23390071	23390091	C	ATGGATTATGTAAGAGAGGTG	80.21	81.35	79.63	73.51	70.39	62.09	1.00	0.81	0.91	0.76	0.51	0.39
phasiR_37	*AT1G63080*	1	23390156	23390176	C	AAAGCTTCCGAAGCTGTGGCT	3.57	2.79	3.31	3.77	2.63	1.36	1.00	0.87	0.92	1.06	0.76	0.42
phasiR_14	*AT1G63150*	1	23419961	23419981	C	TTAGAGTTGTGAATGTAAAGG	1.32	1.24	0.98	1.01	0.58	0.20	1.00	1.06	0.74	0.76	0.47	0.14
phasiR_34	*AT1G63150*	1	23420005	23420025	W	AAAGCTTCAGAAGCAGTGGCT	1.49	1.29	1.08	1.21	1.25	1.55	1.00	0.85	0.64	0.98	0.64	0.68
phasiR_35	*AT1G63150*	1	23420047	23420067	W	AGAGGATGTCAACCAGATCTG	89.22	94.31	88.10	79.29	73.60	74.23	1.00	0.84	0.92	0.92	0.72	0.63
phasiR_36	*AT1G63150*	1	23420089	23420109	W	AACGGATTATGTAAGAGAGGT	59.55	61.49	63.62	56.50	47.44	44.58	1.00	0.88	0.99	0.88	0.65	0.60
phasiR_27	*AT1G63070*	1	23386480	23386500	C	ATGGATTATGTAAGAGAGGTG	80.21	81.35	79.63	73.51	70.39	62.09	1.00	0.81	0.91	0.76	0.51	0.39
phasiR_28	*AT1G63070*	1	23386481	23386501	C	AATGGATTATGTAAGAGAGGT	75.43	84.88	78.76	73.84	64.91	65.68	1.00	0.95	1.02	0.88	0.63	0.70
phasiR_29	*AT1G63070*	1	23386544	23386564	C	TTAGTTGAACGGATGGTTGTG	9.17	8.82	10.26	8.82	6.42	6.81	1.00	0.64	0.97	0.75	0.31	0.25
phasiR_30	*AT1G63070*	1	23386565	23386585	C	AAAGCTTCCGAAGCTGTGGCT	3.57	2.79	3.31	3.77	2.63	1.36	1.00	0.87	0.92	1.06	0.76	0.42
phasiR_13	*PPR RFL9*	1	23299622	23299642	C	TTAGAGTTGTGAATGTAAAGG	1.32	1.24	0.98	1.01	0.58	0.20	1.00	1.06	0.74	0.76	0.47	0.14
phasiR_23	*PPR RFL9*	1	23299666	23299686	W	AAAGCTTCAGAAGCAGTGGCT	1.49	1.29	1.08	1.21	1.25	1.55	1.00	0.85	0.64	0.98	0.64	0.68
phasiR_24	*PPR RFL9*	1	23299708	23299728	W	AGAGGATGTCAACCAGATCTG	89.22	94.31	88.10	79.29	73.60	74.23	1.00	0.84	0.92	0.92	0.72	0.63
phasiR_25	*PPR RFL9*	1	23299750	23299770	W	AACGGATTATGTAAGAGAGGT	59.55	61.49	63.62	56.50	47.44	44.58	1.00	0.88	0.99	0.88	0.65	0.60
phasiR_22	*PPR-AC*	1	23178482	23178502	C	AATGGATTATGTAAGAGAGGT	75.43	84.88	78.76	73.84	64.91	65.68	1.00	0.95	1.02	0.88	0.63	0.70
phasiR_26	*RPF3*	1	23307215	23307235	W	AACGGATTATGTAAGAGAGGT	59.55	61.49	63.62	56.50	47.44	44.58	1.00	0.88	0.99	0.88	0.65	0.60
phasiR_2	*RPF6*	1	23413452	23413472	C	CCACTGCTTCTGAAGCTCTGT	0.59	1.16	0.55	1.25	0.70	0.34	1.00	0.74	2.89	4.85	2.92	1.64
phasiR_32	*RPF6*	1	23413454	23413474	W	AGAGCTTCAGAAGCAGTGGCT	2.15	1.60	1.85	2.09	1.70	1.83	1.00	0.38	0.56	8.82	0.49	5.55
phasiR_33	*RPF6*	1	23413538	23413558	W	AATGGATTATGTAAGAGAGGT	75.43	84.88	78.76	73.84	64.91	65.68	1.00	0.95	1.02	0.88	0.63	0.70
phasiR_3	*TAS1a*	2	11721946	11721966	W	ACGATATCTTCCATTTCTCTA	1.98	2.70	1.50	1.95	1.27	1.57	1.00	1.22	0.60	0.89	0.63	0.66
phasiR_4	*TAS1a*	2	11722030	11722050	W	ATTTTCTAAGATCTTATCGAA	6.43	9.61	10.56	7.18	9.30	13.47	1.00	1.08	1.46	0.69	1.24	1.35
phasiR_15	*TAS1a*	2	11722009	11722029	W	CGCTATGTTAGACTTAAAATA	1.30	0.31	0.37	0.35	0.21	0.26	1.00	0.52	0.63	0.62	0.47	0.54
phasiR_16	*TAS1a*	2	11722051	11722071	W	CGCTATGTTGGACTTAGGATG	4.14	0.19	0.47	0.24	0.46	0.53	1.00	0.16	0.69	0.35	0.99	0.76
atTAS1a-siR255	*TAS1a*	2	11721965	11721985	C	TTCTAAGTCCAACATAGCGTA	35.77	23.71	38.83	20.56	22.20	37.68	1.00	1.35	1.42	1.47	0.79	1.16
phasiR_38	*TAS1a*	2	11721902	11721922	C	AAACTAGAAAAAGCATTGGAT	1.98	1.73	1.55	2.01	1.56	1.63	1.00	0.38	0.34	10.56	0.34	0.36
phasiR_39	*TAS1a*	2	11721986	11722006	C	TGATTGGATCTTAGGAAATTA	653.95	723.79	773.61	548.26	666.22	860.06	1.00	0.90	1.10	0.85	0.88	0.93
phasiR_40	*TAS1a*	2	11721988	11722008	W	ATTTCCTAAGATCCAATCAAA	2.30	2.66	3.18	1.95	2.89	3.56	1.00	1.55	1.45	1.05	1.04	1.04
atTAS1a-siR438(+)	*TAS1a*	2	11722007	11722027	C	TTTTAAGTCTAACATAGCGTT	1.97	2.51	2.43	1.84	2.17	2.11	1.00	1.37	1.22	0.94	1.11	1.01
atTAS1a-siR752	*TAS1a*	2	11722049	11722069	C	TCCTAAGTCCAACATAGCGTT	5.43	5.60	3.89	5.21	4.73	4.39	1.00	1.07	0.84	1.13	0.78	0.68
phasiR_43	*TAS1a*	2	11722070	11722090	C	TACAAGCGAATGAGTCATTCA	7.25	5.79	6.58	4.91	4.54	5.54	1.00	0.96	1.67	0.98	0.99	1.04
phasiR_53	*TAS1a*	2	11721923	11721943	C	ATGATATTTGTAGTAATGGCG	1889.97	2087.17	2139.56	1914.57	1910.48	1810.83	1.00	0.67	0.38	0.63	0.34	0.53
phasiR_1	*TAS1b*	1	18549483	18549503	W	ATTCCGGACATCTCCCATTTT	34.23	28.83	27.99	21.59	12.64	10.37	1.00	1.57	0.98	1.04	0.70	0.59
phasiR_5	*TAS1c*	2	16537710	16537730	C	TTTCAAGTCGTCTAAAGAACA	1.64	1.94	1.72	1.81	0.57	2.50	1.00	1.00	18.98	0.99	0.49	9.85
phasiR_6	*TAS1c*	2	16537711	16537731	C	TTTTCAAGTCGTCTAAAGAAC	0.63	0.58	0.49	0.73	0.62	0.61	1.00	0.75	4.26	0.98	1.31	2.77
atTAS1c-siR850	*TAS1c*	2	16537816	16537836	C	TTCTAAGTTCAACATATCGAC	66.72	64.28	57.60	63.59	35.10	35.83	1.00	1.00	1.35	1.12	0.87	1.06
phasiR_8	*TAS1c*	2	16537858	16537878	C	TCGGTGGATCTTAGAAAATTA	7.74	8.76	7.35	7.40	6.68	7.35	1.00	1.27	1.00	1.20	0.89	1.10
phasiR_9	*TAS1c*	2	16537860	16537880	W	ATTTTCTAAGATCCACCGATA	22.84	18.92	21.76	15.32	11.30	12.20	1.00	1.15	1.75	0.95	1.03	1.56
atTAS1c-siR255	*TAS1c*	2	16537837	16537857	C	TTCTAAGTCCAACATAGCGTA	35.77	23.71	38.83	20.56	22.20	37.68	1.00	1.35	1.42	1.47	0.79	1.16
phasiR_44	*TAS1c*	2	16537712	16537732	W	TTCTTTAGACGACTTGAAAAT	158.43	185.29	137.15	123.58	121.16	159.51	1.00	0.77	18.18	0.61	0.52	13.49
phasiR_45	*TAS1c*	2	16537713	16537733	W	TCTTTAGACGACTTGAAAATC	2.02	2.00	1.38	1.50	1.22	1.49	1.00	0.57	3.43	0.42	0.28	2.84

doi:10.6342/NTU201702588

phasiR_46	*TAS1c*	2	16537731	16537751	C	ATGTGTTCAAGTAAATGAGAT	3.49	4.13	4.23	2.89	2.89	4.40	1.00	0.56	2.33	0.39	0.46	0.75
phasiR_47	*TAS1c*	2	16537773	16537793	C	TATTCCAGGATATGCAAAAGA	2.20	2.79	2.42	2.21	2.34	2.93	1.00	0.84	4.20	0.56	0.49	4.42
phasiR_48	*TAS1c*	2	16537794	16537814	C	AACTAGAAAAGACATTGGACA	12.96	15.43	15.21	11.53	12.36	16.28	1.00	0.85	17.03	0.58	0.52	13.88
phasiR_49	*TAS1c*	2	16537795	16537815	C	GAACTAGAAAAGACATTGGAC	8.03	6.94	6.91	6.52	5.08	4.57	1.00	0.95	0.95	0.84	0.70	0.72
phasiR_50	*TAS1c*	2	16537796	16537816	W	TCCAATGTCTTTTCTAGTTCG	1.43	1.22	1.33	1.23	1.06	1.24	1.00	0.89	0.84	0.88	0.59	0.66
phasiR_10	*TAS2*	2	16539833	16539853	C	CCGTAAAAAAAGTTGTAACTC	1.13	1.95	1.36	1.21	1.10	0.97	1.00	3.37	7.29	0.77	5.08	2.76
phasiR_11	*TAS2*	2	16539898	16539918	W	GAATACTTGAACTACCATCTA	2.25	4.22	2.64	3.88	2.24	1.11	1.00	1.61	1.15	1.54	0.84	0.42
phasiR_12	*TAS2*	2	16539919	16539939	W	AATCTATTGAACATCGTGTTT	1.07	1.59	1.32	1.26	0.98	1.12	1.00	1.92	1.82	1.31	1.38	1.77
atTAS2-3'D6(-)	*TAS2*	2	16539877	16539897	W	ATATCCCATTTCTACCATCTG	14.17	10.07	14.82	7.48	6.96	9.64	1.00	0.76	1.01	0.53	0.45	0.58
phasiR_51	*TAS2*	2	16539812	16539832	C	TTGTTGATCGGATGGTAGAAA	4.83	4.69	5.22	4.38	4.41	4.08	1.00	15.52	20.03	0.59	12.02	8.65
phasiR_52	*TAS2*	2	16539980	16540000	C	TCCAAGCGAATGATGATACTT	125.07	123.24	106.38	84.95	79.22	91.36	1.00	0.87	0.80	0.54	0.51	0.55
phasiR_54	*TAS2*	2	16539856	16539876	W	ATAAGACTGAAACATATATGT	9.65	11.06	9.29	8.28	8.37	8.31	1.00	0.95	0.86	0.83	0.74	0.63
phasiR_55	*TAS2*	2	16539938	16539958	C	TTTGAACTTGTGTATTTTGAA	29.07	47.64	35.77	36.13	45.01	52.47	1.00	1.18	1.10	0.83	1.09	0.97
phasiR_56	*TAS2*	2	16539961	16539981	W	ATAATCAAGTGAATAGTTTAA	3.08	3.40	3.32	2.18	1.93	3.09	1.00	0.83	1.02	0.74	0.46	0.52
phasiR_57	*TAS3*	3	5862267	5862287	C	TTGAGAAGAGATAGAATAGAA	32.48	29.88	32.61	28.50	33.74	36.88	1.00	0.33	0.36	0.31	20.31	0.62
phasiR_58	*TAS3*	3	5862330	5862350	C	ATAGACAAGGTAGGAGAAAAT	9.60	9.49	7.94	8.61	8.80	8.77	1.00	0.34	0.28	0.30	2.09	0.31

doi:10.6342/NTU201702588

Table 5. Expressed siRNAs in de-etiolating seedlings, with average RPM listed.
Due to the large amount of dataset, please visit the link below and see table S4 for the detailed information of expressed siRNAs.
https://bmcgenomics.biomedcentral.com/articles/10.1186/s12864-017-3937-6

doi:10.6342/NTU201702588

Table 6. miRNA-mRNA and phasiRNA-mRNA pairs from cross comparisons of sRNA transcriptome and mRNA degradome.

miR family/*PHAS* loci	Potential targets	Identified target	sRNA	Target	Target gene	Cleavage site	CleaveLand Category	p-value	Identified condition	Dark_RPKM (Repeat 1)	Dark_RPKM (Repeat 2)	W4h_RPKM (Repeat 1)	W4h_RPKM (Repeat 2)	Light/Dark ratio (Repeat 1)	Light/Dark ratio (Repeat 2)
miR156/miR157	150	15	miR156a-3p	*AT3G59550.1*	*SYN3*	2044	0	0.012325634	Dark/light	0.47	0.91	0.67	1.30	1.42	1.42
			miR156c-5p	*AT5G64640.1*		1371	0	0.019753693	Dark/light	3.23	4.76	2.22	2.12	0.69	0.45
			miR156c-5p	*AT3G03440.1*		586	0	0.034963151	Dark	4.28	3.59	8.45	6.84	1.98	1.90
			miR156c-5p	*AT2G04940.1*		162	0	0.037561517	Dark/light	8.15	10.18	5.57	7.71	0.68	0.76
			miR156d-5p	*AT3G13870.1*	*RHD3*	1478	0	0.014984952	Dark/light	54.40	63.74	46.80	45.79	0.86	0.72
			miR156f-5p	*AT2G33810.1*	*SPL3*	797	0	0.004841287	Dark/light	0.94	0.98	0.34	0.50	0.36	0.51
			miR156f-5p	*AT2G42200.1*	*SPL9*	947	0	0.001616374	Dark/light	0.06	0.31	0.95	2.71	14.83	8.84
			miR156f-5p/miR157b-5p	*AT5G43270.2*	*SPL2*	1159	0	0.000539082	Dark/light	9.42	14.73	13.92	15.68	1.48	1.06
			miR156g	*AT5G50570.1*	*SPL13A*	1112	0	0.001616374	Dark/light	2.66	5.51	1.86	3.62	0.70	0.66
			miR156g	*AT5G50670.1*	*SPL13B*	1112	0	0.002692504	Dark/light	2.90	6.18	2.01	4.03	0.69	0.65
			miR156g	*AT3G13760.1*		344	0	0.031313649	Dark/light	0.38	1.44	0.40	0.31	1.08	0.21
			miR156i	*AT1G27360.1*	*SPL11*	1263	0	0.000539082	Dark/light	0.50	1.09	0.83	1.90	1.68	1.74
			miR156i	*AT3G15270.1*	*SPL5*	655	0	0.004841287	Dark/light	0.17	0.68	0.18	0.36	1.06	0.53
			miR156i	*AT3G57920.1*	*SPL15*	855	0	0.001077873	Dark/light	0.32	1.10	0.92	2.43	2.84	2.20
			miR156j	*AT1G27370.1*	*SPL10*	2378	0	0.000539082	Dark/light	2.18	3.88	3.69	4.82	1.70	1.24
miR158	7	2	miR158a-3p	*AT1G62860.1*	*PPR (Pseudogene)*	425	2	0.049377248	Light	1.00	2.45	1.09	2.21	1.09	0.90
			miR158b	*AT4G26910.1*	*PPR (RFL9)*	1568	1	0.00474464	Light	16.74	21.54	12.70	15.36	0.76	0.71
			miR159a	*AT4G26930.1*	*MYB97*	676	0	0.017637109	Dark	0.24	0.20	0.13	0.13	0.53	0.62
miR159	33	4	miR159a	*AT2G34010.1*		449	0	0.006985441	Dark/light	1.22	3.14	1.92	1.88	1.57	0.60
			miR159c	*AT3G11440.1*	*MYB65*	1166	0	0.001077873	Dark/light	3.11	4.95	2.49	2.91	0.80	0.59
			miR159c	*AT5G06100.2*	*MYB33*	1172	0	0.001616374	Dark/light	6.62	9.34	5.12	5.77	0.77	0.62
			miR160c-5p	*AT1G77850.1*	*ARF17*	1420	0	0.000539082	Dark/light	3.08	5.67	2.40	3.27	0.78	0.58
			miR160c-5p	*AT4G30080.1*	*ARF16*	1519	0	0.001077873	Dark/light	10.22	16.11	7.14	10.03	0.70	0.62
miR160	3	3	miR160c-5p	*AT2G28350.1*	*ARF10*	1340	0	0.001616374	Dark/light	14.73	20.45	12.08	17.84	0.82	0.87
miR161	36	6	miR161.1	*AT1G64583.1*	*TPR*	739	0	0.000539082	Dark/light	0.90	1.25	1.30	1.20	1.44	0.96
			miR161.2	*AT1G62590.1*	*PPR*	1050	1	0.001113098	Dark	0.87	2.77	2.19	4.31	2.52	1.56
			miR161.2	*AT1G62930.1*	*RPF3*	985	2	0.049377248	Light	2.81	4.77	3.10	3.91	1.10	0.82
			miR161.2	*AT4G04780.1*	*MED21*	132	0	0.03808035	Dark/light	6.82	8.49	7.15	8.37	1.05	0.99
			miR161.2	*AT1G63330.1*	*PPR*	775	0	0.003767475	Dark	0.00	0.00	0.00	0.00	-	-
			miR161.2	*AT1G62910.1*	*PPR (RFL9)*	997	0	0.000539082	Dark	0.32	0.61	0.66	0.75	2.06	1.23
miR163	26	1	miR163	*AT1G66700.1*	*PXMT1*	358	0	0.001121786	Light	0.19	0.53	0.23	0.14	1.19	0.26
miR164	11	5	miR164a	*AT5G07680.1*	*NAC080*	854	0	0.001616374	Dark/light	8.01	8.11	10.69	10.74	1.33	1.33
			miR164b-5p	*AT3G15170.1*	*CUC1*	675	0	0.000539082	Dark/light	0.22	0.37	0.80	1.41	3.59	3.76
			miR164b-5p	*AT3G12977.1*		728	0	0.003230135	Dark/light	9.84	7.99	4.75	2.31	0.48	0.29
			miR164b-5p	*AT5G39610.1*	*NAC6*	781	0	0.006985441	Dark/light	20.92	5.02	15.54	2.92	0.74	0.58
			miR164b-5p	*AT1G56010.2*	*ANAC021*	813	0	0.002692504	Dark/light	42.88	49.77	33.68	32.94	0.79	0.66
miR165	12	3	miR165a-3p	*AT1G30490.1*	*PHV*	806	0	0.001077873	Dark/light	6.68	8.92	7.77	9.88	1.16	1.11
			miR165b	*AT5G60690.1*	*REV*	1273	0	0.000539082	Dark/light	7.93	11.52	7.98	13.72	1.01	1.19
			miR165b	*AT2G34710.1*	*PHB*	881	0	0.001077873	Dark/light	12.29	14.70	14.54	17.03	1.18	1.16
miR166	10	3	miR166d	*AT4G32880.1*	*HB-8*	945	0	0.001077873	Dark	7.05	7.34	6.75	7.22	0.96	0.98
			miR166e-3p	*AT1G52150.2*	*ATHB-15*	1279	0	0.000539082	Dark/light	15.11	17.65	14.12	15.20	0.93	0.86
			miR167b	*AT5G37020.1*	*ARF8*	2381	0	0.002154584	Dark/light	7.70	14.22	13.99	23.34	1.82	1.64
			miR167b	*AT1G30330.2*	*ARF6*	3247	0	0.002692504	Dark/light	29.99	35.36	22.78	20.28	0.76	0.57
			miR167d	*AT3G19630.1*		783	0	0.002692504	Dark	11.20	11.76	10.78	10.29	0.96	0.87
miR168	7	2	miR168a-5p	*AT2G28671.1*		1275	1	0.015572056	Light	247.02	330.19	211.34	198.71	0.86	0.60
			miR168b-5p	*AT1G48410.2*	*AGO1*	522	2	0.049377248	Light	48.68	55.40	50.15	59.07	1.03	1.07
miR169	33	9	miR169a-5p	*AT3G20910.1*	*NF-YA9*	1046	0	0.006985441	Dark/light	2.61	3.20	1.90	2.57	0.73	0.80

doi:10.6342/NTU201702588

miR169			miR169a-5p	*AT1G17590.1*	*NF-YA8*	1243	0	0.001077873	Dark/light	1.16	2.57	1.16	2.12	1.00	0.82
			miR169c	*AT5G12840.1*	*NF-YA1*	1048	0	0.002692504	Dark/light	13.85	11.22	14.22	11.24	1.03	1.00
			miR169g-3p	*AT4G40070.1*		993	1	0.001900564	Light	9.85	4.00	8.04	4.49	0.82	1.12
			miR169h	*AT5G06510.1*	*NF-YA10*	1078	0	0.002692504	Dark/light	0.38	0.64	0.55	1.15	1.46	1.80
			miR169h	*AT1G54160.1*	*NF-YA5*	1295	0	0.001077873	Dark	0.45	1.00	0.59	0.60	1.30	0.60
			miR169h	*AT1G72830.2*	*NF-YA3*	1503	0	0.000539082	Dark/light	2.25	3.09	1.36	2.00	0.61	0.65
			miR169j	*AT1G48500.1*	*JAZ4*	975	0	0.042737279	Dark	1.53	1.84	1.67	4.21	1.09	2.30
			miR169m	*AT3G05690.1*	*NF-YA2*	1194	0	0.002692504	Dark/light	1.79	4.12	2.46	4.93	1.38	1.20
miR170	7	1	miR170-3p	*AT4G00150.1*	*LOM3*	867	0	0.000539082	Dark/light	25.05	21.14	17.46	12.15	0.70	0.57
miR171	25	5	miR171a-3p	*AT2G45160.1*	*LOM1*	1014	0	0.000539082	Dark/light	10.74	11.92	10.12	7.98	0.94	0.67
			miR171a-3p	*AT3G60630.1*	*LOM2*	1056	0	0.001077873	Dark/light	8.64	13.29	8.64	8.11	1.00	0.61
miR172	67	5	miR172a	*AT2G28550.3*	*RAP2.7*	1613	0	0.002802106	Light	23.33	30.12	41.54	51.94	1.78	1.72
			miR172a	*AT5G60120.2*	*TOE2*	1821	0	0.000539082	Dark/light	13.40	26.47	20.12	37.03	1.50	1.40
			miR172c	*AT4G36920.1*	*AP2*	1340	2	0.049377248	Light	6.42	7.55	3.91	5.67	0.61	0.75
			miR172e-3p	*AT3G54990.1*	*SMZ*	976	0	0.000539082	Dark/light	9.74	8.99	23.30	38.93	2.39	4.33
miR173	5	4	miR173-5p	*AT1G50055.1*	*TAS1B*	374	0	0.005913942	Dark/light	0.06	0.16	0.13	0.13	2.29	0.77
			miR173-5p	*AT2G27400.1*	*TAS1A*	379	0	0.002154584	Dark/light	0.12	0.06	0.22	0.14	1.87	2.40
			miR173-5p	*AT2G39675.1*	*TAS1C*	379	0	0.001616374	Dark/light	0.07	0.00	0.17	0.19	2.49	-
			miR173-5p	*AT2G39681.1*	*TAS2*	418	0	0.002692504	Dark/light	0.10	0.10	0.09	0.12	0.85	1.26
miR319	21	3	miR319b	*AT1G30210.1*	*TCP24*	1142	0	0.003767475	Dark/light	4.82	9.62	7.02	9.38	1.46	0.97
			miR319c	*AT1G53230.1*	*TCP3*	1195	0	0.001616374	Dark/light	3.70	6.98	14.08	12.72	3.81	1.82
			miR319c	*AT3G15030.1*	*TCP4*	1487	0	0.000539082	Dark/light	3.38	7.50	10.11	10.43	2.99	1.39
miR3440	17	1	miR3440b-5p	*AT2G25830.1*		950	1	0.021949864	Light	2.04	8.30	7.91	21.20	3.88	2.55
miR390	22	3	miR390a-5p	*AT5G02480.1*		1375	0	0.042220958	Dark	59.45	82.03	74.78	92.28	1.26	1.12
			miR390b-3p	*AT1G62400.1*	*HT1*	618	0	0.025550813	Dark	0.98	0.48	0.80	0.55	0.81	1.16
			miR390b-5p	*AT3G17185.1*	*TAS3*	472	0	0.005377759	Dark/light	0.23	0.23	0.67	0.32	2.89	1.37
miR393	7	3	miR393a-5p	*AT1G12820.1*	*AFB3*	1895	0	0.002154584	Dark	23.84	28.02	16.77	18.83	0.70	0.67
			miR393a-5p	*AT3G26810.1*	*AFB2*	2010	0	0.002692504	Dark/light	52.57	67.99	35.92	41.28	0.68	0.61
			miR393a-5p	*AT3G62980.1*	*TIR1*	1722	2	0.049377248	Light	75.17	58.57	53.14	45.92	0.71	0.78
miR395	20	2	miR395d	*AT1G35405.1*	copia-like retrotransposon family	1897	0	0.04978776	Light	0.00	0.00	0.00	0.00	-	-
miR396	41	12	miR396a-5p	*AT1G10120.1*	*CIB4*	1317	0	0.01179291	Dark/light	8.93	15.22	7.44	11.37	0.83	0.75
			miR396a-5p	*AT2G36400.1*	*GRF3*	757	0	0.003767475	Dark/light	6.78	10.73	10.14	8.64	1.50	0.81
			miR396b-5p	*AT2G38370.1*	*DUF827*	1140	0	0.033400765	Dark/light	4.53	3.82	4.58	4.41	1.01	1.16
			miR396b-5p	*AT2G45480.1*	*GRF9*	525	0	0.006985441	Dark/light	1.00	2.50	1.13	2.68	1.13	1.07
			miR396b-5p	*AT5G53660.1*	*GRF7*	540	0	0.005377759	Dark	6.98	48.90	0.26	0.26	0.04	0.01
			miR396b-5p	*AT5G61440.1*	*ACHT5*	719	0	0.03235777	Dark	16.39	21.28	22.55	17.56	1.38	0.83
			miR396b-5p	*AT3G52910.1*	*GRF4*	753	0	0.004304526	Dark/light	0.34	0.45	0.63	1.59	1.84	3.54
			miR396b-5p	*AT3G14110.3*	*FLU*	774	0	0.044799783	Dark/light	24.24	44.09	32.30	58.79	1.33	1.33
			miR396b-5p	*AT2G22840.1*	*GRF1*	792	0	0.003767475	Dark/light	5.36	9.34	6.13	6.62	1.14	0.71
			miR396b-5p	*AT4G24150.1*	*GRF8*	848	0	0.006449836	Dark/light	0.55	2.09	0.21	0.18	0.39	0.09
			miR396b-5p	*AT4G37740.1*	*GRF2*	921	0	0.003230135	Dark/light	3.26	12.48	4.37	4.03	1.34	0.32
			miR396b-5p	*AT2G38760.1*	*ANNAT3*	317	1	0.044327387	Light	27.87	25.50	20.37	26.35	0.73	1.03
miR397	22	2	miR397a	*AT2G38080.1*	*IRX12*	760	0	0.000539082	Dark/light	10.94	26.20	11.11	19.08	1.02	0.73
			miR397b	*AT3G60250.1*	*CKB3*	243	0	0.002154584	Dark/light	43.13	49.17	19.69	19.29	0.46	0.39
miR398	24	9	miR398a-3p	*AT1G08830.1*	*CSD1*	128	0	0.003230135	Dark/light	118.26	121.29	111.12	81.98	0.94	0.68
			miR398a-3p	*AT3G27200.1*		269	0	0.046343743	Dark/light	4.06	18.20	7.08	16.10	1.74	0.88
			miR398a-3p	*AT2G27550.1*	*ATC*	351	0	0.026076121	Dark	0.69	2.93	0.79	0.80	1.14	0.27
			miR398a-3p	*AT1G12520.1*	*CCS*	736	0	0.012325634	Dark/light	25.18	21.98	33.97	17.49	1.35	0.80
			miR398a-3p	*AT5G20230.1*	*BCB*	98	0	0.001077873	Dark/light	24.45	4.76	23.03	4.10	0.94	0.86
			miR398a-3p	*AT3G15640.1*		106	0	0.002692504	Dark/light	22.96	37.79	20.05	27.96	0.87	0.74

doi:10.6342/NTU201702588

miR398			miR398a-3p	*AT4G12610.2*	*RAP74*	964	0	0.009659137	Dark	10.37	13.61	9.58	10.41	0.92	0.76
			miR398a-3p	*AT5G14550.1*		1662	2	0.049377248	Light	10.76	15.35	8.34	9.13	0.78	0.60
			miR398b-3p	*AT2G28190.1*	*CSD2*	487	0	0.004841287	Dark/light	28.74	23.19	67.21	33.02	2.34	1.42
miR400	32	4	miR400	*AT1G06580.1*	*PPR*	1096	0	0.000539082	Dark/light	1.36	1.47	1.17	1.22	0.86	0.83
			miR400	*AT2G31400.1*	*GUN1*	1605	0	0.002692504	Dark/light	57.08	54.17	123.80	116.61	2.17	2.15
			miR400	*AT1G62720.1*	*NG1 (PPR)*	996	0	0.001077873	Dark/light	0.10	0.28	0.69	0.34	6.95	1.23
			miR400	*AT3G16710.1*	*PPR*	996	0	0.003230135	Dark/light	0.92	1.20	1.01	1.54	1.10	1.29
miR401	10	1	miR401	*AT1G74260.1*	*PUR4*	3411	0	0.013378686	Light	16.48	12.70	16.33	11.59	0.99	0.91
miR403	19	1	miR403-3p	*AT1G31280.1*	*AGO2*	3233	0	0.000539082	Dark/light	6.48	8.38	5.81	8.29	0.90	0.99
miR404	3	1	miR404	*AT4G29150.1*	*IQD25*	302	0	0.017798354	Light	0.06	0.05	0.13	0.22	2.13	4.80
miR408	10	3	miR408-3p	*AT2G47020.1*		1501	2	0.049377248	Light	2.13	2.45	1.90	1.39	0.89	0.57
			miR408-5p	*AT2G47020.1*		1568	2	0.049377248	Light	2.13	2.45	1.90	1.39	0.89	0.57
miR413	28	1	miR413	*AT1G09932.1*		339	0	0.016046673	Dark	1.02	2.12	0.74	0.83	0.72	0.39
miR447	35	2	miR447c-3p	*AT1G26370.1*		819	0	0.041217074	Dark	6.30	5.88	6.45	6.03	1.02	1.03
			miR447c-3p	*AT3G31370.1*		218	0	0.024390761	Dark	0.00	0.00	0.00	0.00	-	-
			miR472-3p	*AT5G43740.1*	*CC-NBS-LRR*	617	2	0.049377248	Light	0.52	0.58	1.43	1.55	2.73	2.70
miR5022	6	1	miR5022	*AT5G52060.1*	*BAG1*	1453	2	0.049377248	Light	34.56	57.19	41.51	94.52	1.20	1.65
miR5024	14	2	miR5024-5p	*AT3G02750.3*		2115	2	0.049377248	Light	44.56	39.83	31.99	29.59	0.72	0.74
miR5635	9	1	miR5635b	*AT3G02010.1*	*PPR*	85	0	0.043366966	Light	0.41	0.24	0.73	0.43	1.80	1.84
miR5638	10	1	miR5638b	*AT1G12775.1*	*PPR*	1836	1	0.023499149	Light	0.93	1.78	1.43	2.31	1.54	1.30
miR5648	30	2	miR5648-3p	*AT4G04710.1*	*CPK22*	388	0	0.036902785	Light	0.51	0.76	0.37	0.30	0.71	0.40
			miR5648-3p	*AT5G14890.1*		885	0	0.021865716	Dark/light	1.51	0.86	1.79	0.88	1.18	1.03
miR5998	33	1	miR5998a	*AT1G68250.1*		142	0	0.028174522	Dark/light	6.72	0.90	7.86	0.99	1.17	1.09
miR822	15	1	miR822-3p	*AT1G19390.1*		1648	0	0.04118748	Dark/light	0.62	0.39	0.27	0.04	0.44	0.09
miR823	6	1	miR823	*AT1G69770.1*	*CMT3*	2037	0	0.000539082	Dark/light	4.19	5.48	3.69	7.37	0.88	1.35
			miR824-5p	*AT3G57230.1*	*AGL16*	796	0	0.000539082	Dark/light	8.10	17.14	3.97	7.54	0.49	0.44
miR826	12	1	miR826b	*AT3G46560.1*	*TIM9*	372	0	0.013922085	Dark	9.81	16.69	9.62	14.41	0.98	0.86
miR827	4	1	miR827	*AT1G02860.1*	*NLA*	269	0	0.000539082	Dark/light	103.83	57.89	78.61	26.30	0.76	0.45
miR830	24	2	miR830-3p	*AT2G17360.1*	*RPS4A*	49	0	0.039635172	Dark/light	63.23	82.31	56.08	79.72	0.89	0.97
			miR830-5p	*AT3G56730.2*		516	0	0.04993662	Dark	1.38	0.79	1.23	0.87	0.89	1.10
miR838	111	1	miR838	*AT5G60548.1*	*CPuORF62*	639	1	0.035548599	Dark	10.17	17.18	11.95	16.08	1.18	0.94
miR840	16	1	miR840-3p	*AT3G48350.1*	*CEP3*	960	0	0.037042404	Dark	6.21	8.38	52.96	103.99	8.53	12.42
miR846	37	1	miR846-3p	*AT5G49850.1*		799	0	0.001616374	Dark	0.27	1.61	0.20	1.06	0.74	0.66
miR854	76	1	miR854c	*AT4G00180.1*	*YAB3*	563	1	0.040228018	Light	10.93	19.49	16.83	17.85	1.54	0.92
miR858			miR858a	*AT5G49330.1*	*MYB111*	386	0	0.009659137	Dark/light	0.18	3.24	0.37	5.12	2.03	1.58
			miR858a	*AT1G06180.1*	*MYB13*	403	0	0.01179291	Dark/light	0.49	0.74	4.89	10.16	10.07	13.82
			miR858a	*AT1G66230.1*	*MYB20*	469	0	0.008590523	Dark/light	5.20	5.60	5.83	4.15	1.12	0.74
			miR858b	*AT3G17140.1*		62	0	0.024390761	Light	0.00	0.00	0.00	0.00	-	-
			miR858b	*AT3G49690.1*	*MYB84*	509	0	0.018900174	Light	1.32	1.38	2.52	2.98	1.91	2.16
miR862	9	1	miR862-5p	*AT4G26095.1*		1127	0	0.018166683	Dark/light	0.00	0.00	0.00	0.00	-	-
			miR864-3p	*AT5G31662.1*		261	0	0.039117177	Dark/light	0.00	0.00	0.00	0.00	-	-
miR868	14	2	miR868-3p	*AT4G25160.1*		1555	1	0.003007558	Light	0.20	0.90	0.06	0.12	0.28	0.14
			miR868-5p	*AT4G31310.1*		553	0	0.020810274	Dark	4.55	8.30	5.10	8.70	1.12	1.05
miR870	23	2	miR870-3p	*AT4G39050.1*		3245	1	0.010708195	Dark	13.84	17.04	12.53	14.93	0.90	0.88
			miR870-3p	*AT4G34160.1*	*CYCD3;1*	710	0	0.047885208	Dark	4.20	6.00	7.88	12.95	1.88	2.16
TAS2	-	4	phasiR_11	*AT5G03090.1*		151	0	0.035483385	Dark	4.22	2.82	4.36	3.68	1.03	1.30
			phasiR_17	*AT1G10110.1*		917	1	0.043114588	Light	0.56	0.48	0.40	0.30	0.71	0.62
			phasiR_18	*AT5G18065.1*		737	2	0.049377248	Light	1.46	2.07	1.47	2.63	1.01	1.27
PPR RFL9	-	1	phasiR_23	*AT5G15400.1*		3019	2	0.049377248	Light	14.36	16.35	14.54	13.14	1.01	0.80

doi:10.6342/NTU201702588

TAS1a	-	4	phasiR_3	*AT2G27400.1*	*TAS1A*	514	2	0.049377248	Light	0.12	0.06	0.22	0.14	1.87	2.40
			phasiR_43	*AT4G07830.1*		2434	0	0.033921841	Dark	0.11	0.08	0.07	0.07	0.60	0.90
			phasiR_45	*AT1G51055.1*		376	0	0.004841287	Dark	0.00	0.03	0.04	0.09	-	2.70
			phasiR_50	*AT2G39675.1*	*TAS1C*	473	2	0.049377248	Light	0.07	0.00	0.17	0.19	2.49	-
TAS1c	-	4	phasiR_51	*AT5G50460.1*		236	1	0.043569568	Light	27.04	43.20	40.57	61.37	1.50	1.42
			phasiR_53	*AT3G20540.2*	*POLGAMMA1*	2963	1	0.015572056	Light	13.66	10.51	17.79	13.52	1.30	1.29
			phasiR_57	*AT3G17185.1*	*TAS3*	396	2	0.049377248	Light	0.23	0.23	0.67	0.32	2.89	1.37
			phasiR_6	*AT1G52790.1*		181	1	0.000556704	Dark	0.28	0.31	0.23	0.57	0.82	1.86
TAS3	-	1	phasiR_8	*AT3G17720.1*		431	1	0.027097795	Dark	0.04	0.00	0.05	0.00	1.41	-

Category 4: Just one read at that position
Category 3: >1 read, but below or equal to the average depth of coverage on the transcript

Category 2: >1 read, above the average depth, but not the maximum on the transcript
Cateogry 1: >1 read, equal to the maximum on the transcript, when there is >1 position at maximum value
Cateogry 0: >1 read, equal to the maximum on the transcript, when there is just 1 position at the maximum value

For reference, please see http://sites.psu.edu/axtell/software/cleaveland4/

Source of mRNA level information:

The Plant Cell 2013; 25:3699-710.

doi:10.6342/NTU201702588

Table 7. siRNA-mRNA pairs from cross comparisons of sRNA transcriptome and mRNA degradome.

sRNA	Sequence	Target	Target gene	Cleavage site	CleaveLand Category	p-value	Identified condition	Dark_RPKM (Repeat 1)	Dark_RPKM (Repeat 2)	W4h_RPKM (Repeat 1)	W4h_RPKM (Repeat 2)
sRNA4758723	AGACCCAGTCCCGGACGTCTCGGC	*AT1G01470.1*	*LEA14*	453	1	0.002375141	Light	53.54	52.10	85.19	82.33
sRNA12145183	CGCCGGAACTACTTGAGATTATGG	*AT1G03106.1*		709	0	0.008382784	Light	53.54	52.10	85.19	82.33
sRNA16978125	GGAGATTCTCATGGATAAGGCTT	*AT1G06970.1*	*CHX14*	1977	0	0.027125887	Dark	10.35	6.33	6.14	1.84
sRNA21191644	TCGAGAATTTCTGGAAGGGCT	*AT1G07160.1*		838	0	0.034196501	Light	0.06	0.12	0.03	0.14
sRNA20788705	TCCATCAAAGATCGTACGGCT	*AT1G07250.1*	*UGT71C4*	1358	2	0.049377248	Light	0.03	0.07	0.05	0.17
sRNA5813552	AGGAGAAGAAGGAACCGAGAA	*AT1G07640.3*	*OBP2*	1217	1	0.02628168	Light	19.27	13.34	25.66	20.34
sRNA3230120	ACCAACTAAGAACGGCCATGCACC	*AT1G07890.3*	*APX1*	848	0	0.002692504	Dark/light	10.67	8.50	11.61	9.16
sRNA19546430	TACCATCTGGAATACTTGAACT	*AT1G11180.2*	*SCAMP2*	599	0	0.028698415	Dark	133.74	215.28	215.09	352.46
sRNA23813697	TTATCAAGATCCATCTTACTC	*AT1G12775.1*		1514	0	0.004304526	Dark	15.55	9.22	16.53	13.17
sRNA3726636	ACGAGACAGAAACAGAGGCGGAGC	*AT1G13250.1*	*GATL3*	859	0	0.008055784	Dark/light	0.93	1.78	1.43	2.31
sRNA22218664	TGACAGAAGTGAGTGAGCAC	*AT1G13380.1*		13	0	0.028698415	Dark/light	6.81	11.18	9.64	14.55
sRNA7677998	ATCGTGGATCTTGGGCGGTACCA	*AT1G14940.1*		95	0	0.01179291	Dark/light	15.92	16.17	17.05	17.65
sRNA15263601	GAGGGAGACGGAAGAGATAGAATC	*AT1G19660.1*		33	0	0.008055784	Dark/light	0.09	0.03	0.00	0.02
sRNA5882784	AGGAGTTCGTAGTCTCCGGGTCGG	*AT1G20390.1*	TE	2700	0	0.024499347	Dark/light	105.59	54.23	102.86	53.70
sRNA9982741	CATCACCAGATCTTTTGTCGG	*AT1G22065.1*		255	1	0.034294636	Dark	17.83	38.65	14.67	17.16
sRNA21261407	TCGCACGGCGGTCTGACAGGT	*AT1G23320.1*	*TAR1*	369	0	0.014453662	Dark	7.27	3.16	7.85	1.95
sRNA22633394	TGCCATCTTGAGATTGTAAGGA	*AT1G25055.1*		1366	1	0.013825019	Dark	0.00	0.00	0.00	0.00
sRNA22633394	TGCCATCTTGAGATTGTAAGGA	*AT1G25211.1*		1343	1	0.014739862	Dark	1.25	0.95	1.40	0.88
sRNA3070270	ACAGGAGGAGCAGAGGCTGAAGCC	*AT1G25420.1*		879	1	0.001267444	Light	83.85	55.26	77.46	47.42
sRNA3514973	ACCGGAAACCCCTGAAATTCCAGA	*AT1G25422.1*		821	0	0.006449836	Dark	12.99	14.04	14.02	12.18
sRNA25165781	TTTGGCATTCTGTCCACCTCC	*AT1G27340.1*	*LCR*	1384	2	0.049377248	Light	0.02	0.10	0.27	0.43
sRNA22213130	TGACAGAAGAGAGTGAGCACTCT	*AT1G34044.1*		420	0	0.016046673	Dark	25.07	27.12	25.71	27.93
sRNA20686690	TCATTCCGGACATCTCCCATTT	*AT1G35980.1*	Pseudogene	335	0	0.034738366	Light	0.23	0.75	0.14	0.21
sRNA8142022	ATGGCAGAGTGAATGAACCGGGAT	*AT1G37340.1*	TE	1671	0	0.005913942	Dark/light	0.00	0.00	0.00	0.00
sRNA1565034	AAGACAGATTGGGATGGTTCTGCT	*AT1G40100.1*		64	0	0.017637109	Dark/light	0.00	0.00	0.00	0.00
sRNA21122202	TCCTTGTGCTCGAGTGTCTGGTTG	*AT1G41726.1*	TE	370	0	0.016046673	Dark/light	0.00	0.00	0.00	0.00
sRNA8854813	ATTTGTTTCGTCAACACGTTGGGT	*AT1G41870.1*	TE	435	0	0.016695296	Light	0.00	0.00	0.00	0.00
sRNA10450109	CCATCGAGTCTTTGAACGCA	*AT1G47420.1*	*SDH5*	407	2	0.049377248	Light	0.00	0.00	0.00	0.00
sRNA2580695	AATGTCGGATCACCCTTTAAGCGG	*AT1G47870.1*	*E2FC*	811	0	0.0106063	Light	59.06	77.42	55.20	72.06
sRNA6486298	AGTGAACAGATTGAGTGCATC	*AT1G51860.1*		2620	0	0.012858071	Dark	2.47	3.71	2.52	3.87
sRNA15286383	GAGGTAAAGATGAAAAGGACT	*AT1G52850.1*	TE	277	1	0.004444964	Dark	0.16	0.62	0.30	0.33
sRNA15865969	GCACATGCGTATTAGGAAGGACA	*AT1G54750.1*	TE	146	0	0.022198223	Light	0.00	0.00	0.01	0.00
sRNA6063884	AGGCTTACAAGATCGGGTTGCGGT	*AT1G56610.1*		1650	0	0.01393223	Light	0.12	0.00	0.07	0.03
sRNA13414160	CTGAAAGTGACTACATCGGGG	*AT1G62670.1*	*RPF2*	980	0	0.000539082	Dark/light	4.01	3.34	4.20	3.34
sRNA25350469	TTTTGCATATACTCGAATACC	*AT1G62930.1*	*RPF3*	1469	0	0.001616374	Dark/light	1.26	2.33	1.45	2.03
sRNA24307275	TTGAAAGTGACTACATCGGGA	*AT1G63080.1*		1512	0	0.003230135	Dark/light	2.81	4.77	3.10	3.91
sRNA25350469	TTTTGCATATACTCGAATACC	*AT1G63080.1*		1512	0	0.003230135	Dark/light	1.34	2.37	1.82	2.40
sRNA20045769	TATATCCCATTTCTACCATCTG	*AT1G63130.1*		662	0	0.001616374	Dark/light	1.34	2.37	1.82	2.40
sRNA20045777	TATATCCCATTTCTACCATCTGT	*AT1G63130.1*		662	0	0.001616374	Dark/light	3.00	6.04	4.37	7.18
sRNA20045769	TATATCCCATTTCTACCATCTG	*AT1G63150.1*		547	0	0.030268401	Dark/light	3.00	6.04	4.37	7.18
sRNA22216991	TGACAGAAGAGATTGAGCACC	*AT1G64600.1*		894	0	0.012325634	Dark	1.02	2.21	1.26	1.90
sRNA3734086	ACGAGAGTGCAGAAGTCGTCCGCT	*AT1G65590.1*	*HEXO3*	1671	0	0.024390761	Light	1.59	1.67	1.84	1.64
sRNA21039116	TCCGTTGTAGTCTAGCTGGTC	*AT1G67328.1*		867	0	0.016046673	Dark	53.50	38.72	53.89	26.16
sRNA22211284	TGACAGAAGAGAGTGAGCACG	*AT1G69170.1*		1307	2	0.049377248	Light	0.00	0.00	0.00	0.00

doi:10.6342/NTU201702588

sRNA22580969	TGCACTGCCTCTTCCCTGGCTT	*AT1G72230.1*		823	0	0.010726599	Dark/light	1.64	4.08	1.81	3.73
sRNA22401838	TGAGGATGGATTAGATTAGGGTAA	*AT1G74045.1*	*TET17*	563	0	0.010193012	Dark	28.26	30.59	29.69	39.83
sRNA11858555	CGAGAATCGTTGTTTCGGCTTCA	*AT1G76640.1*		184	0	0.02962277	Dark	0.00	0.00	0.00	0.00
sRNA3664172	ACCTTTAAGTACTTTTTCGGGCA	*AT1G77300.1*	*EFS*	3273	0	0.048911467	Dark/light	0.20	1.04	0.00	0.11
sRNA5727320	AGGAAGAGAGGATGATTTAGGAAC	*AT1G79890.1*		1942	0	0.03808035	Dark	12.38	8.81	15.08	9.22
sRNA15424431	GATAAGGTTTAGTGGACTTCT	*AT2G01010.1*		1738	2	0.049377248	Light	0.34	0.99	0.42	0.64
sRNA6105008	AGGGACGTAGTCAACGCGAGCTA	*AT2G01010.1*		1618	2	0.049377248	Light	76.80	67.18	52.51	55.76
sRNA20821085	TCCCAAATGTAGCCAAAGCA	*AT2G01130.1*		308	0	0.022920021	Dark/light	76.80	67.18	52.51	55.76
sRNA22580969	TGCACTGCCTCTTCCCTGGCTT	*AT2G02850.1*	*ARPN*	107	0	0.001077873	Dark/light	4.16	6.23	2.96	3.41
sRNA1120530	AACCCATTGATCAGTGAACTA	*AT2G05185.1*		226	0	0.025025222	Dark	0.99	3.47	1.71	3.31
sRNA24037552	TTCCGAGAAGTGATTGTCGAAACC	*AT2G06390.1*	TE	17	0	0.001077873	Dark	1.40	4.16	1.34	3.54
sRNA3642520	ACCTGTAGCGTTCGTGATTGGCCT	*AT2G07711.1*		450	2	0.049377248	Light	0.17	0.00	0.18	0.00
sRNA12272336	CGGAAAATTCAGGAGAACATGATC	*AT2G13570.1*	*NF-YB7*	40	0	0.007826124	Light	7.99	4.94	5.50	4.34
sRNA5362550	AGCACATGTAGAGAAGGTTTGG	*AT2G14720.1*	*MTV4*	1854	0	0.042737279	Dark/light	0.00	0.03	0.04	0.03
sRNA6200968	AGGGTAAACATAGATTGTGATTGT	*AT2G19470.1*	*ckl5*	1160	0	0.008055784	Dark/light	49.00	41.48	39.45	33.69
sRNA2140823	AAGTGCATTCGGGTCATATGGTAC	*AT2G21550.1*		501	0	0.012858071	Dark	11.41	13.76	13.83	15.39
sRNA4493483	AGAACATGATCGTTTGGTACGAAT	*AT2G25355.1*		346	0	0.0111614	Light	1.26	4.72	1.92	4.60
sRNA4566467	AGAAGAGAAGTAGAAACAGAGTT	*AT2G26210.1*		77	0	0.048911467	Dark	1.35	1.67	2.05	2.55
sRNA4846714	AGACTGTGAAACTGCGAATGG	*AT2G26760.1*	*CYCB1;4*	13	2	0.049377248	Light	40.04	31.46	19.02	16.37
sRNA8325932	ATGTTGTGATGATGGTTGTATAGC	*AT2G28810.1*		1055	0	0.047885208	Dark	11.45	12.81	7.30	10.22
sRNA18072336	GTAGAGGACGTTAGCCATTGCTTT	*AT2G29290.2*		985	0	0.015591	Light	5.18	4.59	4.78	4.46
sRNA24281184	TTCTTGACCTTGTAAGACCC	*AT2G33860.1*		1685	0	0.000539082	Dark/light	0.72	2.41	15.13	13.41
sRNA24281186	TTCTTGACCTTGTAAGACCCC	*AT2G33860.1*	*ETT*	1685	0	0.000539082	Dark/light	7.85	7.54	10.75	13.17
sRNA25028402	TTTCTTGACCTTGTAAGACCC	*AT2G33860.1*		1685	0	0.000539082	Dark/light	7.85	7.54	10.75	13.17
sRNA24409539	TTGATAAGTAGATTGCCTTGGC	*AT2G35530.1*	*bZIP16*	1677	0	0.021865716	Dark	7.85	7.54	10.75	13.17
sRNA24100543	TTCGAGAATCGTTGTTTCGGCTA	*AT2G38560.1*	*TFIIS*	221	0	0.029850621	Light	5.43	6.48	7.28	7.54
sRNA5250676	AGATGATGGGCTTAGATGATTGGC	*AT2G39120.1*	*WTF9*	145	0	0.008382784	Light	17.84	15.99	17.79	14.75
sRNA11262654	CCGGATCACCAGCTAAGGCC	*AT2G39210.1*		1685	0	0.025550813	Dark	1.12	0.63	2.11	0.91
sRNA19382772	TAAGTAACTGTATTAGCAACT	*AT2G39675.1*	*TAS1C*	579	2	0.049377248	Light	94.84	38.44	51.84	13.62
sRNA20045777	TATATCCCATTTCTACCATCTGT	*AT2G39681.1*	*TAS2*	418	0	0.009124974	Dark/light	0.07	0.00	0.17	0.19
sRNA25264601	TTTTACGGGGATAAGACTGAA	*AT2G39681.1*	*TAS2*	563	2	0.049377248	Light	0.10	0.10	0.09	0.12
sRNA22580951	TGCACTGCCTCTTCCCTGGCTC	*AT2G44790.1*	*UCC2*	709	0	0.003767475	Dark/light	0.10	0.10	0.09	0.12
sRNA19359176	TAAGCTTCATCGTCGAGAGGGA	*AT2G45000.1*	*EMB2766*	1958	1	0.00474464	Light	360.67	283.46	149.01	78.37
sRNA12297780	CGGAATCGAGAGCTCCAAGTG	*AT2G45530.1*		674	0	0.008055784	Dark	10.69	7.31	11.98	5.86
sRNA24345808	TTGACAGAAGATACAGAGCAC	*AT2G46080.1*	*BPS2*	1216	0	0.041704358	Dark/light	23.99	12.25	17.13	10.87
sRNA7986567	ATGCACTGCCTCTTCCCTGGCTC	*AT2G47020.1*		1501	2	0.049377248	Light	25.63	18.95	36.60	25.42
sRNA24621975	TTGGGCGAGAGTAGTACTAGGA	*AT2G47730.1*	*GSTF8*	1454	0	0.021865716	Dark/light	2.13	2.45	1.90	1.39
sRNA4970854	AGAGAGTCAAAGAGTGCTTG	*AT2G47730.1*		1454	0	0.021865716	Dark/light	91.98	92.77	162.50	129.38
sRNA4897389	AGAGAAGTAGAAACAGAGTTT	*AT3G02555.1*		18	1	0.001113098	Dark	91.98	92.77	162.50	129.38
sRNA19409117	TAATAGGCAGAACCCAAATGGC	*AT3G06435.1*		1493	0	0.000539082	Dark/light	11.12	11.90	9.84	10.29
sRNA19898258	TAGGCAGAACCCAAATGGCTGG	*AT3G06435.1*		593	2	0.049377248	Light	1.58	1.32	1.06	0.65
sRNA22831528	TGGACAATGAATCAGAAGCAT	*AT3G06435.1*		1493	0	0.000539082	Dark/light	1.58	1.32	1.06	0.65
sRNA8105427	ATGGAGAGGAACAACAATGGAGAT	*AT3G07273.1*		54	0	0.003361584	Light	1.58	1.32	1.06	0.65
sRNA20978904	TCCGGAAGTGCTCGTGCGTGC	*AT3G07350.1*		829	0	0.028215879	Light	15.75	10.95	10.84	5.74
sRNA7115903	ATAGTTTGTTTGATGGTAAC	*AT3G13750.1*	*BGAL1*	2618	2	0.049377248	Light	36.41	6.50	24.91	6.65
sRNA22286734	TGACTCGAACGAATTAGAGGT	*AT3G17185.1*	*TAS3*	439	2	0.049377248	Light	469.89	153.12	634.22	130.05
sRNA7015962	ATAGAGAACGACAATGATTTTGAA	*AT3G18485.1*	*ILR2*	846	0	0.018900174	Light	0.23	0.23	0.67	0.32
sRNA23731940	TTAGATTCACGCACAAACTCC	*AT3G22590.1*	*CDC73*	1294	0	0.028174522	Dark	0.18	0.14	0.63	0.30
sRNA6715395	ATAAACCCGTCTGACTCCTGGTGT	*AT3G23540.1*		1872	0	0.00615427	Light	4.41	7.35	5.57	7.87

doi:10.6342/NTU201702588

sRNA16051497	GCATTTTCGTGATTTGGGCTATA	*AT3G24030.1*		759	0	0.038522914	Light	21.74	17.39	21.85	15.70
sRNA4751527	AGACCAAGGATCTGATGGGGAAGG	*AT3G30837.1*	TE	1952	0	0.002692504	Dark/light	6.50	10.05	7.27	7.79
sRNA1443796	AACTTGACACATCAGCACATGAGA	*AT3G42433.1*	TE	1619	2	0.049377248	Light	0.00	0.00	0.02	0.00
sRNA14331062	GAAGAGGAACTCCAACGGCTATT	*AT3G47750.1*	*ABCA4*	1435	0	0.021338137	Dark	0.00	0.00	0.01	0.00
sRNA17035978	GGAGTACAAGGAAAAGGTAAAACT	*AT3G50480.1*	*HR4*	972	2	0.049377248	Light	0.85	2.82	2.41	4.87
sRNA24997818	TTTCTACCATCCGATCAACAAG	*AT3G52570.1*		643	0	0.015591	Light	26.43	15.44	11.15	2.85
sRNA383725	AAACCCAGAAGTTGATCGGCGAGT	*AT3G53850.1*		253	1	0.002410147	Dark	8.27	13.16	3.82	5.13
sRNA17382479	GGGACAATAATAGAGATAAGGAGA	*AT3G54410.1*		459	1	0.007765716	Dark/light	3.38	6.07	6.61	8.22
sRNA23735193	TTAGCAACTGTTCTTTAGACGT	*AT3G55605.1*		637	1	0.012176161	Dark/light	0.23	0.18	0.17	0.04
sRNA17353593	GGGAAAGACTTTGAAATTGGCATC	*AT3G60500.1*	*CER7*	1224	0	0.004444964	Dark	2.80	4.22	3.71	4.70
sRNA22983846	TGGCCTTGAAGACGACGACTCTGT	*AT3G60930.1*	TE	1570	0	0.028761099	Light	3.91	6.05	3.55	5.75
sRNA1715666	AAGATTCCCGGTCGTGACAGCGTT	*AT3G63220.2*		925	0	0.004841287	Dark/light	4.26	2.78	2.00	1.33
sRNA24253714	TTCTGGGCTGAAGCGCGTAATTCC	*AT4G00120.1*	*EDA33*	1511	2	0.049377248	Light	10.45	7.26	8.84	5.41
sRNA24991825	TTTCGTGGAGAATGAAATCACA	*AT4G02540.1*		1780	2	0.049377248	Light	0.03	0.01	0.00	0.01
sRNA7994867	ATGCAGTGGGACAACAATGGAGAT	*AT4G03410.2*		761	0	0.01179291	Dark/light	19.84	24.70	15.59	21.31
sRNA12725338	CGTGATTTGGGCTATATTACGGA	*AT4G06477.1*	TE	3826	2	0.049377248	Light	2.52	1.92	2.55	2.38
sRNA14689129	GACCTTTAAGTACTTTTTCGGGCC	*AT4G06477.1*	TE	3854	2	0.049377248	Light	1.24	0.31	2.55	0.26
sRNA18118622	GTAGTACTAGGATGGCTGACCTCC	*AT4G06477.1*	TE	4069	2	0.049377248	Light	1.24	0.31	2.55	0.26
sRNA18462938	GTGATTTGGGCTATATTACGGACC	*AT4G06477.1*	TE	3825	2	0.049377248	Light	1.24	0.31	2.55	0.26
sRNA19950377	TAGTACTAGGATGGGTGACC	*AT4G06477.1*	TE	4068	2	0.049377248	Light	1.24	0.31	2.55	0.26
sRNA24975580	TTTCGGAAAGCCCAAAGACAGCCC	*AT4G06477.1*	TE	3938	2	0.049377248	Light	1.24	0.31	2.55	0.26
sRNA3664171	ACCTTTAAGTACTTTTTCGGGC	*AT4G06477.1*	TE	3853	2	0.049377248	Light	1.24	0.31	2.55	0.26
sRNA4363923	ACTTGGCATGTGATACTTTTTCGG	*AT4G06477.1*	TE	3956	2	0.049377248	Light	1.24	0.31	2.55	0.26
sRNA4770560	AGACCGTGAGGCCAAACTTGGCAT	*AT4G06477.1*	TE	3971	2	0.049377248	Light	1.24	0.31	2.55	0.26
sRNA5588482	AGCGTGCTTGGGCGAGAGTAGTAC	*AT4G06477.1*	TE	4086	2	0.049377248	Light	1.24	0.31	2.55	0.26
sRNA644135	AAAGCTCGTTAAGACTAGATGGG	*AT4G06477.1*	TE	4251	2	0.049377248	Light	1.24	0.31	2.55	0.26
sRNA7881398	ATGACTCTATAACTTCTATACCGT	*AT4G06477.1*	TE	3988	2	0.049377248	Light	1.24	0.31	2.55	0.26
sRNA8145530	ATGGCATGTGATACCTTTTCGGAA	*AT4G06477.1*	TE	3954	2	0.049377248	Light	1.24	0.31	2.55	0.26
sRNA8288131	ATGTGATACCTTTTCGGAAAGCCC	*AT4G06477.1*	TE	3949	2	0.049377248	Light	1.24	0.31	2.55	0.26
sRNA22983846	TGGCCTTGAAGACGACGACTCTGT	*AT4G06603.1*	TE	1745	0	0.029850621	Light	1.24	0.31	2.55	0.26
sRNA24579151	TTGGCAGAAGATAGAGAGCAC	*AT4G08850.1*		3260	0	0.026601145	Dark	0.02	0.00	0.01	0.00
sRNA1627261	AAGAGAGGATGATCTAGGAACTC	*AT4G09020.1*	*ISA3*	1573	0	0.03311186	Light	34.31	20.25	28.47	13.98
sRNA7545550	ATCCTACGTTCTTCCATACTCTGA	*AT4G12640.1*		1138	0	0.028698415	Dark/light	2.89	5.48	3.12	4.97
sRNA11040075	CCCTTGAAAATCCGGAGGAC	*AT4G14165.1*		578	0	0.005038136	Light	7.93	8.23	6.95	6.39
sRNA5080336	AGAGGATGGAGAGGGTAGACCGTT	*AT4G16900.1*		3306	0	0.03235777	Dark/light	0.03	0.05	0.08	0.02
sRNA20477977	TCACTCGGAGCATAGACACAAA	*AT4G18100.1*		561	0	0.006711868	Light	7.09	9.37	4.67	5.61
sRNA21024034	TCCGTAGTCTGTAGAATGGTTA	*AT4G19400.1*		415	0	0.029745355	Dark/light	86.30	141.16	76.09	115.09
sRNA14880318	GAGAAGATTGAGACGACATGGTT	*AT4G21940.2*	*CPK15*	148	0	0.038522914	Light	0.52	0.58	0.30	0.64
sRNA17917194	GGTTTCGTGGTGTAGTTGGTTATC	*AT4G24830.1*		1406	1	0.011258938	Dark	0.32	0.51	0.82	1.20
sRNA1600791	AAGAGAAACCTTGAATCGATGCGG	*AT4G26400.2*		1257	0	0.0111614	Light	5.63	11.19	11.75	19.14
sRNA7545550	ATCCTACGTTCTTCCATACTCTGA	*AT4G27880.1*		883	1	0.013458845	Dark	28.81	33.99	14.43	9.25
sRNA24004565	TTCCATGAGAGCTTTGAGGCATA	*AT4G29210.1*	*GGT4*	2062	1	0.028361103	Dark/light	21.76	18.64	14.68	12.68
sRNA8495680	ATTCCATGAGAGCTTTGAGGCATA	*AT4G29210.1*		2062	0	0.028361103	Dark/light	18.62	24.42	20.89	21.86
sRNA25048695	TTTGAAGAGAAGATTGTATTGGCT	*AT4G36090.3*		1437	0	0.034442636	Dark	18.62	24.42	20.89	21.86
sRNA20756113	TCCACTGTAACCTCGTCGGGTTTG	*AT4G37409.1*		1067	0	0.044799783	Dark/light	4.83	5.80	4.09	4.40
sRNA20756113	TCCACTGTAACCTCGTCGGGTTTG	*AT4G37432.1*		671	0	0.045314714	Dark	0.00	0.00	0.34	0.28
sRNA14975183	GAGAGATGGCTGAGTGGACT	*AT4G38280.1*		498	0	0.045829367	Dark/light	0.04	0.00	0.00	0.00
sRNA22628530	TGCCAGAAGAGAGTGAGCAC	*AT4G38920.1*	*ATVHA-C3*	405	2	0.049377248	Light	10.98	16.22	8.91	10.39
sRNA24461846	TTGCCAGAAGAGAGTGAGCAC	*AT4G38920.1*	*ATVHA-C3*	406	2	0.049377248	Light	118.92	163.51	100.18	126.33

doi:10.6342/NTU201702588

sRNA10431761	CCATACATGAATAATAATTACC	*AT5G02350.1*		1219	0	0.000539082	Dark/light	118.92	163.51	100.18	126.33
sRNA17917194	GGTTTCGTGGTGTAGTTGGTTATC	*AT5G03415.1*	*DPB*	1387	0	0.020000758	Light	0.39	1.22	0.30	0.52
sRNA10033004	CATCTACTTACACTTAAGGTCG	*AT5G03552.1*	*MIR822A*	13	0	0.000539082	Dark/light	5.84	5.04	6.18	4.97
sRNA11592679	CCTTACTATGTCTGGACCTGGTA	*AT5G06300.1*	*LOG7*	728	0	0.01945062	Light	11.11	26.47	4.57	4.01
sRNA14721190	GACGATGGAGAGGCGGTGAGAAGC	*AT5G07370.2*	*IPK2A*	70	0	0.039635172	Dark	13.93	9.63	10.44	5.73
sRNA17160439	GGCAGAGAGAAATGGATCGTCGTC	*AT5G08120.1*	*MBP2C*	342	0	0.009124974	Dark/light	21.64	35.33	25.41	30.81
sRNA21239183	TCGATGAAGTCTCGGACCTGGTC	*AT5G10230.1*	*ANNAT7*	541	0	0.019224975	Dark	12.10	13.06	9.07	9.91
sRNA21253276	TCGCAAATGTAGACAAAGCA	*AT5G10540.1*		1960	0	0.001682207	Light	1.00	1.78	1.00	3.29
sRNA4654106	AGAATACGCGGCGCTTTCGGAGAA	*AT5G15070.2*		3231	0	0.005377759	Dark	37.61	29.26	20.13	19.75
sRNA24945576	TTTCCGAGTGACTGAGAATTGGCG	*AT5G15490.1*	*UGD3*	1311	0	0.012325634	Dark/light	0.95	2.55	0.75	1.11
sRNA13414160	CTGAAAGTGACTACATCGGGG	*AT5G16640.1*		825	0	0.01179291	Dark	27.62	60.78	27.28	43.82
sRNA19366519	TAAGGAGGTGGAAGATGATTCTA	*AT5G17040.1*		825	0	0.023295107	Light	0.73	0.86	1.28	1.21
sRNA9893496	CAGTCGAAGAATGAACGTAGTTGC	*AT5G22110.1*	*DPB2*	1440	0	0.041704358	Dark/light	0.05	0.21	0.03	0.77
sRNA1120530	AACCCATTGATCAGTGAACTA	*AT5G22608.2*		248	0	0.025550813	Dark	0.68	1.32	0.84	1.43
sRNA24059876	TTCCTAAATGTAGACAAAGCA	*AT5G23070.1*		767	1	0.00789522	Light	4.45	5.09	3.54	3.11
sRNA16962147	GGAGAGGGTGTAGAGGTAAGGCTC	*AT5G25475.4*		196	0	0.036523011	Dark/light	4.54	4.12	8.50	8.33
sRNA22983846	TGGCCTTGAAGACGACGACTCTGT	*AT5G28430.1*	TE	845	0	0.028215879	Light	1.86	2.63	1.50	1.30
sRNA906968	AAATTTGAATGATGCGTCGCCAGC	*AT5G32408.1*	TE	1006	0	0.002242313	Light	0.94	1.79	0.63	1.13
sRNA6749118	ATAACAGGTCTGTGATGCCC	*AT5G32620.1*	TE	43	0	0.029745355	Dark	0.00	0.00	0.00	0.00
sRNA4751527	AGACCAAGGATCTGATGGGGAAGG	*AT5G32825.1*	TE	2080	1	0.003481608	Light	0.01	0.00	0.03	0.00
sRNA4751527	AGACCAAGGATCTGATGGGGAAGG	*AT5G40605.1*	TE	4486	2	0.049377248	Light	0.00	0.00	0.00	0.00
sRNA24307780	TTGAAAGTGACTACATCGGGT	*AT5G41170.1*		884	0	0.002154584	Dark/light	0.02	0.01	0.02	0.04
sRNA4869716	AGAGAAAGAGACGGAGAAATTCA	*AT5G44210.1*	*ERF9*	167	1	0.024928303	Dark	0.49	0.83	0.96	1.53
sRNA4977731	AGAGATAAGGAGACATTTTGGAGC	*AT5G45095.1*		123	0	0.024390761	Light	3.50	4.30	2.38	1.38
sRNA2977201	ACACTGAGAAGGCTGGTCATTCGG	*AT5G47010.1*	*UPF1*	3234	1	0.007213027	Dark/light	1.61	1.10	2.05	0.71
sRNA3653706	ACCTTCCGAGAAGTGATTGTCGAA	*AT5G48730.1*		257	1	0.005737686	Dark/light	32.90	22.69	35.25	20.20
sRNA1759482	AAGCAGGACAATGGAACTTTTCC	*AT5G50320.1*	*ELO3*	1506	0	0.021865716	Dark/light	2.35	4.44	5.02	5.49
sRNA21423958	TCGGGCAAGAAGAAGAAACT	*AT5G51410.1*		116	0	0.010726599	Dark	13.33	12.30	9.82	9.16
sRNA7869687	ATGACCGATAGAACCAAACCGCAT	*AT5G52250.1*	*RUP1*	990	0	0.006985441	Dark/light	17.38	17.87	12.29	12.49
sRNA23136498	TGGTACTCAGAATAAATGGATGGT	*AT5G52415.1*	Pseudogene	800	0	0.006985441	Dark/light	16.02	5.19	23.45	22.15
sRNA15022912	GAGATCAACAGATAGGAGGAGACT	*AT5G54206.1*	Pseudogene	1023	0	0.010050889	Light	0.00	0.00	0.00	0.00
sRNA25438712	TTTTTTACGGGGATAAGACTG	*AT5G55280.1*	*FTSZ1-1*	1406	0	0.04118748	Dark	0.00	0.00	0.00	0.00
sRNA25327079	TTTTCTTGACCTTGTAAGACC	*AT5G60450.1*	*ARF4*	1885	0	0.001077873	Dark/light	2.72	5.60	11.89	12.92
sRNA20756113	TCCACTGTAACCTCGTCGGGTTTG	*AT5G65160.1*	*TPR14*	1549	0	0.030938921	Light	9.22	17.63	12.68	24.91
sRNA5727320	AGGAAGAGAGGATGATTTAGGAAC	*AT5G66190.1*	*FNR1*	238	0	0.006985441	Dark	0.85	0.67	0.68	0.63
sRNA16722360	GCTTGAGAGTCTCTGTTGCGGTGG	*AT5G67600.1*	*WIH1*	252	0	0.037983174	Light	16.06	37.45	153.50	201.87
sRNA16903585	GGACTAAAGCGTTGGATTGCT	*ATCG00090.1*	*TRNS.1*	63	2	0.049377248	Light	32.75	48.11	31.76	39.00
sRNA18528735	GTGGACTAAAGCTTTGGATTGC	*ATCG00090.1*	*TRNS.1*	65	2	0.049377248	Light	374.88	259.72	592.09	245.29

TE: Transposable element.

doi:10.6342/NTU201702588

Table 8. Differentially expressed miRNAs in de-etiolating *Arabidopsis* seedlings, with average log_2 fold-change listed.

Cluster I	**W0h**	**W1h**	**W3h**	**W6h**	**W12h**	**W24h**
miR163	0	3.230582	5.070049	6.036598	5.963276	6.724631
Cluster II	**W0h**	**W1h**	**W3h**	**W6h**	**W12h**	**W24h**
miR5026	0	-0.19729	0.609021	-0.33921	0.435821	0.256526
miR825	0	-0.55657	-0.0974	0.484967	0.475439	0.143117
miR869.2	0	-0.44551	-0.24714	0.236649	-0.06937	0.766993
miR156c-3p	0	0.008901	0.458674	-0.41258	0.129615	0.571201
miR170-3p	0	0.199128	0.233507	0.359504	0.420726	-0.0398
miR2933a	0	-0.73393	0.087544	0.296233	-0.12048	0.00611
miR2933b	0	-0.73393	0.087544	0.296233	-0.12048	0.00611
miR5642a	0	-0.12856	0.102902	0.354152	0.920248	0.760898
miR157d	0	0.366314	0.311192	0.17222	0.304513	0.640368
miR167a-3p	0	0.046902	0.474899	0.574704	0.480747	0.881156
miR833b	0	1.053165	0.727714	0.849033	0.892631	0.279323
miR858a	0	0.657713	0.522465	0.833586	0.69362	0.780516
miR157a-3p	0	0.119139	0.300398	0.181048	0.842913	1.197978
miR157b-3p	0	0.112265	0.292249	0.169389	0.833254	1.186319
miR157c-3p	0	0.18009	0.174448	1.165619	1.299035	2.35774
Cluster III	**W0h**	**W1h**	**W3h**	**W6h**	**W12h**	**W24h**
miR158b	0	0.068148	-0.23119	0.046673	-0.49671	-0.77436
miR162a-3p	0	0.216902	-0.35089	-0.001	-0.53321	-1.32163
miR390a-5p	0	0.041912	-0.24039	-0.52191	-0.83531	-0.94731
miR398c-3p	0	0.233205	-0.74225	0.337007	-0.5905	-1.54736
miR399b	0	-0.32628	-0.03547	-0.57065	-0.81218	-1.16872
miR399c-3p	0	-0.13086	0.021596	-0.5015	-0.75814	-1.10903
miR829-3p.1	0	-0.19326	-0.0353	-0.14504	-0.74384	-0.90991
miR829-5p	0	0.017165	-0.29223	-0.32674	-0.66067	-0.74456
miR162b-3p	0	0.215734	-0.35239	-0.00193	-0.53434	-1.32203
miR162b-5p	0	0.057888	-0.1911	0.175723	-0.742	-1.07194
miR169a-3p	0	-0.35672	-0.10399	-0.09992	-0.43079	-0.99436
miR173-5p	0	-0.04189	-0.26578	-0.30136	-0.5118	-0.95313
miR390b-5p	0	0.041759	-0.2396	-0.52135	-0.83081	-0.94673
miR396b-3p	0	-0.19923	-0.26739	-0.52009	-0.66862	-1.11049
miR398b-3p	0	0.233205	-0.74225	0.337007	-0.5905	-1.54736
miR823	0	-0.25067	0.109541	-0.45625	-0.76484	-0.99271
miR839-5p	0	-0.9158	0.276875	-0.35478	-0.56659	-1.1664

doi:10.6342/NTU201702588

Cluster III (Continued)	W0h	W1h	W3h	W6h	W12h	W24h
miR166a-3p	0	0.141355	0.079493	-0.11147	-0.50323	-0.56368
miR166b-3p	0	0.158125	0.078693	-0.10249	-0.52608	-0.57401
miR166c	0	0.157754	0.078204	-0.10279	-0.52633	-0.57431
miR166d	0	0.1578	0.078219	-0.1028	-0.52637	-0.5743
miR166e-3p	0	0.157828	0.07835	-0.10235	-0.52615	-0.57403
miR166f	0	0.157829	0.078349	-0.10233	-0.5261	-0.574
miR166g	0	0.157513	0.077882	-0.10266	-0.52644	-0.57431
miR169b-3p	0	0.046702	0.084603	-0.51457	0.08493	-0.43209
miR169i	0	-0.21387	0.036407	-0.3923	-0.08524	-0.29972
miR171c-5p	0	-0.24785	-0.51146	-0.30205	-0.45579	-0.08671
miR319b	0	0.101478	0.007334	0.230599	-0.43223	-0.64435
miR393b-3p	0	-0.22189	-0.24646	-0.14695	-0.49096	-0.49076
miR408-3p	0	-0.24897	-0.16535	0.122217	-0.11517	-0.57962
miR5644	0	-0.46437	-0.21745	-0.08393	-0.26968	-0.45617
miR156h	0	-0.44634	-0.37253	-0.19148	-0.36689	-0.10394
miR160c-3p	0	-0.17658	-0.29051	-0.33976	-0.00825	0.041016
miR169m	0	-0.12627	0.064869	-0.27125	0.118007	-0.32789
miR166a-5p	0	-0.14566	-0.30587	-0.69082	-1.16879	-1.42452
miR395e	0	-0.52798	-0.63659	-0.291	-1.43631	-1.91425
miR5646	0	-0.55674	-0.18855	-0.6301	-1.65092	-1.82573
miR166b-5p	0	-0.14566	-0.30587	-0.69082	-1.16879	-1.42452
miR166e-5p	0	-0.49789	-0.68724	-1.10023	-1.47964	-1.73891
miR390b-3p	0	-0.32255	-0.76324	-0.65686	-1.66625	-1.99135
miR395a	0	-0.52798	-0.63659	-0.29058	-1.43631	-1.91425
miR395b	0	-0.30231	-0.53107	-0.43895	-1.02895	-2.04242
miR395c	0	-0.30231	-0.53107	-0.43895	-1.02895	-2.04242
miR395d	0	-0.52798	-0.63659	-0.29058	-1.43631	-1.91425
miR395f	0	-0.30231	-0.57998	-0.43895	-1.02895	-2.04242
miR396a-3p	0	-0.16376	-0.71517	-0.7776	-1.56218	-2.04976
miR408-5p	0	-0.44974	-0.17004	-0.65167	-1.20912	-1.72316
miR5012	0	-0.37776	-0.43595	-0.68763	-1.5225	-1.78667
miR5024-3p	0	-0.59768	-0.10816	-0.63027	-1.32052	-2.05354
miR5634	0	-0.19003	-0.51725	-0.68077	-0.88666	-1.19981

doi:10.6342/NTU201702588

Table 9. Expression levels of *GRF*s.

miRNA	Expression level (RPKM)							
miR396	W0h (R1)	W4h (R1)	W0h (R2)	W4h (R2)	Gene	Light/dark ratio (R1)	Light/dark ratio(R2)	MFE (miR396-GRF, kcal/mol)
AT2G22840	5.36	6.13	9.34	6.62	*GRF1*	1.14	0.71	-28.20
AT4G37740	3.26	4.37	12.48	4.03	*GRF2*	1.34	0.32	-28.20
AT2G364 0	6.78	10.14	10.73	8.64	*GRF3*	1.50	0.81	-28.60
AT3G52910	0.34	0.63	0.45	1.59	*GRF4*	1.84	3.54	-28.60
AT3G13960	0.59	0.72	1.27	0.91	*GRF5*	1.20	0.72	-
AT2G06200	0.27	0.26	2.64	0.85	*GRF6*	0.96	0.32	-
AT5G53660	6.98	0.26	48.90	0.26	*GRF7*	0.04	0.01	-28.10
AT4G24150	0.55	0.21	2.09	0.18	*GRF8*	0.39	0.09	-28.00
AT2G45480	1.00	1.13	2.50	2.68	*GRF9*	1.13	1.07	-28.00

MFE was calculated from the miRNA/target pairing regions by RNAHybrid.
GRF5 and GRF6 mRNAs lack miR396 target sites.

doi:10.6342/NTU201702588

參考文獻

1. Sullivan JA, Deng XW. From seed to seed: the role of photoreceptors in Arabidopsis development. *Dev Biol* 2003;260:289-97.
2. Kami C, Lorrain S, Hornitschek P, Fankhauser C. Light-Regulated Plant Growth and Development. *Curr Top Dev Biol* 2010;91:29-66.
3. Wu SH. Gene expression regulation in photomorphogenesis from the perspective of the central dogma. *Annu Rev Plant Biol* 2014;65:311-33.
4. Yeh KC, Wu SH, Murphy JT, Largarias JC. A Cyanobacterial Phytochrome Two-Component Light Sensory System. *Science* 1997;277:1505-8.
5. Ahmad M, Jarillo JA, Cashmore AR. Chimeric Proteins between cry1 and cry2 Arabidopsis Blue Light Photoreceptors Indicate Overlapping Functions and Varying Protein Stability. *Plant Cell* 1998;10:197-207.
6. Rizzini L, Favory JJ, Cloix C, Faggionato D, O'Hara A, Kaiserli E, Baumeister R, Schäfer E, Nagy F, Jenkins GI, Ulm R. Perception of UV-B by the Arabidopsis UVR8 protein. *Science* 2011;332:103-6.
7. Wang H, Wang H. Phytochrome signaling: time to tighten up the loose ends. *Mol Plant* 2015;8:540-51.
8. Yin R, Arongaus AB, Binkert M, Ulm R. Two distinct domains of the UVR8 photoreceptor interact with COP1 to initiate UV-B signaling in Arabidopsis. *Plant Cell* 2015;27:202-13.
9. Ma L, Li J, Qu L, Hager J, Chen Z, Zhao H, Deng XW. Light control of Arabidopsis development entails coordinated regulation of genome expression and cellular pathways. *Plant Cell* 2001;13:2589-607.
10. Chattopadhyay S, Ang LH, Puente P, Deng XW, Wei N. Arabidopsis bZIP protein HY5 directly interacts with light-responsive promoters in mediating light control of gene expression. *Plant Cell* 1998;10:673-83.
11. Liu MJ, Wu SH, Chen HM, Wu SH. Widespread translational control contributes to the regulation of Arabidopsis photomorphogenesis. *Mol Syst Biol* 2012;8:566.
12. Liu MJ, Wu SH, Wu JF, Lin WD, Wu YC, Tasi TY, Tsai HL, Wu SH. Translational Landscape of Photomorphogenic Arabidopsis. *Plant Cell* 2013;25:3699-710.
13. Meister G, Tuschl T. Mechanisms of gene silencing by double-stranded RNA. *Nature* 2004;431:343-9.
14. Chen HM, Li YH, Wu SH. Bioinformatic prediction and experimental validation of a microRNA-directed tandem trans-acting siRNA cascade in Arabidopsis. *Proc Natl Acad Sci U S A* 2007;104:3318-23.
15. Fei Q, Xia R, Meyers BC. Phased, secondary, small interfering RNAs in posttranscriptional regulatory networks. *Plant Cell* 2013;25:2400-15.
16. Allen E, Xie Z, Gustafson AM, Carrington JC. microRNA-directed phasing during trans-acting siRNA biogenesis in plants. *Cell* 2005;121:207-21.
17. Law JA, Jacobsen SE. Establishing, maintaining and modifying DNA methylation patterns in plants and animals. *Nat Rev Genet* 2010;11:204-20.
18. Matzke MA, Mosher RA. RNA-directed DNA methylation: an epigenetic pathway of increasing complexity. *Nat Rev Genet* 2014;15:394-408.
19. Bartel DP. MicroRNAs: Genomics, Biogenesis, Mechanism, and Function. *Cell* 2004;116:281-97.
20. Chen X. Small RNAs and Their Roles in Plant Development. *Annu Rev Cell Dev*

doi:10.6342/NTU201702588

Biol 2009;35:21-44.
21. Guleria P, Mahajan M, Bhardwaj J, Yadav SK. Plant Small RNAs: Biogenesis, Mode of Action and Their Roles in Abiotic Stresses. *Genomics Proteomics Bioinformatics* 2011;9:183-99.
22. Ruiz-Ferrer V, Voinnet O. Roles of Plant Small RNAs in Biotic Stress Responses. *Annu Rev Plant Biol* 2009;60:485-510.
23. Bollman KM. HASTY, the Arabidopsis ortholog of exportin 5/MSN5, regulates phase change and morphogenesis. *Development* 2003;130:1493-504.
24. Sorin C, Bussell JD, Camus I, Ljung K, Kowalczyk M, Geiss G, McKhann H, Garcion C, Vaucheret H, Sandberg G, Bellini C. Auxin and light control of adventitious rooting in Arabidopsis require ARGONAUTE1. *Plant Cell* 2005;17:1343-59.
25. Tsai HL, Li YH, Hsieh WP, Lin MC, Ahn JH, Wu SH. HUA ENHANCER1 is involved in posttranscriptional regulation of positive and negative regulators in Arabidopsis photomorphogenesis. *Plant Cell* 2014;26:2858-72.
26. Cho SK, Ben Chaabane S, Shah P, Poulsen CP, Yang SW. COP1 E3 ligase protects HYL1 to retain microRNA biogenesis. *Nat Commun* 2014;5:5867.
27. Zhang H, He H, Wang X, Wang X, Yang X, Li L, Deng XW. Genome-wide mapping of the HY5-mediated gene networks in Arabidopsis that involve both transcriptional and post-transcriptional regulation. *Plant J* 2011;65:346-58.
28. Schneider CA, Rasband WS, Eliceiri KW. NIH Image to ImageJ: 25 years of image analysis. *Nature Methods* 2012;9:671-5.
29. Franco-Zorrilla JM, Valli A, Todesco M, Mateos I, Puga MI, Rubio-Somoza I, Leyva A, Weigel D, Garcia JA, Paz-Ares J. Target mimicry provides a new mechanism for regulation of microRNA activity. *Nat Genet* 2007;39:1033-7.
30. Langmead B, Trapnell C, Pop M, Salzberg SL. Ultrafast and memory-efficient alignment of short DNA sequences to the human genome. *Genome Biol* 2009;10:R25.
31. Stocks MB, Moxon S, Mapleson D, Woolfenden HC, Mohorianu I, Folkes L, Schwach F, Dalmay T, Moulton V. The UEA sRNA workbench: a suite of tools for analysing and visualizing next generation sequencing microRNA and small RNA datasets. *Bioinformatics* 2012;28:2059-61.
32. Dai X, Zhao PX. psRNATarget: a plant small RNA target analysis server. *Nucleic Acids Res* 2011;39:W155-9.
33. Jones-Rhoades MW, Bartel DP. Computational identification of plant microRNAs and their targets, including a stress-induced miRNA. *Mol Cell* 2004;14:787-99.
34. Addo-Quaye C, Eshoo TW, Bartel DP, Axtell MJ. Endogenous siRNA and miRNA targets identified by sequencing of the Arabidopsis degradome. *Curr Biol* 2008;18:758-62.
35. German MA, Pillay M, Jeong DH, Hetawal A, Luo S, Janardhanan P, Kannan V, Rymarquis LA, Nobuta K, German R, et al. Global identification of microRNA-target RNA pairs by parallel analysis of RNA ends. *Nat Biotechnol* 2008;26:941-6.
36. Gregory BD, O'Malley RC, Lister R, Urich MA, Tonti-Filippini J, Chen H, Millar AH, Ecker JR. A link between RNA metabolism and silencing affecting Arabidopsis development. *Dev Cell* 2008;14:854-66.

doi:10.6342/NTU201702588

37. Addo-Quaye C, Miller W, Axtell MJ. CleaveLand: a pipeline for using degradome data to find cleaved small RNA targets. *Bioinformatics* 2009;25:130-1.
38. Brousse C, Liu Q, Beauclair L, Deremetz A, Axtell MJ, Bouche N. A non-canonical plant microRNA target site. *Nucleic Acids Res* 2014;42:5270-9.
39. Wang Y, Wu JF, Nakamichi N, Sakakibara H, Nam HG, Wu SH. LIGHT-REGULATED WD1 and PSEUDO-RESPONSE REGULATOR9 form a positive feedback regulatory loop in the Arabidopsis circadian clock. *Plant Cell* 2011;23:486-98.
40. Kozomara A, Griffiths-Jones S. miRBase: integrating microRNA annotation and deep-sequencing data. *Nucleic Acids Res* 2011;39:D152-7.
41. Cheng Y, Chen X. Posttranscriptional control of plant development. *Curr Opin Plant Biol* 2004;7:20-5.
42. Vazquez F, Vaucheret H, Rajagopalan R, Lepers C, Gasciolli V, Mallory AC, Hilbert JL, Bartel DP, Crete P. Endogenous trans-acting siRNAs regulate the accumulation of Arabidopsis mRNAs. *Mol Cell* 2004;16:69-79.
43. Baumberger N, Baulcombe D. Arabidopsis ARGONAUTE1 is an RNA Slicer that selectively recruits microRNAs and short interfering RNAs. *Proc Natl Acad Sci U S A* 2005;102:11928-33.
44. Arvey A, Larsson E, Sander C, Leslie CS, Marks DS. Target mRNA abundance dilutes microRNA and siRNA activity. *Mol Syst Biol* 2010;6:363.
45. Ragan C, Zuker M, Ragan MA. Quantitative Prediction of miRNA-mRNA Interaction Based on Equilibrium Concentrations. *PLoS Comput Biol* 2011;7:e1001090.
46. Vaucheret H, Vazquez F, Crete P, Bartel DP. The action of ARGONAUTE1 in the miRNA pathway and its regulation by the miRNA pathway are crucial for plant development. *Genes Dev* 2004;18:1187-97.
47. Chung PJ, Park BS, Wang HI, Jang IC, Chua NH. Light-Inducible MiR163 Targets PXMT1 Transcripts to Promote Seed Germination and Primary Root Elongation in Arabidopsis. *Plant Physiol* 2016;170:1772-82.
48. Liu D, Song Y, Chen Z, Yu D. Ectopic expression of miR396 suppresses GRF target gene expression and alters leaf growth in Arabidopsis. *Physiol Plant* 2009;136:223-36.
49. Kim JH, Choi D, Kende H. The AtGRF family of putative transcription factors is involved in leaf and cotyledon growth in Arabidopsis. *Plant J* 2003;36:94-104.
50. Kim JS, Mizoi J, Kidokoro S, Maruyama K, Nakajima J, Nakashima K, Mitsuda N, Takiguchi Y, Ohme-Takagi M, Kondou Y, et al. Arabidopsis growth-regulating factor7 functions as a transcriptional repressor of abscisic acid- and osmotic stress-responsive genes, including DREB2A. *Plant Cell* 2012;24:3393-405.
51. Chen HM, Chen LT, Patel K, Li YH, Baulcombe DC, Wu SH. 22-Nucleotide RNAs trigger secondary siRNA biogenesis in plants. *Proc Natl Acad Sci U S A* 2010;107:15269-74.
52. Lee BH, Ko JH, Lee S, Lee Y, Pak JH, Kim JH. The Arabidopsis GRF-INTERACTING FACTOR gene family performs an overlapping function in determining organ size as well as multiple developmental properties. *Plant Physiol* 2009;151:655-68.
53. Li J, Yang Z, Yu B, Liu J, Chen X. Methylation protects miRNAs and siRNAs from

doi:10.6342/NTU201702588

a 3'-end uridylation activity in Arabidopsis. *Curr Biol* 2005;15:1501-7.
54. Park MY, Wu G, Gonzalez-Sulser A, Vaucheret H, Poethig RS. Nuclear processing and export of microRNAs in Arabidopsis. *Proc Natl Acad Sci U S A* 2005;102:3691-6.
55. Vaucheret H, Mallory AC, Bartel DP. AGO1 homeostasis entails coexpression of MIR168 and AGO1 and preferential stabilization of miR168 by AGO1. *Mol Cell* 2006;22:129-36.
56. Yang L, Liu Z, Lu F, Dong A, Huang H. SERRATE is a novel nuclear regulator in primary microRNA processing in Arabidopsis. *Plant J* 2006;47:841-50.
57. Creasey KM, Zhai J, Borges F, Van EF, Regulski M, Meyers BC, Martienssen RA. miRNAs trigger widespread epigenetically activated siRNAs from transposons in Arabidopsis. *Nature* 2014;508:411-5.
58. Martinez G, Choudury SG, Slotkin RK. tRNA-derived small RNAs target transposable element transcripts. *Nucleic Acids Res* 2017;45:5142-52.
59. Aravin AA, Sachidanandam R, Girard A, Fejes-Toth K, Hannon GJ. Developmentally regulated piRNA clusters implicate MILI in transposon control. *Science* 2007;316.
60. Sato K. The epigenetic regulation of transposable elements by PIWI-interacting RNAs in Drosophila. *Genes Genet Syst* 2013;88:9-17.

doi:10.6342/NTU201702588

Appendices

doi:10.6342/NTU201702588

Appendix 1. Primers used in this study

Primer	Sequence (5' to 3')
Genotyping	
SALK_006163-LP	AAGTTCTTCCGCTCTAGCGTC
SALK_006163-RP	CAGGGTTATGTGATGGACACC
mir396a-LP	TGATTATGGAATCAATCACGC
mir396a-RP	AATTTCCTCCACCCAATTTTG
SAIL_1256_F08-LP	GCACAAGATTGAAGAAAGGCC
SAIL_1256_F08-RP	GCACAATTGAAGGAGCTTGAG
LBb1.3	ATTTTGCCGATTTCGGAAC
LB1_SAIL	GCCTTTTCAGAAATGGATAAATAGCCTTGCTTCC
qRT-PCR	
AGO1-FW	GAGCTGCCGACCTCTAGAAT
AGO1-RV	CCAAGCCATCCCCCAATGAT
GRF1-FW	CGTCGCATAAACAAGCCTCG
GRF1-RV	ATTTCAGCTCTTCGGGCCAA
GRF2-FW	TGTTCATGTTCTTGGGTCGGT
GRF2-RV	CGTTGCAAGCAATCCTCACC
GRF3-FW	CCATACGAGTCCCACATCGG
GRF3-RV	CTGAGCTCATGGGGCTTGAA
GRF7-FW	CCGATGTCTACCACACCTGG
GRF7-RV	TCACTCTAGACGGGGACGAG
UBQ10-FW	AGAAGTTCAATGTTTCGTTTCATGTAA
UBQ10-RV	GAACGGAAACATAGTAGAACACTTATTCA
MIM396 cloning	
MIM396-FW	AACAGTTCAAGAACTAAGCTGTGGAAAGCTTCGGTTCCCCTCG
MIM396-RV	CTTTCCACAGCTTAGTTCTTGAACTGTTTCTAGAGGGAGATAA
SalI-*IPS1*-A1	GTGTCGACAAGAAAAATGGCCATCCCCTAGC
SacI-*IPS1*-B2	CTGGAGCTCGAGGAATTCACTATAAAGAGAATCG
Northern blotting	
miR168a-AS	TTCCCGACCTGCACCAAGCGA
miR396b-AS	AAGTTCAAGAAAGCTGTGGAA

doi:10.6342/NTU201702588

Appendix 2. Accepted research article.

doi:10.6342/NTU201702588

Lin et al. BMC Genomics (2017) 18:559
DOI 10.1186/s12864-017-3937-6

BMC Genomics

RESEARCH Open Access

Unraveling multifaceted contributions of small regulatory RNAs to photomorphogenic development in *Arabidopsis*

Meng-Chun Lin[1,2], Huang-Lung Tsai[1], Sim-Lin Lim[1], Shih-Tong Jeng[2] and Shu-Hsing Wu[1*]

Abstract

Background: Post-transcriptional control of gene expression mediated by small regulatory RNAs (sRNAs) is vital for growth and development of diverse organisms. The biogenesis of sRNAs is regulated by both positive and negative regulators known to regulate photomorphogenic development. Two microRNAs (miRNAs), miR157 and miR319, also regulate photomorphogenesis. However, genome-wide profiling of sRNAs and their regulation of target genes during photomorphogenesis has been missing. We provide a comprehensive view of sRNA-controlled gene expression in this developmental process.

Results: By profiling sRNAs and the 5′ ends of degraded mRNAs during the first 24 h of photomorphogenic development in *Arabidopsis*, we identified 335 sRNA-mediated mRNA cleavage events in de-etiolating seedlings. These cleavage events are primarily resulted from actions of highly expressed miRNAs and irrelevant to the abundance of target mRNAs. In the light, the expression of the slicer protein gene *ARGONAUTE1* in the miRNA functioning pathway could be fine-tuned by miRNA168a/b. We also found that miR396a/b positively regulates de-etiolation by suppressing *GROWTH REGULATING FACTOR*s. Our results suggest that the miRNAs are required to tune down the target mRNAs and regulate photomorphogenesis.

Conclusion: sRNAs may have a broad impact on gene expression regulation for optimized photomorphogenic development. With both positive and negative regulators under the control of sRNAs, young *Arabidopsis* seedlings can have a timely but not exaggerated developmental adaptation to light.

Keywords: Light, Small regulatory RNA, Post-transcriptional regulation, Photomorphogenesis

Background

Plants have evolved a plethora of morphological alterations to adapt to their surroundings. Photomorphogenesis, or de-etiolation, is one such process when seedlings first experience light irradiation. The rate of hypocotyl elongation decreases in seedlings under light exposure, which allows for the formation of firm structural support for seedlings emerging from the soil surface. Also, the cotyledons open and expand to maximize the area of light perception and to expose the shoot apical meristem for the development of true leaves. Light also triggers the development of chloroplasts for photosynthesis so that plants can utilize light energy for autotrophic growth and development [1–3].

In *Arabidopsis*, photomorphogenesis is under the control of at least three types of photoreceptors, including the red (R)–far-red (FR) light photoreceptor phytochromes (phys), blue light (B) photoreceptor cryptochromes (crys) and the UV-B photoreceptor, UVR8 [3–8]. The perceived light signals trigger signaling cascades that reprogram gene expression for photomorphogenic development. Transcriptional profiling for *Arabidopsis* seedlings exposed to B, FR, R light and the light–dark transition have revealed differential expression of approximately one-third

* Correspondence: shuwu@gate.sinica.edu.tw
[1]Institute of Plant and Microbial Biology, Academia Sinica, Taipei 11529, Taiwan
Full list of author information is available at the end of the article

doi:10.6342/NTU201702588

of the genome [9]. The light-regulated genome-wide transcriptomic adjustment requires the actions of transcription factors. One of the most well-characterized transcription factors conveying light signals to changes of gene expression is ELONGATED-HYPOCOTYL 5 (HY5). HY5 is a light-regulated bZIP transcription factor that upregulates the expression of many light-responsive genes during de-etiolation [10]. In addition to activating transcription, light also enhances the translational efficiency of thousands of genes, especially those committed to the translation apparatus and chloroplast functions [11, 12].

Plant small regulatory RNAs (sRNAs) are 20 to 24 nt long and can be classified into microRNAs (miRNAs) and small interfering RNAs (siRNAs) primarily according to different modes of biogenesis. MiRNAs originate from stem-loop structures of primary transcripts, and siRNAs are mostly derived from double-stranded RNAs [13]. Phased siRNAs (phasiRNAs) are a special group of siRNAs generated from mRNAs cleaved by 22-nt miRNAs or siRNAs [14–16]. Plant miRNAs can mediate the cleavage or translation inhibition of target mRNAs, whereas siRNAs function via RNA-dependent DNA methylation (RdDM) for transcriptional gene silencing or post-transcriptional target mRNA cleavage [17–22].

Previous studies have implied that sRNAs are involved in gene expression regulation during de-etiolation. Mutants defective in genes for miRNA biogenesis and functions have altered light responses. For example, in *Arabidopsis*, light hypersensitive phenotypes have been observed to carry mutations in the miRNA processor HYPONASTIC LEAVES 1 (HYL1), the sRNA methyltransferase HUA ENHANCER1 (HEN1), the sRNA transporter HASTY (HST), and the slicer protein ARGONAUTE1 (AGO1) [23–25]. A negative regulator of photomorphogenesis, CONSTITUTIVE PHOTOMORPHOGENESIS 1 (COP1), can protect HYL1 against degradation, thereby leading to a stabilized miRNA pool [26]. Transcripts of the positive regulator HY5 and negative regulator TEOSINTE BRANCHED 1, CYCLOIDEA AND PCF TRANSCRIPTION FACTORs (TCPs) of photomorphogenesis were shown to be under regulation by miR157d and miR319, respectively [25]. In addition, HY5 was found to bind to promoter regions of at least 8 miRNAs (*MIR*) loci and required for the accumulation of miR156d, miR402, miR408, miR775 and miR858 [27]. These studies provide a glimpse into photomorphogenic development shaped by the actions of a few sRNAs. A global investigation of sRNAs and their targets would greatly help in assessing the impact of post-transcriptional regulation in photomorphogenic development. However, such information is currently missing in de-etiolating seedlings.

In this study, we profiled sRNAs at 6 times during the first 24 h of *Arabidopsis* photomorphogenic development. We also sequenced 5′ ends of degraded mRNAs (degradome) in both dark- and light-grown seedlings to reveal sRNA-mediated cleavage of mRNAs during de-etiolation. Pairwise studies of sRNAs and their target mRNAs indicated that a high sRNA-to-target ratio is a key determinant for successful mRNA target repression by sRNAs. The high ratio is mainly contributed by the abundance of sRNAs. A total of 335 sRNA-target mRNA regulatory pairs were identified in de-etiolating seedlings, with several sRNAs demonstrated to regulate photomorphogenesis. The action of miR168 leads to reduced expression of *AGO1* under light, thereby offering a feedback regulation of miRNA functioning during de-etiolation. miR396 were identified to act as positive regulators of photomorphogenesis. In addition, we revealed that some 24-nt siRNAs had potential to cause target cleavage in de-etiolating seedlings. Our data indicate that sRNAs function in multiple regulatory circuits for optimized seedling growth under light illumination.

Results

The expression and actions of small RNAs in de-etiolating *Arabidopsis* seedlings

We first used deep sequencing to survey the sRNAs in de-etiolating *Arabidopsis* seedlings. The sRNAs were isolated from 4-d-old dark-grown (W0 h) seedlings and seedlings that were further treated with continuous white light irradiation for 1 to 24 h (W1 h to W24 h) and subjected to deep sequencing (Fig. 1). Approximately 18–22 million reads were obtained for each sample in 3 biological replicates. For each dataset, 94–98% of the filtered reads (see methods) could be mapped to the TAIR10 genome (Additional file 1: Table S1). We first analyzed miRNAs and phasiRNAs, as they are frequently studied groups of plant sRNAs. Among the 427 *Arabidopsis* miRNAs annotated in miRBase 21 [28], 207 (48.5%) are considered expressed (see methods for criteria) (Additional file 1: Table S2). Overall 58 phasiRNAs derived from 12 phasiRNA-generating loci (*PHAS*, or trans-acting siRNA-generating loci, *TAS*) [14] were expressed in de-etiolating seedlings (Table 1 and Additional file 1: Table S3). In addition to miRNAs and phasiRNAs, 4255 20–24 nt siRNAs were defined expressed in this developmental stage (Additional file 1: Table S4).

Since both miRNAs and siRNAs can target mRNAs for cleavage [19, 29–31], we aimed to identify sRNA–target pairs that may be involved in photomorphogenic development. We performed degradome sequencing followed by CleaveLand analyses [32] to identify target mRNAs cleaved by expressed sRNAs in de-etiolating seedlings. The degraded mRNA samples were obtained from seedlings grown under dark (W0 h) or light (equally mixed from samples treated with W for 1, 3, 6, 12 and 24 h).

doi:10.6342/NTU201702588

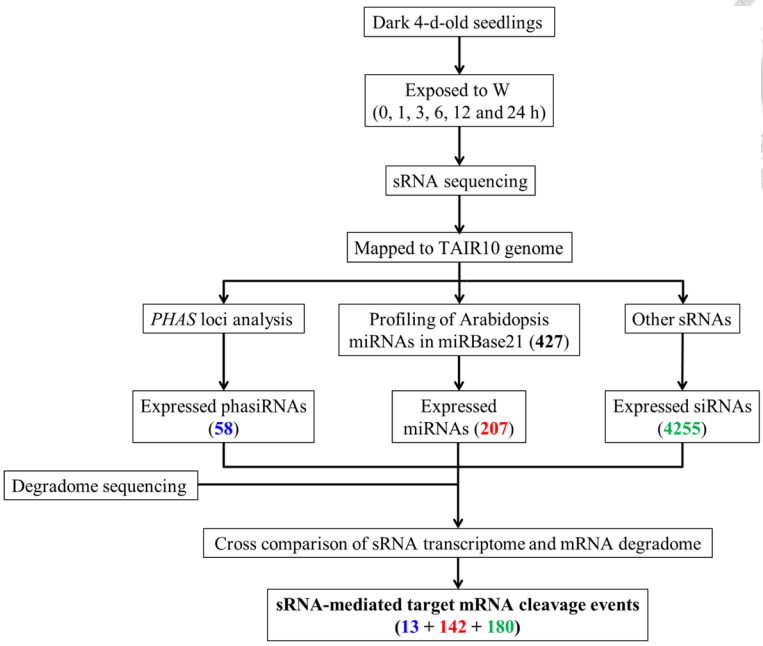

Fig. 1 Pipeline for investigating sRNA-mediated regulation in de-etiolating *Arabidopsis* seedlings. Four-d-old dark-grown seedlings (W0 h) were exposed to continuous white light (W; 100 μE) for 1, 3, 6, 12 and 24 h; 18–22 million (M) reads per library were acquired. Degradome sequencing for dark- (Dark) and light- (equally pooled from the five light-treated time points) grown seedlings were used for identifying sRNA-mediated cleavage of target mRNA. Colored numbers in parentheses indicate the number of sRNAs/targets passing the corresponding filtering criteria

Approximately 50 million reads for each of the libraries were obtained; 81–85% could be mapped to TAIR10 cDNAs (Additional file 1: Table S1). Our analyses suggested that 262 non-redundant sRNAs could mediate the cleavage of 306 *Arabidopsis* mRNAs (a total of 335 target cleavage sites). Among them, 142 cleavage events were mediated by miRNAs, 13 by phasiRNAs and 180 by other siRNAs (Fig. 1; Additional file 1: Table S5 and S6). These newly identified sRNA-target pairs are potential players in post-transcriptional gene expression regulation in *Arabidopsis* photomorphogenesis.

sRNA abundance determines the likelihood of target mRNA cleavage

When analyzing the mRNA degradomes, we noticed that although 90 miRNA families were expressed in

Table 1 Expressed *PHAS* loci in de-etiolating seedlings

PHAS locus	Gene	Chromosome	phasiR trigger	Start	End	n	k	*p*-value
At1g62910	*RFL9 (PPR)*	1	TAS2 3′-D6 (−)	23,299,624	23,299,875	77	14	2.0×10^{-7}
At1g63130	*RPF6*	1	ta-siR2140	23,413,391	23,413,642	13	7	7.3×10^{-7}
At1g50055	*TAS1B*	1	miR173	18,549,441	18,549,692	60	12	9.7×10^{-7}
At1g63070	*PPR*	1	ta-siR2140	23,386,420	23,386,671	50	11	1.3×10^{-6}
At1g63150	*	1	TAS2 3′-D6 (−)	23,420,003	23,420,254	80	12	2.7×10^{-5}
At1g62930	*RPF3 (PPR)*	1	miR161.1	23,307,125	23,307,466	99	13	4.5×10^{-5}
At1g63080	*PPR*	1	ta-siR2140	23,389,990	23,390,241	58	10	5.5×10^{-5}
At1g62590	*PPR-AC*	1	TAS2 3′-D6 (−)	23,178,438	23,178,689	27	7	7.1×10^{-5}
At2g39681	*TAS2*	2	miR173	16,539,919	16,540,170	12	9	1.9×10^{-9}
At2g39675	*TAS1C*	2	miR173	16,537,860	16,538,111	10	7	1.5×10^{-8}
At2g27400	*TAS1A*	2	miR173	11,722,009	11,722,260	21	8	6.2×10^{-7}
At3g17185	*TAS3*	3	miR390	5,682,143	5,682,394	80	14	3.4×10^{-7}

n: Number of distinct alignments
k: Number of phased alignments, based on hypergeometric distribution
*: Reported *PHAS* locus
Loci with $p < 10^{-4}$ are listed

doi:10.6342/NTU201702588

de-etiolating seedlings (Additional file 1: Table S2), target cleavage was detected for only members of 49 miRNA families (Additional file 1: Table S5). The results prompted us to investigate factors affecting target cleavage or the identification of degradome signatures. Previous reports have shown that high target abundance will compromise the repression activity of miRNAs and siRNAs when introduced via transfection in animal cell lines [33]. A computational model based on fixed concentration of miRNAs and mRNAs implicated that the concentration of miRNAs has a greater effect on miRNA-mRNA interaction in *Drosophila melanogaster* and in human [34]. In contrast to the seed pairing seen in most animal miRNA-mRNA interactions, most plant miRNAs interact with their target mRNAs at high complementarity that leads to cleavage of target mRNAs [19]. The availability of transcriptome data for mRNAs [12], sRNAs and degradome signatures in this study allowed us to investigate whether miRNAs/siRNAs or target abundance is important for effective miRNA/siRNA-mediated target cleavage in de-etiolating *Arabidopsis* seedlings.

Our analysis indicated that miRNAs causing target cleavage tended to have higher abundance, as compared with miRNAs that failed to generate detectable target degradome signatures (Fig. 2a). The results were similar for miRNAs expressed in both the dark ($p = 5.2 \times 10^{-8}$, D = 0.4327 in Kolmogorov-Smirnov test, K-S test) and light ($p = 3.0 \times 10^{-8}$, D = 0.4394, K-S test) (Fig. 2a). In contrast, for mRNAs with predicted miRNA target sites, the transcript abundance was comparable for mRNAs with or without degradome signatures identified (Fig. 2b). Pair-wise examination of miRNA-to-target ratios revealed relatively higher ratios for miRNA-mRNA pairs with observed cleavage under both dark ($p = 1.3 \times 10^{-12}$,

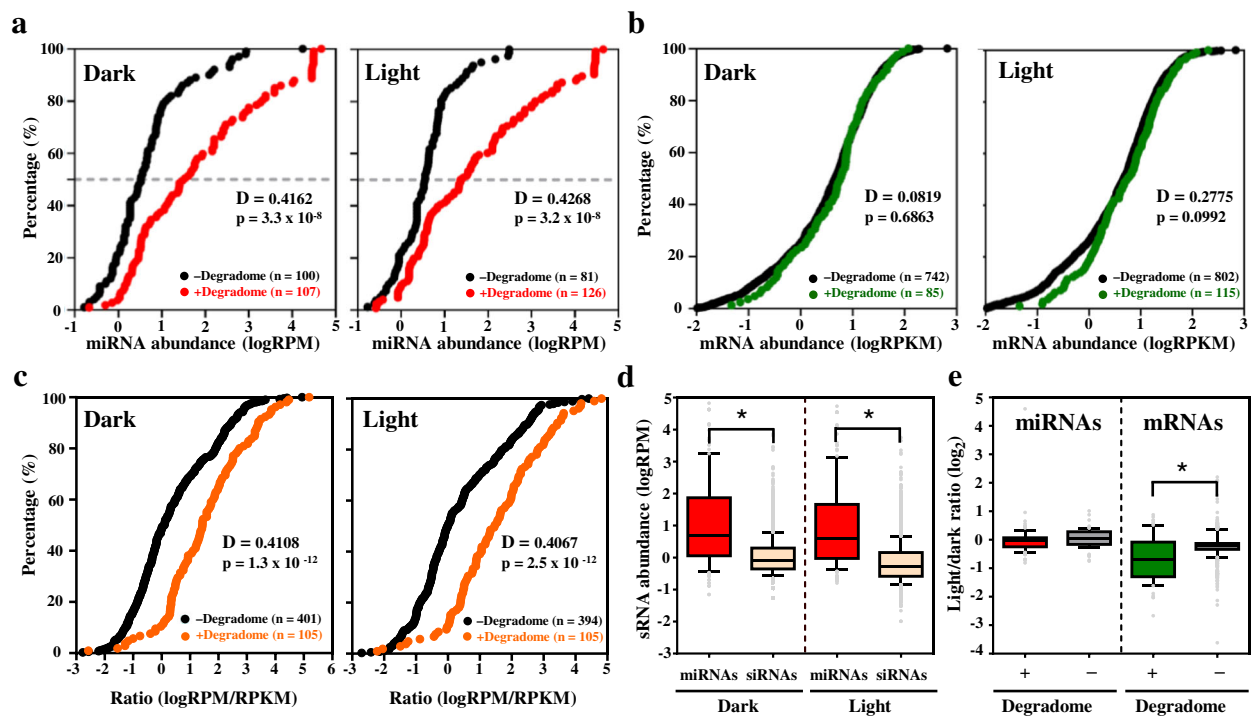

Fig. 2 The miRNA abundance, rather than target mRNA abundance, is the major determinant of target cleavage. **a** miRNAs causing target cleavage tend to have higher abundance. Kolmogorov-Smirnov (KS) plot showing the abundance of expressed miRNAs in dark and light (W3 h). + Degradome (*red*) indicates miRNAs with valid target cleavages identified; – degradome (*black*) indicates expressed miRNAs without target cleavage identified. Dashed lines indicate 50th percentile of sRNAs. **b** Target mRNA abundance was relatively unchanged regardless of being cleaved. KS plot showing the abundance of target mRNA with (*green*) or without (*black*) degradome signatures under dark or light (W4 h). Only expressed target genes with RPKM > 0.01 were plotted. **c** Degradome signatures were preferentially detected in mRNAs with high miRNA-to-target ratios. KS plot showing distribution of pairwise miRNA-to-target ratios in dark and light (W3 h/W4 h). + Degradome (*orange*) indicates miRNA–target pairs with target cleavage identified; – degradome (*black*) indicates miRNA–target pairs without target cleavage identified. **d** The abundance is relatively lower for siRNAs than expressed miRNAs. **e** Target mRNAs, but not miRNAs, are downregulated by light. Light/dark ratios indicate the relative levels of miRNAs (W3 h/W0 h) and mRNAs (W4 h/W0 h). + and – degradome indicate miRNAs/targets with or without identified degradome signatures, respectively. Data are the mean of all biological replicates (three replicates for sRNAs and two for mRNAs). * $p < 0.01$ by Student's t-test. The bottom, middle, and top of the box represent the 25th, 50th, and 75th percentiles, and whiskers are the 10th and 90th percentiles, respectively

doi:10.6342/NTU201702588

D = 0.4108, K-S test) and light (p = 2.5 × 10^{-12}, D = 0.4067, K-S test) (Fig. 2c). Therefore, miRNAs with high abundance may give rise to high miRNA-to-target ratios, thereby leading to successful target mRNA cleavage.

The above notion remains true when applied to siRNA-mediated mRNA cleavage (Additional file 2: Figure S1), although not as significant as for miRNAs (Fig. 2a). Among the 4255 expressed siRNAs, only 180 have degradome signatures identified for their target mRNAs (Additional file 1: Table S6), as compared with 155 targets resulting from 265 miRNA/phasiRNA-mediated cleavages (Additional file 1: Table S5), possibly because of the significantly lower expression of most siRNAs than miRNAs (Fig. 2d).

Although the expression of most of the miRNAs remained unchanged before and after light treatment, light appears to down-regulate the expression of target mRNAs with degradome signatures but not that of mRNAs without evidence of cleavage (Fig. 2e). Therefore, instead of regulating miRNA expression, light signals may potentiate the target-cleavage activities of miRNAs to tune down the expression of their target genes during de-etiolation. Whether this reduction is achieved by regulating the expression or enzymatic activities of slicer complexes remains to be investigated.

Light optimizes miRNA functioning via the action of miR168

Previously, we reported a feedback regulation between *HY5* and *HEN1*, which indicates that an sRNA equilibrium is required during photomorphogenic development [25]. Here, we sought to identify whether light regulates steps in addition to *HEN1* in sRNA biogenesis and functioning. In *Arabidopsis*, miR168 targets the sRNA slicer gene *AGO1* [35]. Deep sequencing and northern blot results indicated that the expression pattern of miR168 only slightly fluctuated under light (Fig. 3a, b). However, the mean abundance of miR168a/b ranged from 880 to 1270 read per million reads (RPM) (Additional file 1: Table S2), which is more than 10 times greater than the median level of miRNAs overall (Fig. 2a). Thus, miR168a/b has high potential in mediating the cleavage of *AGO1* transcript. Indeed, under light, *AGO1* cleavage signatures could be detected (Additional file 1: Table S5), which led to the down-regulation of *AGO1* (Fig. 3c). The detection of *AGO1* cleavage signature only under light is also consistent with preferential light-mediated downregulation of miRNA target mRNAs (Fig. 2e). Thus, miR168a/b have potential to desensitize the sRNA actions by targeting *AGO1* for degradation during photomorphogenesis.

Light regulates the expression of some miRNAs and phasiRNAs

Although most miRNA levels were unchanged before and after light treatment in young *Arabidopsis* seedlings (Fig. 2d; Additional file 1: Table S2), we still observed that 32% (67 of 207) of expressed miRNAs were regulated by light (Fig. 4; Additional file 1: Table S2). Only 8 of 58 expressed phasiRNAs were differentially regulated by light (Additional file 1: Table S3). Because sRNA abundance is a major determinant for target cleavage in seedlings (Fig. 2), any changes in sRNA levels under light may alter their target suppression capacity. Thus, the light regulation of miRNAs and phasiRNAs may provide a timely control of target mRNAs to shape photomorphogenic development. The light responsiveness of the 67 light-regulated miRNAs could be classified into 3 major clusters by k-mean clustering (Fig. 4; Table 2). miR163 belongs to cluster I, whose expression is barely detectable in the dark but is rapidly induced by light. miR163 has been shown to promote seed germination and primary root growth during early seedling development, but not involved in light-induced

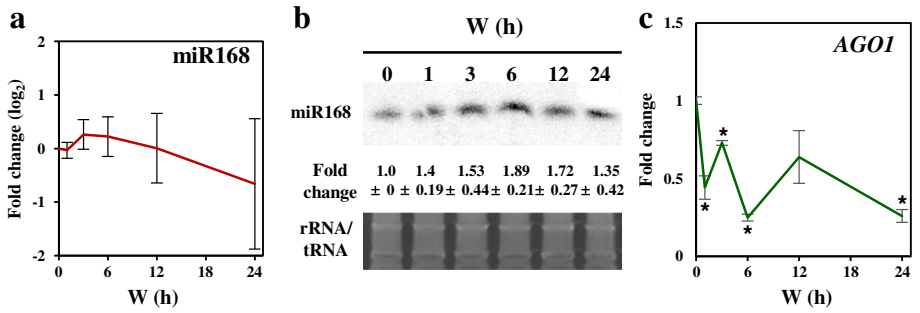

Fig. 3 The expression of miR168 and *AGO1* in de-etiolating *Arabidopsis*. **a** Expression pattern of miR168. Data are mean ± SD from three biological replicates of sRNA sequencing. **b** Northern blot analysis of miR168 level during the times examined. Data are mean ± SD are calculated from three biological replicates. SYBR-gold stained rRNA/tRNA was a loading control. **c** Light down regulates *AGO1*. qRT-PCR results were shown as mean ± SD calculated from three technical repeats. Asterisks indicate $p < 0.01$ in Student's t-test. Three biological replicates have shown similar results

doi:10.6342/NTU201702588

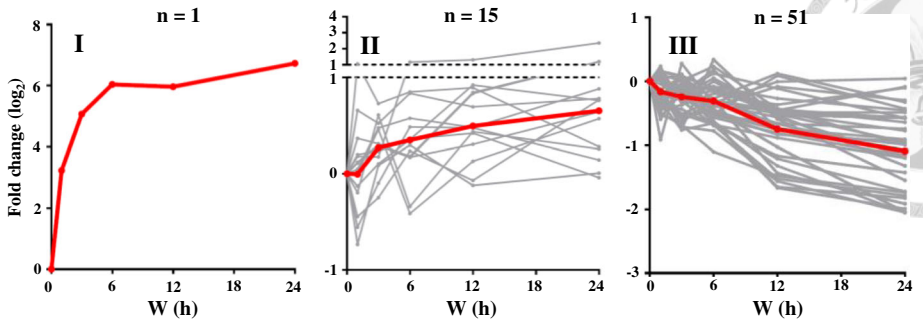

Fig. 4 Cluster analysis of light-regulated miRNAs. Student's t-test was performed to identify miRNAs with significant fold changes against dark (W0 h). The expression patterns of miRNAs in response to light treatments were classified into four clusters by use of k-mean clustering (by Euclidean distance). *Gray lines* indicate the average fold change of each miRNA from three biological replicates; red lines indicate average fold changes within the cluster

inhibition of hypocotyl elongation [36]. Cluster II miRNAs are also upregulated by light, and the up regulation is more prominent after prolonged light exposure. The miRNAs in cluster II include miR157d, reported to target *HY5* during photomorphogenic development [25]. The miRNAs in cluster III were down regulated by light, especially after 6-h light exposure.

miR396 promote photomorphogenesis by tuning *GRF* levels

In de-etiolating seedlings, the degradome signatures were most frequently found for mRNAs targeted by members in the miR156/157 and miR396 families (Fig. 5a). miR157d directly targets *HY5* to desensitize the light signals during photomorphogenesis [25], but the functions of miR396 in photomorphogenic development remain obscure.

The expression of miR396 was slightly decreased upon light treatment (Fig. 5b and c). miR396 can target 7 *GROWTH REGULATING FACTOR*s (*GRF*s) [37, 38], and the cleaved signatures of all 7 *GRF*s were detected in our degradome analysis (Additional file 1: Table S5). *GRF1*, *GRF2*, *GRF3* and *GRF7* showed relatively higher degradome signature reads amongst the *GRF*s (Fig. 5d), and all showed clear down regulation under light (Fig. 5e). *GRF1*, *GRF2* and *GRF3* cooperatively regulate leaf and cotyledon development [39], whereas *GRF7* is a transcriptional repressor of abscisic acid and osmotic stress-responsive genes [40]. However, their functions in photomorphogenesis remain unknown.

To assay the regulatory roles of miR396–*GRF* pairs in photomorphogenesis, we first isolated and analyzed the *mir396a* single mutant (SALK_064047; Additional file 2: Figure S2a). Although overall miR396 levels were reduced, the phenotypes of the *mir396a* mutant were indistinguishable from that of the wild type under dark or light (Additional file 2: Fig. S2a and b). Possibly, the residual amount of miR396b in *mir396a* is sufficient for normal seedling development (Additional file 2: Figure S2a).

Because both miR396a and miR396b can suppress *GRF*s [38], we sought to simultaneously sequester these two miRNAs by generating target mimicry lines (*MIM396*) (Fig. 6a). The levels of *GRF1*, *GRF2*, *GRF3* and *GRF7* were indeed increased in two independent *MIM396* lines (Fig. 6a). The *MIM396* lines showed elongated hypocotyl length under 50 μE white light (Fig. 6b), which suggests that functional miR396 can positively regulate photomorphogenesis. We also examined the hypocotyl lengths of the *MIR396A* overexpression line (*MIR396Aox*) [38] and found that light sensitivity was not further exaggerated (Additional file 2: Figure S2c and d), so the endogenous miR396 pool may be at a saturated level for its functions in light responses.

To further understand the mechanistic roles of miR396 in photomorphogenesis, we examined the hypocotyl lengths of *grf1 grf2 grf3* and *grf7* mutants. Compared to wild-type Ws, the *grf1 grf2 grf3* triple mutant showed short hypocotyl under 50 μE white light, which indicates that the three *GRF*s act as negative regulators of photomorphogenesis. In contrast, *grf7* showed a short hypocotyl only under dark (Fig. 6c). Together with the quick repression of *GRF7* expression by light (Fig. 5e), the major function of *GRF7* is likely to promote hypocotyl elongation under dark. In sum, miR396 can act as a positive regulator of hypocotyl elongation by suppressing the negative regulator *GRF*s.

Varied length and target properties of siRNAs in *Arabidopsis* seedlings

Among the expressed siRNAs in de-etiolating seedlings, 164 are capable of mediating target cleavage (Additional file 1: Table S6). Among them, 70 (> 40%) are 24 nt long (Fig. 7a), which is quite different from the typical 21- or 22-nt miRNAs/phasiRNAs that mediate target mRNA cleavage [14, 19, 41]. Most target genes with degradome

doi:10.6342/NTU201702588

Table 2 Differentially expressed miRNAs in de-etiolating *Arabidopsis* seedlings, with average $\log_2$ fold-change listed

Cluster I	W0 h	W1 h	W3 h	W6 h	W12 h	W24 h
miR163	0	3.230582	5.070049	6.036598	5.963276	6.724631
Cluster II	W0 h	W1 h	W3 h	W6 h	W12 h	W24 h
miR5026	0	−0.19729	0.609021	−0.33921	0.435821	0.256526
miR825	0	−0.55657	−0.0974	0.484967	0.475439	0.143117
miR869.2	0	−0.44551	−0.24714	0.236649	−0.06937	0.766993
miR156c-3p	0	0.008901	0.458674	−0.41258	0.129615	0.571201
miR170-3p	0	0.199128	0.233507	0.359504	0.420726	−0.0398
miR2933a	0	−0.73393	0.087544	0.296233	−0.12048	0.00611
miR2933b	0	−0.73393	0.087544	0.296233	−0.12048	0.00611
miR5642a	0	−0.12856	0.102902	0.354152	0.920248	0.760898
miR157d	0	0.366314	0.311192	0.17222	0.304513	0.640368
miR167a-3p	0	0.046902	0.474899	0.574704	0.480747	0.881156
miR833b	0	1.053165	0.727714	0.849033	0.892631	0.279323
miR858a	0	0.657713	0.522465	0.833586	0.69362	0.780516
miR157a-3p	0	0.119139	0.300398	0.181048	0.842913	1.197978
miR157b-3p	0	0.112265	0.292249	0.169389	0.833254	1.186319
miR157c-3p	0	0.18009	0.174448	1.165619	1.299035	2.35774
Cluster III	W0 h	W1 h	W3 h	W6 h	W12 h	W24 h
miR158b	0	0.068148	−0.23119	0.046673	−0.49671	−0.77436
miR162a-3p	0	0.216902	−0.35089	−0.001	−0.53321	−1.32163
miR390a-5p	0	0.041912	−0.24039	−0.52191	−0.83531	−0.94731
miR398c-3p	0	0.233205	−0.74225	0.337007	−0.5905	−1.54736
miR399b	0	−0.32628	−0.03547	−0.57065	−0.81218	−1.16872
miR399c-3p	0	−0.13086	0.021596	−0.5015	−0.75814	−1.10903
miR829-3p.1	0	−0.19326	−0.0353	−0.14504	−0.74384	−0.90991
miR829-5p	0	0.017165	−0.29223	−0.32674	−0.66067	−0.74456
miR162b-3p	0	0.215734	−0.35239	−0.00193	−0.53434	−1.32203
miR162b-5p	0	0.057888	−0.1911	0.175723	−0.742	−1.07194
miR169a-3p	0	−0.35672	−0.10399	−0.09992	−0.43079	−0.99436
miR173-5p	0	−0.04189	−0.26578	−0.30136	−0.5118	−0.95313
miR390b-5p	0	0.041759	−0.2396	−0.52135	−0.83081	−0.94673
miR396b-3p	0	−0.19923	−0.26739	−0.52009	−0.66862	−1.11049
miR398b-3p	0	0.233205	−0.74225	0.337007	−0.5905	−1.54736
miR823	0	−0.25067	0.109541	−0.45625	−0.76484	−0.99271
miR839-5p	0	−0.9158	0.276875	−0.35478	−0.56659	−1.1664
miR166a-3p	0	0.141355	0.079493	−0.11147	−0.50323	−0.56368
miR166b-3p	0	0.158125	0.078693	−0.10249	−0.52608	−0.57401
miR166c	0	0.157754	0.078204	−0.10279	−0.52633	−0.57431
miR166d	0	0.1578	0.078219	−0.1028	−0.52637	−0.5743
miR166e-3p	0	0.157828	0.07835	−0.10235	−0.52615	−0.57403
miR166f	0	0.157829	0.078349	−0.10233	−0.5261	−0.574
miR166g	0	0.157513	0.077882	−0.10266	−0.52644	−0.57431
miR169b-3p	0	0.046702	0.084603	−0.51457	0.08493	−0.43209
miR169i	0	−0.21387	0.036407	−0.3923	−0.08524	−0.29972

doi:10.6342/NTU201702588

Table 2 Differentially expressed miRNAs in de-etiolating *Arabidopsis* seedlings, with average $\log_2$ fold-change listed *(Continued)*

miR171c-5p	0	−0.24785	−0.51146	−0.30205	−0.45579	−0.08671
miR319b	0	0.101478	0.007334	0.230599	−0.43223	−0.64435
miR393b-3p	0	−0.22189	−0.24646	−0.14695	−0.49096	−0.49076
miR408-3p	0	−0.24897	−0.16535	0.122217	−0.11517	−0.57962
miR5644	0	−0.46437	−0.21745	−0.08393	−0.26968	−0.45617
miR156h	0	−0.44634	−0.37253	−0.19148	−0.36689	−0.10394
miR160c-3p	0	−0.17658	−0.29051	−0.33976	−0.00825	0.041016
miR169m	0	−0.12627	0.064869	−0.27125	0.118007	−0.32789
miR166a-5p	0	−0.14566	−0.30587	−0.69082	−1.16879	−1.42452
miR395e	0	−0.52798	−0.63659	−0.291	−1.43631	−1.91425
miR5646	0	−0.55674	−0.18855	−0.6301	−1.65092	−1.82573
miR166b-5p	0	−0.14566	−0.30587	−0.69082	−1.16879	−1.42452
miR166e-5p	0	−0.49789	−0.68724	−1.10023	−1.47964	−1.73891
miR390b-3p	0	−0.32255	−0.76324	−0.65686	−1.66625	−1.99135
miR395a	0	−0.52798	−0.63659	−0.29058	−1.43631	−1.91425
miR395b	0	−0.30231	−0.53107	−0.43895	−1.02895	−2.04242
miR395c	0	−0.30231	−0.53107	−0.43895	−1.02895	−2.04242
miR395d	0	−0.52798	−0.63659	−0.29058	−1.43631	−1.91425
miR395f	0	−0.30231	−0.57998	−0.43895	−1.02895	−2.04242
miR396a-3p	0	−0.16376	−0.71517	−0.7776	−1.56218	−2.04976
miR408-5p	0	−0.44974	−0.17004	−0.65167	−1.20912	−1.72316
miR5012	0	−0.37776	−0.43595	−0.68763	−1.5225	−1.78667
miR5024-3p	0	−0.59768	−0.10816	−0.63027	−1.32052	−2.05354
miR5634	0	−0.19003	−0.51725	−0.68077	−0.88666	−1.19981

signatures for both miRNAs/phaiRNAs and siRNAs are protein coding genes (Fig. 7b). Intriguingly, 30 cleavage events from the actions of siRNAs were identified from 18 transposable elements (TEs), which is significantly higher than the number targeted by miRNAs/phasiRNAs ($p = 3.2 \times 10^{-3}$ by Fisher's exact test). Most siRNA-targeted transposons are in the gypsy-like retrotransposon and CACTA-like transposase family. Eleven sRNAs that mediate TE mRNA cleavage are also derived from annotated TEs, with 4 sRNAs derived from their target loci (Additional file 1: Table S6), so these TEs may be capable of self-suppressing through TE-derived siRNAs and self-targeted cleavage. Among the 30 cleavage events derived from TE mRNAs, 23 potentially resulted from cleavage mediated by 24-nt siRNAs. The 24-nt siRNAs derived from transposable elements can mediate silencing of their original transposable elements via RNA-dependent DNA methylation (RdDM) [17, 18]. Our results suggest that in addition to RdDM, siRNA-mediated cleavage may function as an additional mechanism to prevent TE mRNA accumulation, which may escape from incomplete RdDM.

Discussion

Light regulates miRNA-target pairs in photomorphogenic development

In addition to the previously discovered miR157d–*HY5* and miR319–*TCP* pairs [25], we found additional miRNA–target pairs that positively regulate photomorphogenesis. In this study, miR168 could tune down *AGO1* level under light (Fig. 3), which can counteract the actions of sRNAs stabilized by the light-induced *HEN1* expression. miR396 can act as positive regulators of photomorphogenesis by suppressing *GRF1*, *GRF2*, *GRF3* and *GRF7*. The *grf7* mutant shows shorter hypocotyl length under dark, so it may positively regulate hypocotyl elongation under dark. Under light conditions, the *grf7* mutant phenotype is comparable to that of the wild type possibly because light also markedly represses *GRF7* expression (Fig. 5e, Additional file 1: Table S8).

We cannot rule out that light down-regulates the expression of *GRFs* at the transcriptional level. However, the detection of the miR396-mediated cleavage events on *GRFs* (Additional file 2: Table S5) suggested that miR396 indeed functions to optimize the *GRF* mRNA levels

doi:10.6342/NTU201702588

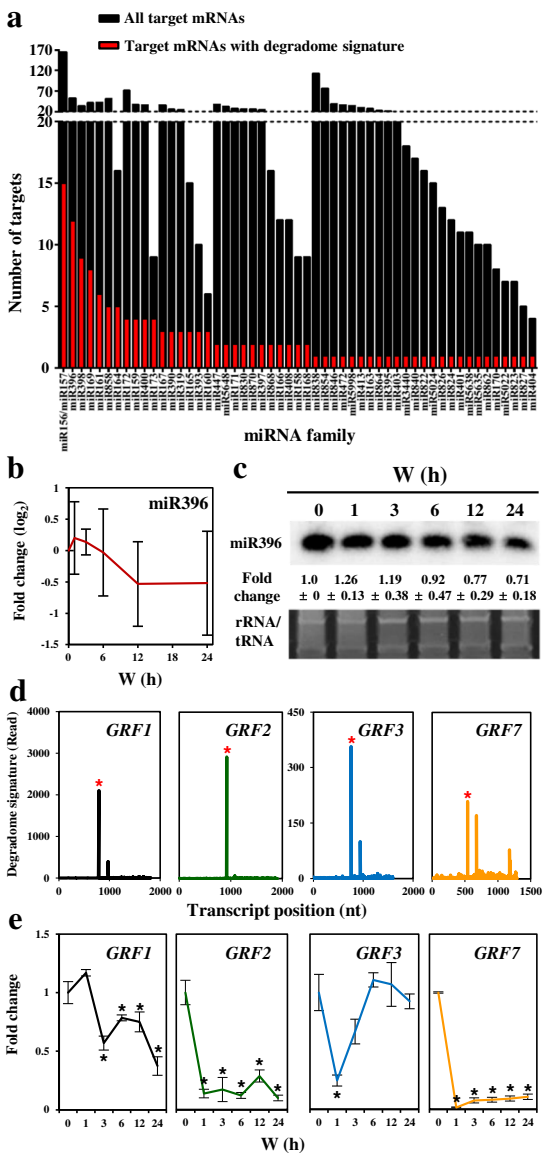

Fig. 5 miRNA families with identified targets and the expression patterns of miR396–*GRF* regulatory pairs in de-etiolating seedlings. **a** Expressed miRNA families with predicted (*black*) or identified (*red*) target cleavages in de-etiolating *Arabidopsis*. **b** Expression of miR396 is transiently upregulated and gradually decreased on W exposure. Data are mean ± SD from three biological replicates of sRNA sequencing. **c** Northern blot analyses confirmed the expression of miR396 in de-etiolating *Arabidopsis*. One representative gel image is shown. Data are mean ± SD for the relative expression from three biological replicates. SYBR-Gold-stained rRNA/tRNA was a loading control. **d** Degradome T-plot marked the miR396-mediated *GRF1/GRF2/GRF3/GRF7* mRNA cleavage in de-etiolating seedlings. Red asterisks indicate the degradome signatures detected at expected cleavage sites for *GRF1*, *GRF2*, *GRF3* and *GRF7*. **e** Light regulation of *GRF1*, *GRF2*, *GRF3* and *GRF7*. Data are mean ± SD from three technical replicates of one representative qRT-PCR experiment. * $p < 0.01$ in Student's t-test. Three biological replicates were performed with similar results

during de-etiolation. GRFs are known as transcription activators [42]; hence, future investigation of GRF downstream genes will help demystify genes regulated by the miR396-*GRF* lineage and provide a future research direction for their contribution in photomorphogenic development.

sRNAs regulate photomorphogenesis from multiple angles

Our results in Fig. 2 and Additional file 2: Figure S1 showed that abundant sRNAs have a better likelihood of mediating target mRNA cleavage during photomorphogenic development. Also, despite no negative correlation between the expression of miR168/miR396 and their target mRNAs (Figs. 3 and 5), degradome signatures from their target mRNAs were observed (Additional file 1: Table S5, Fig. 5). This finding indicated that although light does not affect the accumulation of miR168 and miR396, these miRNAs can contribute to the expression repression of their target mRNAs in de-etiolating seedlings. The steady-state mRNA transcriptome during photomorphogenic growth likely is a finely orchestrated balance between the well-studied transcriptional regulation by light signals and target mRNA cleavage mediated by small regulatory RNAs as examples shown in this study.

Combined with our previous [25] and current discovery, sRNAs could fine-tune the expression of both positive (*HY5*) and negative (*TCPs*, *AGO1*, *GRFs*) regulators of photomorphogenesis (Fig. 8). Clearly, as key regulators of these complex and interlocked regulatory circuits, the whole plethora of sRNAs is crucial for an optimal transcriptome during photomorphogenesis. This observation also explains why mutations of single *MIR* or target gene usually show less prominent phenotypic changes (Fig. 6), as compared with mutants with a defective miRNA pathway [23–25, 30, 43–46]. We have observed a considerable amount of degradome signatures that were predicted to be results of siRNA-mediated mRNA cleavage. This suggests that, in addition to miRNAs, siRNAs also contribute considerably to down regulate their target mRNAs in de-etiolating seedlings. Further investigation of the miRNA- and siRNA-target pairs will continue to shed light on post-transcriptional regulation of photomorphogenic growth.

Finally, our observation suggests that siRNA-mediated TE mRNA cleavage may serve as an additional mode of TE silencing (Fig. 7). In *Arabidopsis*, TE mRNAs could also be cleaved by miR859 [47] and a tRNA-derived small RNA via the association with AGO1 in pollens [48]. In *Drosophila* germ cells, Piwi-interacting RNAs (piRNAs) can interact with Aubergine (Aub) or AGO3 for the cleavage of TE mRNAs [49, 50]. It remains to be clarified with which AGO protein(s) siRNAs interact for silencing plant TE mRNAs.

doi:10.6342/NTU201702588

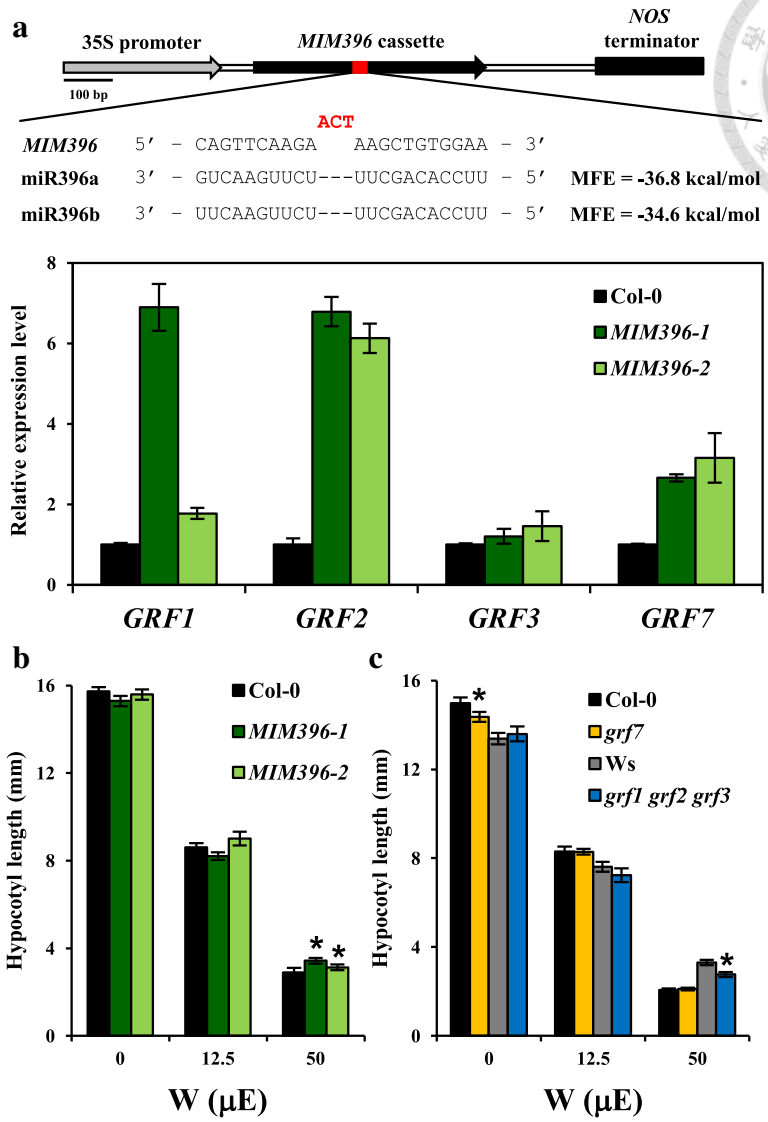

Fig. 6 miR396 positively regulate photomorphogenesis by suppressing *GRF* levels. **a** Illustration of the *35S:MIM396* (*MIM396*) target mimicry construct. The nucleotides generating a bulge at the miR396 target site is highlighted in *red*. Minimum free energy (MFE) for *MIM396* binding to miR396a and miR396b was calculated by RNAHybrid. The expression of *GRF1*, *GRF2*, *GRF3* and *GRF7* is increased in the two independent *MIM396* T_4 lines. Data are mean ± SD calculated from three technical replicates. Three biological replicates were performed with similar results. **b** The *MIM396* T_4 homozygous lines show long hypocotyl length under W at 50 μE. Data are mean ± SE of hypocotyl length for one representative result. * $p < 0.01$ by Student's t-test, $n \geq 30$. Three biological replicates were performed with similar results. **c** The *grf1 grf2 grf3* triple mutant and the *grf7* single mutant shows shorter hypocotyl than their corresponding wild types, Ws and Col-0, under W and dark conditions, respectively. * $p < 0.01$ by Student's t-test, $n \geq 30$. Data are one representative result from three biological replicates performed with similar results

Conclusions

Photomorphogenesis is a coordinated result of gene expression regulation at multiple levels. Our analyses revealed multiple sRNA–mRNA pairs contributing to this important development process. We also confirmed a comprehensive impact of sRNAs on regulating post-transcriptional gene expression during de-etiolation in *Arabidopsis*. sRNAs target multiple positive and negative regulators of photomorphogenesis, offering sophisticated fine-tuning power for regulating gene expression during de-etiolation. The potency of an sRNA in target cleavage is primarily determined by its abundance, adding an extra regulation dimension in addition to target recognition.

Methods

Plant materials and growth conditions

Seeds of wild-type *Arabidopsis*, Col-0, L*er*, Ws, T-DNA insertion lines SALK_064047 (*mir396a*) and SAIL_1256_F08 (*grf7*) were acquired from stock centers, ABRC or NASC. Homozygous lines of T-DNA insertion lines were screened

doi:10.6342/NTU201702588

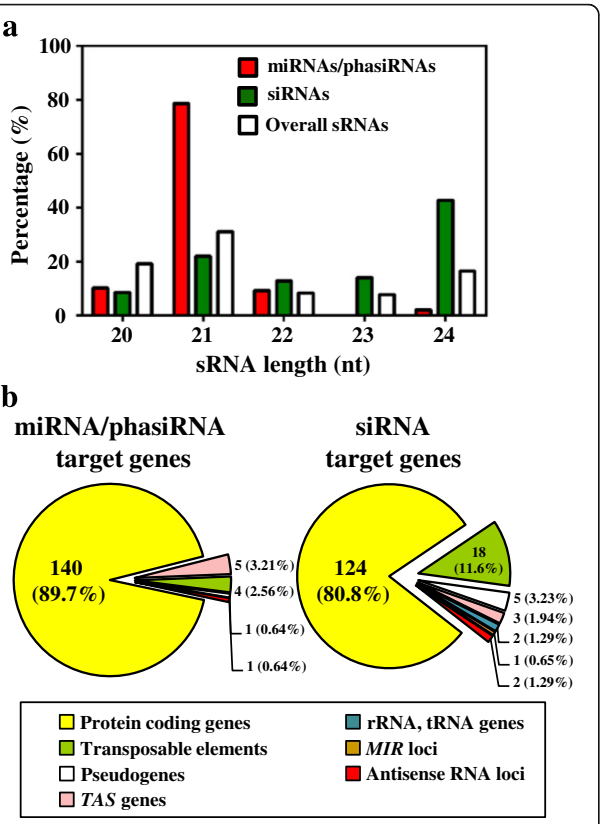

Fig. 7 siRNA sizes and target gene features in de-etiolating seedlings. **a** Length distribution of sRNAs with targeted cleavage signatures identified (*red* and *green*). **b** Categorization of mRNAs with degradome signatures from targeted cleavage by miRNAs/phasiRNAs or siRNAs

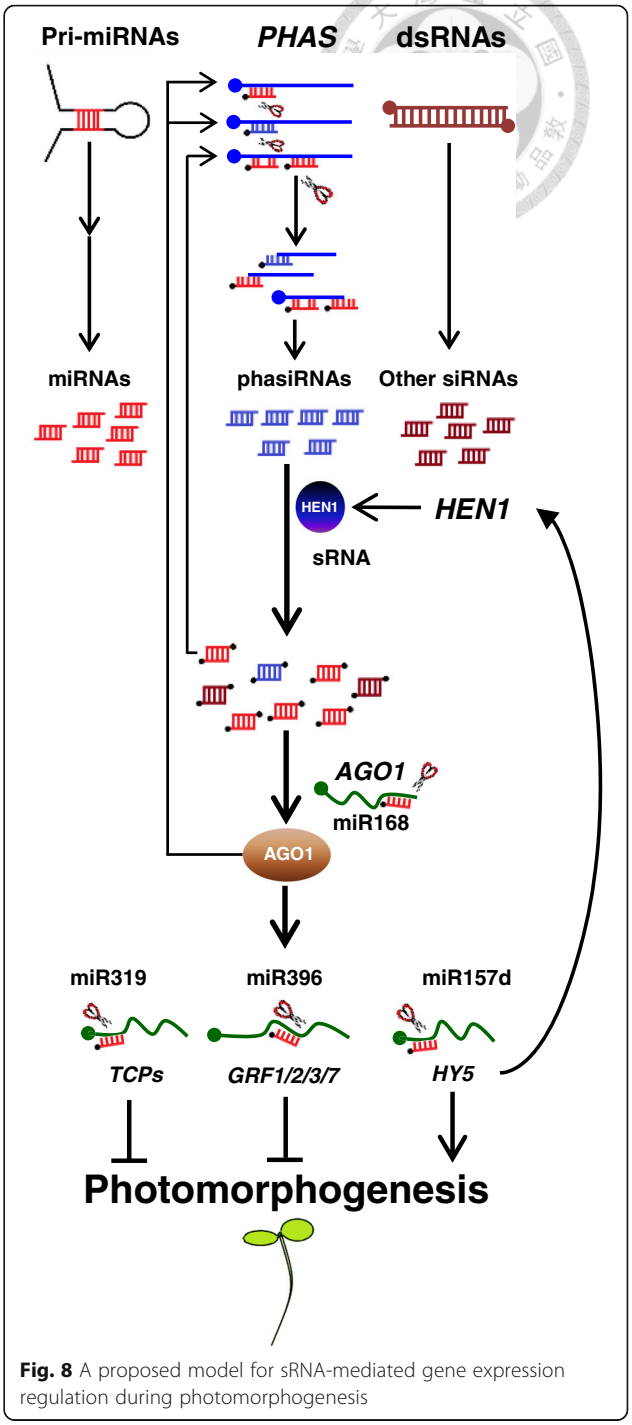

Fig. 8 A proposed model for sRNA-mediated gene expression regulation during photomorphogenesis

and confirmed for phenotype observation. The *grf1 grf2 grf3* triple mutant and *35S:MIR396aox* lines were kindly provided by Drs. Jeong Hoe Kim and DiQiu Yu, respectively. For phenotype observation, *Arabidopsis* seeds were surface-sterilized with 30% bleach and sown on half-strength Murashige and Skoog medium (Duchefa) without supplementing vitamin or sucrose, with 0.8% phyto agar at tissue culture grade (Duchefa, CAS number 9002–18-0). Seeds were stratified (4 °C for 4 days in the dark) to synchronize germination, then exposed to white light for 1 h to stimulate germination, and transferred to different light (W) conditions at 22 °C (Dark, W 12.5 and 50 μE for 4 days). The white light source was a PHILIPS LIFEMAX T-LD 18 W/840 T25 cool white tube. Hypocotyl lengths of seedlings were measured by using ImageJ v1.47 [51]. The means and SEM were calculated from more than 30 seedlings. At least 3 biological replicates for each line were used for each experiment.

Construction of *MIM396* lines

Primer sequences used in this study are listed in Additional file 1: Table S10. *35S:MIM396* target mimicry lines were generated as described [52]. Briefly, the genomic fragment of *IPS1* was amplified by using the iProof High-fidelity PCR kit (Bio-Rad) and cloned into the pGEMT-easy vector (Promega). The miR399 target site on original *IPS1* sequence was modified to sequester miR396a/b, as shown in Fig. 6a, by overlapping PCR during construction [52]. All constructs were then subcloned into the pCambia-1390 binary vector

doi:10.6342/NTU201702588

(CSIRO) digested with *Sal*I and *Sac*I. The constructs were transformed into *Agrobacterium tumefaciens* GV3101 strain, and introduced into *Arabidopsis* Col-0 by floral dipping. Two independent homozygous transgenic lines per construct were used for further analyses.

RNA sequencing and data analyses

For sRNA sequencing and data analyses, 4-d-old dark-grown *Arabidopsis* Col-0 seedlings were exposed to white light (100 μE) for 1, 3, 6, 12 and 24 h. The aerial tissues of approximately 5000 seedlings were collected for RNA isolation. Ten to 15 μg total RNA was size fractionated on 15% Tris-Borate-EDTA-Urea gel. sRNAs ranging from 17 to 30 nucleotides were gel-purified and used for cDNA library construction (Illumina Truseq for replicates 1 and 2, Small RNA v1.5 for replicates 3) and sequencing with the use of an Illumina HiSeq 2500. Twelve barcoded samples were sequenced in one single flowcell (a total of 240 M reads output per flowcell) at a read length of 50 nt. The adaptor-trimmed reads with size >18 nt were mapped to the *Arabidopsis* TAIR10 genome by using Bowtie [53] with the parameters -f –n 0 –e 80 –l 18 –a –m 5 –best –strata. For miRNA profiling, reads that perfectly matched to mature miRNA sequences were counted, normalized to total mapped reads of 20–24 nt and were shown as reads per million reads (RPM). Reads that mapped to miRNA families (e.g., miR156) were weighted by dividing the read count and equally assigning to each miRNA family member. For siRNA quantification, the Bowtie parameters were -f –n 0 –e 80 –l 18 –a –v 2 –best –strata. For phasiRNAs, the prediction of *PHAS* loci involved use of the UEA sRNA Workbench [54]. In brief, adaptor-trimmed reads longer than 16 nt were mapped to the TAIR10 genome, and the 21-nt phasing register was set to detect phasing within a 251-nt window, based on hypergeometric distributions described previously [14]. Among the uniquely mapped miRNA/siRNAs, only those with read counts ≥5 in ≥1 time point for all 3 biological replicates were considered expressed. Light-regulated sRNAs were defined as sRNAs with $p < 0.05$ on Student's t-test compared to dark treatment (W0 h) for all 3 biological replicates. For mRNA transcriptome analysis, the RPKM for sRNA target genes were analyzed by using datasets published previously [12]. Potential targets included those predicted by use of psRNATarget [55] (with UPE = 25, expectation = 3), miRNA targets identified in previous studies [25, 37] and miRNA targets detected in our degradome analysis (see Additional file 1: Table S5). Expressed genes had RPKM > 0.01 in at least one time point in both biological replicates. The transcript levels of target genes with degradome signatures are in Additional file 1: Table S5 and S6.

For degradome sequencing, 100 μg total RNA was isolated from 4-d-old dark-grown seedlings and mixtures of 4-d-old dark-grown seedlings exposed to 1, 3, 6, 12 and 24 h of light. Degradome sequencing was performed as described [56–58]. Putative cleavage sites were identified by using Cleaveland v4.4.3 [32, 59]. Those with CleaveLand category ≤ 2, $p \leq 0.05$ and at least 5 reads at the predicted cleavage site were reported as valid targeting events.

Northern blot analysis and qRT-PCR

In total, 20 to 50 μg total RNA was separated on 15% TBE-Urea gel (Invitrogen). SYBR-Gold (Life Technologies) was used for visualizing RNAs on gels. RNAs were then transferred to Hybond-N+ Nylon membrane (GE Healthcare), by using Transblot SD Semi-Dry Transfer Cell (Bio-Rad) and hybridized with γ-^{32}P-labeled miRNA probes as indicated at 37° Celsius overnight in UltraHyb Oligo buffer (Ambion). Hybridized blots were washed and exposed to Phosphoimager (GE Healthcare), then analyzed by using Typhoon FLA 7000 (GE Healthcare Life Sciences), as described [14]. Images were quantified by using ImageJ v1.47 [51]. For qRT-PCR, cDNA was synthesized from 2 μg total RNA from 4-d-old de-etiolating *Arabidopsis* seedlings. The SuperScript II RT kit (Invitrogen) was used for reverse transcription of mRNA. For qRT-PCR, cDNA with 0.25 ng equivalence of mRNA was used as a template for each sample. PCR amplification and detection was as described [60]. Primers are in Additional file 1: Table S8. Data for one representative biological replicate were shown in Figs. 3c, 5e and 6a. Results for 2 additional biological replicates were shown in Additional file 2: Figure S3.

Additional files

Additional file 1: Table S1. Sequencing and mapping statistics. Description: Contains the number and percentage of mapped sRNA reads in sRNA and degradome sequencing. **Table S2.** Expressed miRNAs in de-etiolating *Arabidopsis* seedlings. Description: Contains the expression level of expressed miRNAs, with RPM and fold changes. **Table S3.** Expressed phasiRNAs in de-etiolating seedlings. Description: Contains the expression level of expressed phasiRNAs, with the corresponding *PHAS* locus, RPM and fold changes. **Table S4.** Expressed siRNAs in de-etiolating seedlings. Description: Contains the expression level of expressed siRNAs, with the sequence, length, RPM and fold changes. **Table S5.** miRNA-mRNA and phasiRNA-mRNA pairs from cross comparisons of sRNA transcriptome and mRNA degradome. Contains the information of miRNA/phasiRNA-mediated target cleavage, including locus number, CleaveLand categories, *p*-values and target mRNA levels. **Table S6.** siRNA-mRNA pairs from cross comparisons of sRNA transcriptome and mRNA degradome. Contains the information of siRNA-mediated target cleavage, including locus number, CleaveLand categories, *p*-values and target mRNA levels. **Table S7.** Expression levels of *GRF*s. Contains the expression level of *GRF*s under dark and light. **Table S8.** Primers used in this study. Contains sequences of the primers that are used in this study. (XLSX 2667 kb)

Additional file 2: Figure S1. miRNAs/siRNAs with target cleavage tend to be more abundant than miRNAs/siRNAs that did not show target cleavage signatures. Contains supplemental figure and legend showing K-S test results of siRNA abundance. **Figure S2.** Molecular and phenotypic analyses of *mir396a* mutant and *MIR396aox* lines. Contains supplemental

doi:10.6342/NTU201702588

figure and legend showing the examination of *mir396a* mutant and *MIR396aox* lines. **Figure S3.** qRT-PCR results of two additional biological replicates for a *AGO1* and b, c *GRF* shown in Figs. 3c, 5e and 6a, respectively. Contains supplemental figure and legend showing the qRT-PCR results of two additional biological replicates in this study. (PDF 1074 kb)

Abbreviations

AGO1: ARGONAUTE1; Aub: Aubergine; B: blue; COP1: CONSTITUTIVE PHOTOMORPHOGENESIS 1; cry: cryptochrome; FR: far-red; GRF: GROWTH REGULATING FACTOR; HEN1: HUA ENHANCER1; HST: HASTY; HY5: ELONGATED-HYPOCOTYL 5; HYL1: HYPONASTIC LEAVES 1; K-S test: Kolmogorov-Smirnov test; miRNA or miR: microRNA; *PHAS*: phasiRNA-generating loci; phasiRNAs: phased siRNA; phy: phytochrome; piRNA: Piwi-interacting RNA; R: red; RdDM: RNA-dependent DNA methylation; RPM: read per million reads; siRNA: small interfering RNA; sRNA: small regulatory RNA; *TAS*: trans-acting siRNA-generating loci; TCP: TEOSINTE BRANCHED 1CYCLOIDEA AND PCF TRANSCRIPTION FACTOR; TE: transposable element

Acknowledgements

We specially thank Ming-Tsung Wu and Shu-Jen Chou for establishing the degradome sequencing system, Bo-Jun Liu and Chi-Yu Chen for assisting in experiments related to *MIM396* under the supervision of MCL and SHW. We also thank Jeong Hoe Kim at Kyungpook National University and Diqiu Yu at Xishuangbanna Tropical Botanical Garden, Chinese Academiy of Sciences, for kindly providing the *grf* mutants and *35S:MIR396aox* line, respectively. Finally, we thank Chih-Ching Lin, Chiung-swey Joanne Chang, Ho-Ming Chen, Ho-Wei Wu, Wen-Ping Hsieh, Yi-Chen Wu and Ying Wang for inspiring discussion and suggestions.

Funding

This research, including design and collection of experimental results, data analyses and preparation of the manuscript, was supported by the Investigator Award to S.-H. Wu from Academia Sinica, Taiwan.

Availability of data and materials

The datasets generated and analyzed in this manuscript can be accessed from Gene Expression Omnibus (GEO) under accession number GSE83646. The other supporting data are included as Additional files.

Authors' contributions

SHW, STJ, MCL and HLT designed the experiments. SLL, HLT and MCL conducted experiments. SHW and MCL wrote the manuscript. All authors have read and approved the final manuscript.

Ethics approval and consent to participate

Not applicable.

Consent for publication

Not applicable.

Competing interests

The authors declare that they have no competing interests.

Author details

[1]Institute of Plant and Microbial Biology, Academia Sinica, Taipei 11529, Taiwan. [2]Institute of Plant Biology, College of Life Science, National Taiwan University, Taipei 106, Taiwan.

Received: 23 April 2017 Accepted: 10 July 2017
Published online: 24 July 2017

References

1. Sullivan JA, Deng XW. From seed to seed: the role of photoreceptors in Arabidopsis development. Dev Biol. 2003;260:289–97.
2. Kami C, Lorrain S, Hornitschek P, Fankhauser C. Light-regulated plant growth and development. Curr Top Dev Biol. 2010;91:29–66.
3. Wu SH. Gene expression regulation in photomorphogenesis from the perspective of the central dogma. Annu Rev Plant Biol. 2014;65:311–33.
4. Yeh KC, Wu SH, Murphy JT, Largarias JC. A cyanobacterial Phytochrome two-component light sensory system. Science. 1997;277:1505–8.
5. Ahmad M, Jarillo JA, Cashmore AR. Chimeric proteins between cry1 and cry2 Arabidopsis blue light photoreceptors indicate overlapping functions and varying protein stability. Plant Cell. 1998;10:197–207.
6. Rizzini L, Favory JJ, Cloix C, Faggionato D, O'Hara A, Kaiserli E, Baumeister R, Schäfer E, Nagy F, Jenkins GI, Ulm R. Perception of UV-B by the Arabidopsis UVR8 protein. Science. 2011;332:103–6.
7. Wang H, Wang H. Phytochrome signaling: time to tighten up the loose ends. Mol Plant. 2015;8:540–51.
8. Yin R, Arongaus AB, Binkert M, Ulm R. Two distinct domains of the UVR8 photoreceptor interact with COP1 to initiate UV-B signaling in Arabidopsis. Plant Cell. 2015;27:202–13.
9. Ma L, Li J, Qu L, Hager J, Chen Z, Zhao H, Deng XW. Light control of Arabidopsis development entails coordinated regulation of genome expression and cellular pathways. Plant Cell. 2001;13:2589–607.
10. Chattopadhyay S, Ang LH, Puente P, Deng XW, Wei N. Arabidopsis bZIP protein HY5 directly interacts with light-responsive promoters in mediating light control of gene expression. Plant Cell. 1998;10:673–83.
11. Liu MJ, Wu SH, Chen HM, Wu SH. Widespread translational control contributes to the regulation of Arabidopsis photomorphogenesis. Mol Syst Biol. 2012;8:566.
12. Liu MJ, Wu SH, Wu JF, Lin WD, Wu YC, Tasi TY, Tsai HL, Wu SH. Translational landscape of Photomorphogenic Arabidopsis. Plant Cell. 2013;25:3699–710.
13. Meister G, Tuschl T. Mechanisms of gene silencing by double-stranded RNA. Nature. 2004;431:343–9.
14. Chen HM, Li YH, Wu SH. Bioinformatic prediction and experimental validation of a microRNA-directed tandem trans-acting siRNA cascade in Arabidopsis. Proc Natl Acad Sci U S A. 2007;104:3318–23.
15. Fei Q, Xia R, Meyers BC. Phased, secondary, small interfering RNAs in posttranscriptional regulatory networks. Plant Cell. 2013;25:2400–15.
16. Allen E, Xie Z, Gustafson AM, Carrington JC. microRNA-directed phasing during trans-acting siRNA biogenesis in plants. Cell. 2005;121:207–21.
17. Law JA, Jacobsen SE. Establishing, maintaining and modifying DNA methylation patterns in plants and animals. Nat Rev Genet. 2010;11:204–20.
18. Matzke MA, Mosher RA. RNA-directed DNA methylation: an epigenetic pathway of increasing complexity. Nat Rev Genet. 2014;15:394–408.
19. Bartel DP. MicroRNAs: genomics, biogenesis, mechanism, and function. Cell. 2004;116:281–97.
20. Chen X. Small RNAs and their roles in plant development. Annu Rev Cell Dev Biol. 2009;35:21–44.
21. Guleria P, Mahajan M, Bhardwaj J, Yadav SK. Plant small RNAs: biogenesis, mode of action and their roles in abiotic stresses. Genomics Proteomics Bioinform. 2011;9:183–99.
22. Ruiz-Ferrer V, Voinnet O. Roles of plant small RNAs in biotic stress responses. Annu Rev Plant Biol. 2009;60:485–510.
23. Bollman KM. HASTY, the Arabidopsis ortholog of exportin 5/MSN5, regulates phase change and morphogenesis. Development. 2003;130:1493–504.
24. Sorin C, Bussell JD, Camus I, Ljung K, Kowalczyk M, Geiss G, McKhann H, Garcion C, Vaucheret H, Sandberg G, Bellini C. Auxin and light control of adventitious rooting in Arabidopsis require ARGONAUTE1. Plant Cell. 2005;17:1343–59.
25. Tsai HL, Li YH, Hsieh WP, Lin MC, Ahn JH, Wu SH. HUA ENHANCER1 is involved in posttranscriptional regulation of positive and negative regulators in Arabidopsis photomorphogenesis. Plant Cell. 2014;26:2858–72.
26. Cho SK, Ben Chaabane S, Shah P, Poulsen CP, Yang SW. COP1 E3 ligase protects HYL1 to retain microRNA biogenesis. Nat Commun. 2014;5:5867.
27. Zhang H, He H, Wang X, Wang X, Yang X, Li L, Deng XW. Genome-wide mapping of the HY5-mediated gene networks in Arabidopsis that involve both transcriptional and post-transcriptional regulation. Plant J. 2011;65:346–58.
28. Kozomara A, Griffiths-Jones S. miRBase: integrating microRNA annotation and deep-sequencing data. Nucleic Acids Res. 2011;39:D152–7.
29. Cheng Y, Chen X. Posttranscriptional control of plant development. Curr Opin Plant Biol. 2004;7:20–5.
30. Vazquez F, Vaucheret H, Rajagopalan R, Lepers C, Gasciolli V, Mallory AC, Hilbert JL, Bartel DP, Crete P. Endogenous trans-acting siRNAs regulate the accumulation of Arabidopsis mRNAs. Mol Cell. 2004;16:69–79.
31. Baumberger N, Baulcombe D. Arabidopsis ARGONAUTE1 is an RNA slicer that selectively recruits microRNAs and short interfering RNAs. Proc Natl Acad Sci U S A. 2005;102:11928–33.
32. Brousse C, Liu Q, Beauclair L, Deremetz A, Axtell MJ, Bouche N. A non-canonical plant microRNA target site. Nucleic Acids Res. 2014;42:5270–9.
33. Arvey A, Larsson E, Sander C, Leslie CS, Marks DS. Target mRNA abundance dilutes microRNA and siRNA activity. Mol Syst Biol. 2010;6:363.

34. Ragan C, Zuker M, Ragan MA. Quantitative prediction of miRNA-mRNA interaction based on equilibrium concentrations. PLoS Comput Biol. 2011;7:e1001090.
35. Vaucheret H, Vazquez F, Crete P, Bartel DP. The action of ARGONAUTE1 in the miRNA pathway and its regulation by the miRNA pathway are crucial for plant development. Genes Dev. 2004;18:1187–97.
36. Chung PJ, Park BS, Wang HI, Jang IC, Chua NH. Light-inducible MiR163 targets PXMT1 transcripts to promote seed germination and primary root elongation in Arabidopsis. Plant Physiol. 2016;170:1772–82.
37. Jones-Rhoades MW, Bartel DP. Computational identification of plant microRNAs and their targets, including a stress-induced miRNA. Mol Cell. 2004;14:787–99.
38. Liu D, Song Y, Chen Z, Yu D. Ectopic expression of miR396 suppresses GRF target gene expression and alters leaf growth in Arabidopsis. Physiol Plant. 2009;136:223–36.
39. Kim JH, Choi D, Kende H. The AtGRF family of putative transcription factors is involved in leaf and cotyledon growth in Arabidopsis. Plant J. 2003;36:94–104.
40. Kim JS, Mizoi J, Kidokoro S, Maruyama K, Nakajima J, Nakashima K, Mitsuda N, Takiguchi Y, Ohme-Takagi M, Kondou Y, et al. Arabidopsis growth-regulating factor7 functions as a transcriptional repressor of abscisic acid- and osmotic stress-responsive genes, including DREB2A. Plant Cell. 2012;24:3393–405.
41. Chen HM, Chen LT, Patel K, Li YH, Baulcombe DC, Wu SH. 22-nucleotide RNAs trigger secondary siRNA biogenesis in plants. Proc Natl Acad Sci U S A. 2010;107:15269–74.
42. Lee BH, Ko JH, Lee S, Lee Y, Pak JH, Kim JH. The Arabidopsis GRF-INTERACTING FACTOR gene family performs an overlapping function in determining organ size as well as multiple developmental properties. Plant Physiol. 2009;151:655–68.
43. Li J, Yang Z, Yu B, Liu J, Chen X. Methylation protects miRNAs and siRNAs from a 3'-end uridylation activity in Arabidopsis. Curr Biol. 2005;15:1501–7.
44. Park MY, Wu G, Gonzalez-Sulser A, Vaucheret H, Poethig RS. Nuclear processing and export of microRNAs in Arabidopsis. Proc Natl Acad Sci U S A. 2005;102:3691–6.
45. Vaucheret H, Mallory AC, Bartel DP. AGO1 homeostasis entails coexpression of MIR168 and AGO1 and preferential stabilization of miR168 by AGO1. Mol Cell. 2006;22:129–36.
46. Yang L, Liu Z, Lu F, Dong A, Huang H. SERRATE is a novel nuclear regulator in primary microRNA processing in Arabidopsis. Plant J. 2006;47:841–50.
47. Creasey KM, Zhai J, Borges F, Van EF, Regulski M, Meyers BC, Martienssen RA. miRNAs trigger widespread epigenetically activated siRNAs from transposons in Arabidopsis. Nature. 2014;508:411–5.
48. Martinez G, Choudury SG, Slotkin RK. tRNA-derived small RNAs target transposable element transcripts. Nucleic Acids Res. 2017;45:5142–52.
49. Aravin AA, Sachidanandam R, Girard A, Fejes-Toth K, Hannon GJ. Developmentally regulated piRNA clusters implicate MILI in transposon control. Science. 2007;316
50. Sato K. The epigenetic regulation of transposable elements by PIWI-interacting RNAs in drosophila. Genes Genet Syst. 2013;88:9–17.
51. Schneider CA, Rasband WS, Eliceiri KW. NIH image to ImageJ: 25 years of image analysis. Nat Methods. 2012;9:671–5.
52. Franco-Zorrilla JM, Valli A, Todesco M, Mateos I, Puga MI, Rubio-Somoza I, Leyva A, Weigel D, Garcia JA, Paz-Ares J. Target mimicry provides a new mechanism for regulation of microRNA activity. Nat Genet. 2007;39:1033–7.
53. Langmead B, Trapnell C, Pop M, Salzberg SL. Ultrafast and memory-efficient alignment of short DNA sequences to the human genome. Genome Biol. 2009;10:R25.
54. Stocks MB, Moxon S, Mapleson D, Woolfenden HC, Mohorianu I, Folkes L, Schwach F, Dalmay T, Moulton V. The UEA sRNA workbench: a suite of tools for analysing and visualizing next generation sequencing microRNA and small RNA datasets. Bioinformatics 2012;28:2059–2061.
55. Dai X, Zhao PX. psRNATarget: a plant small RNA target analysis server. Nucleic Acids Res. 2011;39:W155–9.
56. Addo-Quaye C, Eshoo TW, Bartel DP, Axtell MJ. Endogenous siRNA and miRNA targets identified by sequencing of the Arabidopsis degradome. Curr Biol. 2008;18:758–62.
57. German MA, Pillay M, Jeong DH, Hetawal A, Luo S, Janardhanan P, Kannan V, Rymarquis LA, Nobuta K, German R, et al. Global identification of microRNA-target RNA pairs by parallel analysis of RNA ends. Nat Biotechnol. 2008;26:941–6.
58. Gregory BD, O'Malley RC, Lister R, Urich MA, Tonti-Filippini J, Chen H, Millar AH, Ecker JR. A link between RNA metabolism and silencing affecting Arabidopsis development. Dev Cell. 2008;14:854–66.
59. Addo-Quaye C, Miller W, Axtell MJ. CleaveLand: a pipeline for using degradome data to find cleaved small RNA targets. Bioinformatics. 2009;25:130–1.
60. Wang Y, Wu JF, Nakamichi N, Sakakibara H, Nam HG, Wu SH. LIGHT-REGULATED WD1 and PSEUDO-RESPONSE REGULATOR9 form a positive feedback regulatory loop in the Arabidopsis circadian clock. Plant Cell. 2011;23:486–98.

doi:10.6342/NTU201702588